博士論文

Synthesis and Properties of [7]Helicene Metallocenes with Group 8 Metals

（8 族金属を有する[7]ヘリセンメタロセンの合成と性質）

A dissertation submitted to the University of Tokyo

for the degree of Doctor of Philosophy (Engineering)

Midori Akiyama

秋山 みどり

Midori Akiyama
Department of Chemistry and Biotechnology
Graduate School of Engineering
The University of Tokyo
7-3-1 Hongo, Bunkyo-ku, Tokyo 113-8656, Japan

Table of Contents

List of Abbreviations

List of Abbreviations

Ar	argon
Ar	aryl
atm	atmosphere(s)
a.u.	arbitrary unit
bpy	2,2'-bipyridine
br	broad (spectral)
Bu	butyl
°C	degree Celsius
cal	calorie
calcd.	calculated
CD	circularly dichroism
Cp	cyclopentadienyl
Cp*	pentamethylcyclopentadienyl
CP	circularly-polarized
CPL	circularly-polarized luminescence
CV	cyclic voltammetry
d	doublet (spectral)
δ	chemical shift of NMR signal
Δ	difference
DCM	dichloromethane
DFT	density functional theory
dmso	dimethyl sulfide
DNA	deoxyribonucleic acid
ε	molar absorption coefficient
equiv	equivalent
ESI	electrospray ionization
Et	ethyl
et al.	*et alii*
EWG	electron-withdrawing group
f	oscillator strength
Φ	quantum yield
g	asymmetric factor
G	Gibbs free energy
GPC	gel permeation chromatography
h	hour(s)
H	enthalpy
HOMO	highest occupied molecular orbital
HPLC	high-performance liquid chromatography
HRMS	high resolution mass spectrum
Hz	Hertz
IR	infrared
i	iso
IL	intra-ligand
J	joule
J	coupling constant
λ	wavelength
k	kinetic constant
k_B	Boltzmann constant
K	equilibrium constant
K	kelvin
L	neutral ligand
LMCT	ligand-to-metal charge transfer
ln	natural logarithm
LUMO	lowest unoccupied molecular orbital
m	multiplet

M	mol per liter
M	metal
M	minus (helical chirality)
MC	metal-centered
Me	methyl
MeCN	acetonitrile
MeO	methoxy
MeOH	methanol
min	minute(s)
MLCT	metal-to-ligand charge transfer
MS	mass spectroscopy
m/z	mass-to-charge ratio
n	normal
NLO	nonlinear optics
NMR	nuclear magnetic resonance
OLED	organic light emitting diode
ORTEP	Oak Ridge thermal ellipsoid plot
p	*para*
P	plus (helical chirality)
Ph	phenyl
phen	1,10-phenanthroline
ppy	2-(2'- pyridyl)phenyl
Pr	propyl
PTLC	preparative thin layer chromatography
q	quartet
R	rectus (chirality)
rac	racemic
RT	room temperature
s	singlet (spectral)
s	second(s)
S	singlet (excited/ground state)
S	entropy
S	sinister (chirality)
SCF	self-consistent field
t	triplet (spectral)
t	time
t	tertiary
τ	lifetime of emission
T	triplet (excited state)
T	temperature
TD	time-dependent
Tf	trifluoromethanesulfonyl
THF	tetrahydrofuran
TMS	trimethylsilyl
TS	transition state
UV	ultra-violet
vis	visible
Å	angstrom

Chapter 1.

General Introduction

1-1. Cyclopentadienyl (Cp) complexes

1-1-1. Discovery of ferrocene, the first example of Cp complexes

In 1951, Kealy and Pauson reported a paper titled "A New Type of Organo-Iron Compound".[1] In this report, the reaction of cyclopentadienylmagnesium bromide with iron chloride was reported (Scheme 1-1). The authors aimed at oxidative coupling to afford fulvalene, however, they did not get the desired compound but compound expressed as $C_{10}H_{10}Fe$ in chemical formula instead.

Scheme 1-1. The first report of synthesizing ferrocene

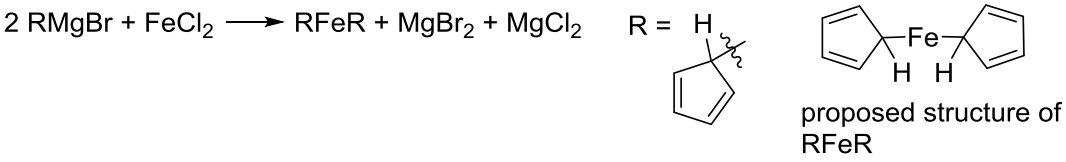

The structure of the obtained complex was suggested as described in Scheme 1-1 in the first report. One year later, Wilkinson *et al.* proposed another structure in which two cyclopentadienyl rings are parallel with an iron atom sandwiched between them, based on the reactivity and physical properties of the organo-iron compound.[2] At the same time, Pfab and Fischer also suggested the same structure as Wilkinson *et al.* did independently.[3] The proposed sandwich-like structure was supported by x-ray-diffraction analysis of a single crystal, reported preliminary by Pepinsky and Eiland,[4] and Orgel and Dunitz (Figure 1-1).[5] In 1956, the structure was confirmed based on the more precise analysis by Orgel, Dunitz, and Rich.[6]

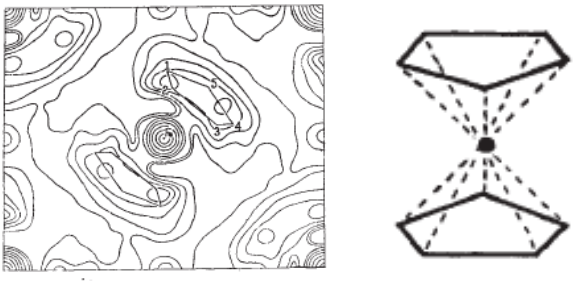

Figure 1-1. The first reported crystallographic structure of ferrocene

Ferrocene was not only the first example of cyclopentadienyl complexes but also the first example of organo-iron compounds. It was remarkably stable and easily isolated, in contrast that trials to prepare organo-iron complexes so far had been resulted in failure. Why is ferrocene so stable? Kealy and Pauson mentioned in their first report that the stability came from the aromaticity of the cyclopentadienyl anion.[1] After the structure was confirmed, it has been widely accepted that the central iron atom satisfies 18 electrons rule, 6 d-electrons from Fe(II) and 6 π-electrons from each of the cyclopentadienyl anions, which makes ferrocene stable.

1-1-2. Variety of Cp complexes

After the novel discovery of ferrocene, many kinds of cyclopentadienyl metal complexes have been synthesized, which greatly contributed to the growth of organometallic chemistry. A wide variety of metals have been incorporated in Cp complexes, not only transition-metals, but also main group metals[7,8]and lanthanides.[9]

Since Dunitz *et al.* described ferrocene as a "molecular sandwich" based on its structure in their manuscript,[5] organometallic compounds with two Cp ligands like ferrocene are called "sandwich complexes" nowadays. Metal complexes bearing only one Cp ligand are often described as "half-sandwich complexes," or "piano-stool complexes" according to their stool-like structure in which the ligands other than Cp are regarded as legs.

Cp complexes are utilized in various ways because of the great stability of the Cp–Metal bond, for example, as homogeneous catalysts,[9–15] redox reagents,[16] building blocks,[17,18] electronic and optical materials,[10,19] bioactive compounds,[20–22] and so on.

1-1-3. Chiral Cp complexes

1-1-3-1. Class of chiral Cp complexes

There are lots of examples of Cp complexes possessing chirality. They can be classified into three types:[23] (i) Complexes with Cp ligand(s) bearing substituent(s) with central or axial chirality, (ii) complexes composed of prochiral Cp ligand(s) arranged in either C_2 or C_1 symmetry, and (iii) metal-centred chiral complexes with three different ligands other than Cp.

1-1-3-1-1. Complexes with Cp ligand(s) bearing substituent(s) with central or axial chirality

In 1975, Leblanc and Moise reported preparation of cyclopentadienyl anion with a central-chiral substituent by asymmetric reduction of 6,6-disubstituted fulvene in the presence of (−)-quinine or (+)-cinchonine, which was treated with $CpTiCl_3$ to afford a chiral Cp titanium complex.[24] Chiral Cp complexes with zirconium, ruthenium and iron complexes were also synthesized by the same procedure.[25,26] In 1978 and later, cyclopentadienes bearing a substituent derived from natural products such as menthol, camphor, and so on, were synthesized and used as precursors of chiral Cp ligands.[27–30] In the last decade, annulated Cp ligands with several chiral centers were developed.[31–34]

In 1989, the first example of axially-chiral Cp complexes was reported by Halterman and Colleti.[35] They synthesized titanium, zirconium, and iron complexes with this C_2-symmetric ligand (Figure 1-2).[36,37] Recently, iridium, rhodium, ruthenium, scandium, yttrium, and

gadolinium complexes were also synthesized for the sake of homogeneous catalysis.

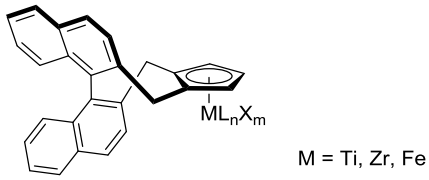

Figure 1-2. Cp complexes with axial chirality synthesized by Halterman *et al.*

1-1-3-1-2. Complexes composed of prochiral Cp ligand(s) arranged in either C_2 or C_1 symmetry

Ansa-metallocene is a metallocene in which two of the Cp ligands are bridged. If an *ansa*-metallocene has a substituent at appropriate position on each Cp ring, the complex is chiral. The first example of an *ansa*-metallocene was reported by Brintzinger and Schnutenhaus in 1979 (Figure 1-3).[38] The complex was prepared by deprotonation of 1,3-bis(2-tert-butylcyclopentadienyl)propane to afford the corresponding dianion and the following treatment with titanium trichloride. The complex was successfully resolved into enantiomers by selective conversion of one of the enantiomers to the corresponding binaphtholate. After this report, tremendous kinds of chiral *ansa*-metallocenes with early-transition metals, such as titanium, zirconium, and hafnium were synthesized.[23] Other than the central metals, bridging groups and substituents on the Cp ring were also varied. Especially, C_2-symmetrical bis-indenyl metal complexes, whose first example was reported by Brintzinger *et al.* in 1982,[39] have been vigorously studied because they showed great potentials for stereo-selective polymerization (See **1-1-3-2-1**).

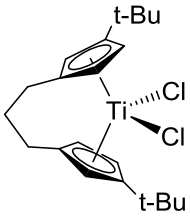

Figure 1-3. The first *ansa*-metallocene

1,2-Disubstituted Cp complexes with two different ligands have planar chirality. The first example was dimethyl(2-vinylferrocenyl)methylamine, reported by Hauser and Lednicer in 1959 (Figure 1-4a).[40] The first reported enantiopure planar-chiral Cp complex was obtained by resolution *via* diastereomer-salt formation (Figure 1-4b).[41] Diastereoselective synthesis of planar-chiral ferrocene by using a chiral directing group was reported by Nozaki *et al.* in 1969,[42,43] and by Ugi *et al.* in 1970.[44] With these two reports as a trigger, a number of 1,2-disubstituted ferrocenes with various chiral directing groups have been synthesized. After 26 years from the development of diastereoselective method, enantioselective lithiation of ferrocene by a chiral lithium salt,[45] and using butyllithium in the presence of an optically-active compound[46,47] was reported.

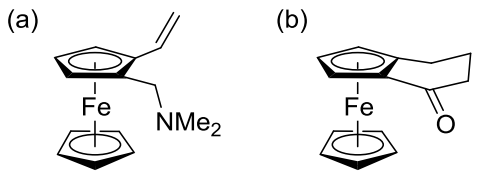

Figure 1-4. Examples of planar-chiral Cp complexes

Asymmetric catalysts for synthesizing planar-chiral Cp complexes have been developed.[48] In 1990s, kinetic resolution of planar-chiral ferrocenes catalyzed by enzymes were studied.[49] The first report of asymmetric synthesis of planar-chiral compound catalyzed by a non-

enzymatic compound was reported by Schmaltz *et al.*, in which one substituted ferrocene was desymmetrized by stereoselective intramolecular cyclization (Scheme 1-2).[50] It was 9 years later from the Schmaltz's report that the first non-enzymatic kinetic resolution of 1,2-disubstituted ferrocenes using Sharpless asymmetric dihydroxylation was reported.[51] In recent 10 years, a certain number of studies on catalytic asymmetric planar-chiral Cp complexes (mainly substituted ferrocenes) have been reported. Ogasawara *et al.* used molybdenum- or ruthenium-catalyzed olefin metathesis for catalytic kinetic resolution and desymmetrization of planar-chiral Cp complexes.[52–58] Rhodium-catalyzed 1,4-addition to an α,β-unsaturated ketone,[59] ruthenium-catalyzed reduction of ketone,[60] and *ortho*-lithiation in the presence of catalytic amount of chiral auxiliary ligand,[61] were also used in the asymmetric catalytic synthesis of planar-chiral Cp complexes. Most recently, palladium-catalyzed cross-coupling reactions and Heck reaction using amino-acid derivatives as ligands have been developed.[62,63] Organocatalysts also have been employed for asymmetric synthesis of planar-chiral Cp complexes.[64–66]

Scheme 1-2. The first catalytic asymmetric synthesis of a planar-chiral ferrocene

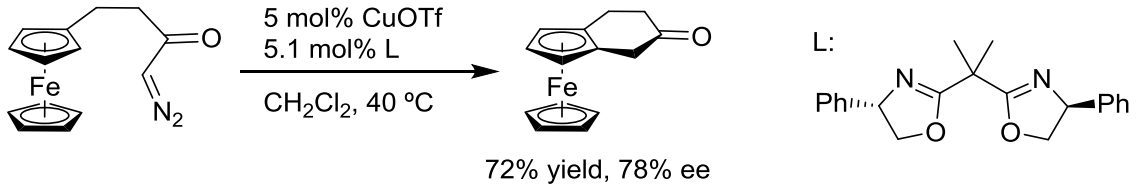

1-1-3-1-3. Metal-centred chiral complexes

The first organometallic compound with metal-centered chirality was a Cp manganese complex with a carbonyl, a nitrosyl, and a phosphine ligand, synthesized by Brunner *et al.* in 1969 (Figure 1-5).[67,68] Their racemic mixture was treated with an optically-active nucleophile to afford a pair of diastereomers, able to be separated on the basis of the different solubilities. Removal of the

auxiliary part gave an enantiopure metal-centered chiral complex. After this report, metal-centered chiral Cp complexes possessing three different ligands other than Cp were synthesized with iron, molybdenum, rhenium, and rhodium, and their chiroptical properties, stability of the chirality, and reactivity with other molecules were investigated.[69]

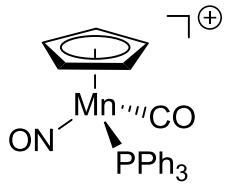

Figure 1-5. The first metal-centered chiral Cp complex

Diastereoselective formations of a chiral metal center were also reported. The methods can be classified into two ways; reaction of a bidentate ligand possessing a chiral substituent with achiral Cp metal precursor,[70–72] and a ligand substitution of chiral Cp complex possessing a chiral substituent on Cp or planar-chirality.[36–41]

All of the examples mentioned above in this section are three-legged piano-stool complexes. It is notable that there is one example of a metal-centred chiral complex with four legs showing square-pyramidal structure (Figure 1-6).[79,80]

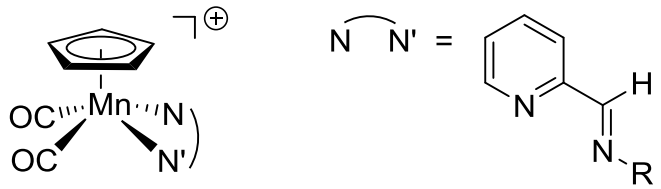

Figure 1-6. Metal-centered chiral Cp complex with four legs

1-1-3-2. Use of chiral Cp complexes

Chiral Cp complexes are mainly applied in the field of stereo-selective catalysis. Representative

examples are reviewed in this section.

1-1-3-2-1. Catalysts for stereoselective polymerization[81]

C_2-symmetric *ansa*-metallocenes with early-transition metals are widely used for stereoselective polymerization.[11] Kaminsky *et al*. reported polymerizations of propylene with a racemic mixture of a chiral zirconocene catalyst activated by methylaluminoxane.[82] They found that the obtained polymer was highly isotactic. Since this polymerization was reported, considerable numbers of *ansa*-metallocenes with a group 4 metal were applied to polymerization of propylene. With regards to the central metal, zirconium is the best choice in terms of cost, activity, stability of the complexes. Hafnium is better suited for producing polypropylene with higher molecular weight, while the catalytic activity is lower. The stereoselectivities of the polymerization are comparable between zirconium and hafnium. Most of the reported *ansa*-titanocenes shows lower catalytic activity and stereoselectivity compared to zirconocenes and hafnocenes, and are unstable under high temperature. The abilities of catalysts also depend on the bridging moiety and the substituents on the Cp ring.

In catalytic polymerization of propylene, C_2-symmetric *ansa*-metallocenes give isotactic polymer, while C_s-symmetric ones afford syndiotactic polymer. The stereoselectivity is originated from the enantioface-selective insertion of propylene to the metal center; in the case of a bis-indenyl complex for example, insertion of re-face of propylene is much likely to occur with (*R*,*R*)-*ansa*-metallocene, which makes a stereocenter as (*S*).

Ansa-zirconocene have been applied for synthesis of isotactic polymers of 1-butene[82] and longer α-olefins.[83,84] Kaminsky and his coauthors reported polymerization of cyclopentene by a bis-indenyl zirconium catalyst,[85] and later Collins *et al.* carefully studied the regio- and stereo-selectivity in polymerization of cyclopentene by various *ansa*-zirconocenes.[86–88] There are

also reports of stereoregular cyclopolymerization of non-conjugated dienes, such as 1,5-hexadiene by *ansa*-zirconocene catalysts.[89] For polymerization of styrene, bis-indenyl complexes with yttrium and neodymium showed high isotactic selectivity.[90]

1-1-3-2-2. Asymmetric catalysts for transformation of small molecules

In the 20th century, several examples of asymmetric catalytic reactions with chiral Cp complexes were reported, such as hydrogenation, epoxidation, and isomerization of alkenes, reductions of ketone, and aldol reactions, although they resulted in moderate selectivities.[23]

In 2004, Gutnov and Heller *et al.* reported the first example of asymmetric reactions catalyzed by an optically-active Cp late-transition metal complex. They used Cp cobalt complexes with a menthyl substituent for asymmetric [2+2+2] cycloaddition reaction to afford axially chiral compounds in a good enantioselectivity (Scheme 1-3).[91,92] The authors supposed that cobaltacyclopentadiene was formed diastereoselectively as an intermediate, which originated the enantioselective reaction.

Scheme 1-3. Catalytic enantioselective [2+2+2] addition using a chiral Cp cobalt complex

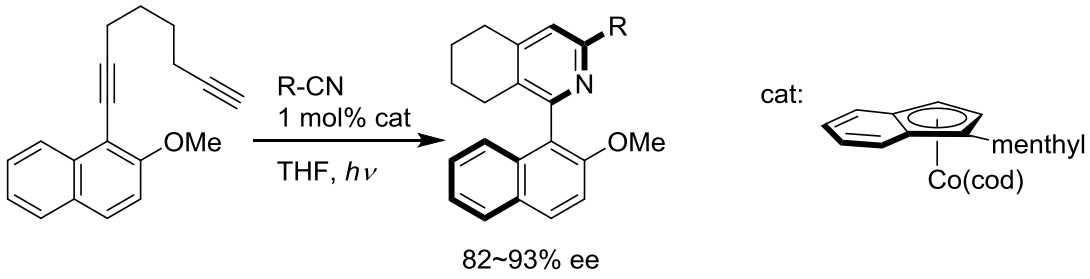

In 2012, Cramer and Ye reported enantioselective cycloaddition of olefin through cleavege of a C–H bond, which was catalyzed by a Cp rhodium complex with chiral cyclohexane annulated (Scheme 1-4).[93,94] The reaction afforded chiral dihydroquinolones in a good

stereoselectivity. The authors mentioned about the mechanism of enantioselectivity-determining step as follows: the two methyl substituents on the cyclohexane ring acted as “side wall” and controled the orientation of the arene substrate, while the substituents on the acetal moiety woked as “back wall” and controled the direction from which the olefin approached to the rhodium center (Figure 1-7). Cramer and Ye also reported stereoselective catalytic reaction by a rhodium complex with an axial-chiral Cp ligand.[95] They achieved enantioselective C–H allylation of benzamides. With these two reports as a trigger, asymmetric catalytic reactions by chiral Cp complexes were developed at an accelerating speed.[96] In addition to rhodium,[97–102] iridium,[103] ruthenium,[104] and lanthanide (scandium, yttrium, and gadolinium)[105] complexes with chiral Cp ligands were applied to asymmetric catalysis.

Scheme 1-4. Catalytic enantioselective cycloaddition using a chiral Cp rhodium complex

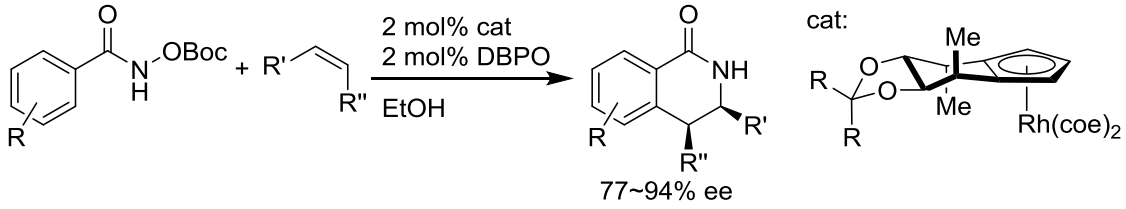

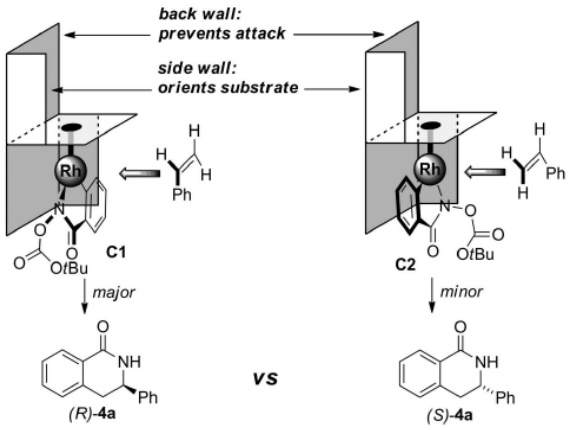

Figure 1-7. Mechanism of the enantioselective reactions catalyzed by a chiral Cp complex[93]

1-1-3-2-3. Chiral ligands of organometallic complexes for asymmetric catalysis

Ferrocene derivatives have been widely used as a ligand for organometallic catalyst because of its great properties such as low price, thermal and chemical stability, and high tolerance to moisture and oxygen.[10] Especially chiral ferrocenes are useful ligands for asymmetric catalysis (Figure 1-8).[106–111] Some of them, for example, ppfa, Josiphos, Taniaphos, Fc-Phox, Trap, and FerroTANE, have already been established and commercially available. Tremendous kinds of other chiral ferrocene ligands were also reported, helped by a variety of general methods for its functionalization. They are applied to various asymmetric reactions, such as hydrogenation of unsaturated bonds, addition of hydrogen–heteroatom and heteroatom–heteroatom bonds to unsaturated bonds, cross-coupling reactions, allylic substitutions, nucleophilic additions, and so on.

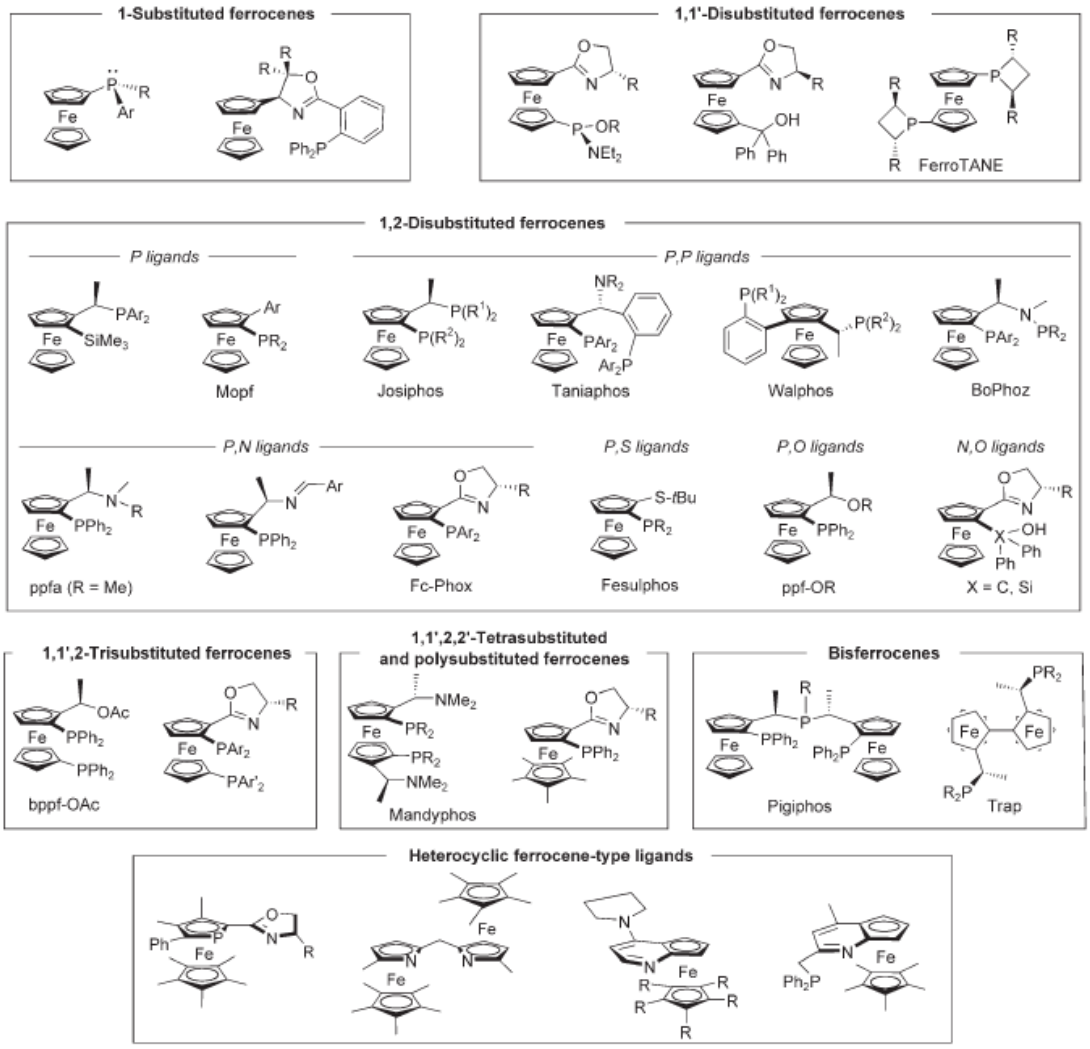

Figure 1-8. Variety of chiral ferrocene ligands[108]

1-1-3-2-4. Organocatalysts

Fu *et al.* reported asymmetric catalytic esterification by a chiral ferrocene possessing amine moiety (Scheme 1-5).[112]

Scheme 1-5. Kinetic resolution by a organocatalyst possessing planar-chiral ferrocene moiety

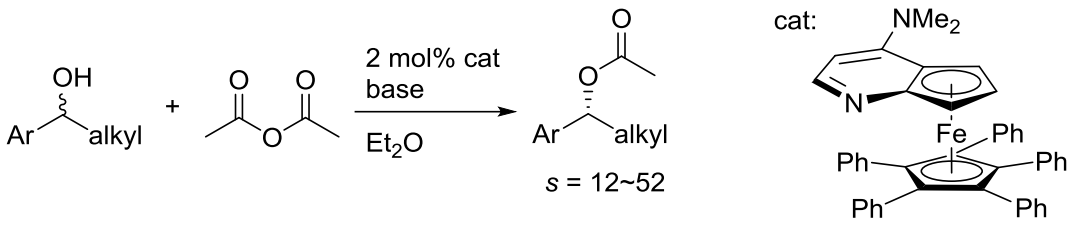

1-2. Phosphorescence from transition-metal complexes

Phosphorescence is an emission involving change in spin multiplicity, usually from triplet excited state to the singlet ground state. Phosphorescent molecules can be thought as candidates for OLED materials, chemical sensors, photovoltaics, and bio-imaging.[113–116] From this point of view, the 2nd and 3rd row transition metal complexes attract much attention because the heavy atom effect enable them emitting phosphorescence.[115,117]

1-2-1. Classification of excited states in organometallic complexes[118,119]

Excited states in organometallic compounds are classified based on the character of the electron transitions; (i) metal-centered (MC) excited states arising from electron transition between the metal's d-orbitals, (ii) metal to ligand charge-transfer (MLCT) excited states derived from electron excitation from a metal-centered d-orbital to a ligand-localized orbital, (iii) ligand to metal charge-transfer (LMCT) excited states involving electron transition from a d-orbital to an orbital of the ligand, (iv) intra-ligand (IL) excited states in which an electron transit between orbitals localized on the ligand. For bimetallic complexes involving a metal-metal bond, (v) metal to metal charge transfer (MMCT) excited states arising from electron transition between d-orbitals of the different two metal, are possible.[120]

1-2-2. Representative examples of phosphorescent metal complexes[113]

There are tremendous number of reports on photoluminescence from metal complexes. In this paragraph, only selected examples showing strong phosphorescence enough to be observed at room temperature will be mentioned (Figure 1-9).

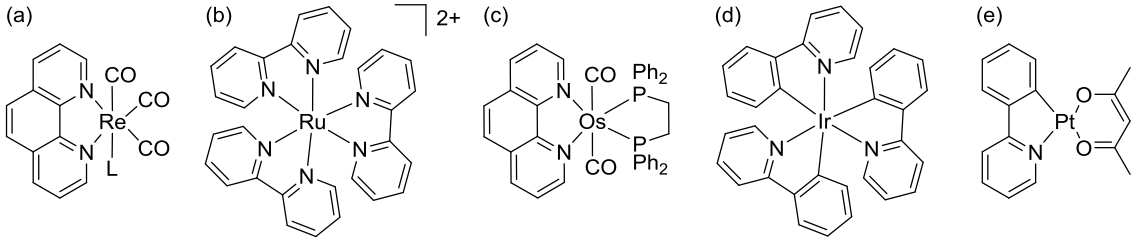

Figure 1-9. Representative examples of phosphorescent metal complexes

In early days before 1970s, the photochemistry of metal carbonyl complexes were widely studied because of their high reactivity for photochemical reactions.[118,121,122] Among them, group 7 metal complexes exhibit a relatively strong emission. Especially, tricarbonylrhenium α,α'-diimine complexes ([Re(N^N)$(CO)_3$(L)]) are known to show phosphorescence at ambient temperature (Figure 1-9a).[123,124] The emission originated from either ^{3}MLCT localized on diimine ligand or IL $^3\pi$-π^* diimine excited state.

In 1971, Ru$(bpy)_3^{2+}$ was found to act as a triplet photosensitizer, and show strong phosphorescence (Figure 1-9b).[125,126] From then, a variety of Ru$(bpy)_3^{2+}$ analogs have been designed by introducing substituents or changing ancillary ligands.[127–132] Experimental[133–135] and theoretical[136–139] studies were conducted to disclose that the phosphorescence originates from the ^{3}MLCT transition localized on one of the three bipyridine ligands. In addition to these cationic ruthenium(II) pyridyl complexes, neutral ones, such as bis(pyridyl pyrazolate)diphosphine complexes and bis(benzo[*h*]quinolinate)carbonylphosphine complexes were also reported to

exhibit phosphorescence in the last decade.[140–142] The osmium analogues of these complexes were also synthesized. Although simple osmium tris(α,α'-diimine) complexes, such as $[Os(bpy)_3]^{2+}$ and $[Os(phen)_3]^{2+}$ emit in near-IR region,[143,144] the emission wavelength could be blue-shifted by introducing a diphosphine ligand instead of the diimine ligand (Figure 1-9c).[145]

Iridium cyclometalated complexes, $Ir(ppy)_3$ and its derivatives, also exhibit intense emission (Figure 1-9d).[114,146–149] The origin of phosphorescence is usually assigned to be ^{3}MLCT excited state,[150] but introducing electron-withdrawing ligands, which decrease the energy of IL excited states, sometimes makes it mixed with IL character.[151,152]

From the late 1980s, cyclometalated platinum complexes were found to show phosphorescence at room temperature (Figure 1-9e).[153,154] While bipyridine or terpyridine platinum complexes hardly exhibit emission because of radiationless deactivation from ^{3}MC excited states, cyclometalated ligands, for example 2-phenyl pyridine, have strong electron-donating ability to raise the energy of MC excited state, which makes the complex showing emission from either IL or MLCT excited states.[154]

Other than the examples mentioned above, rhodium, palladium, silver, and gold complexes were reported to show phosphorescence at room temperature.[155] There are also several examples of phosphorescent copper complexes, although the emission is weak due to smaller spin-orbital coupling in the first-row transition-metals.[156]

1-2-3. Photoluminescence properties of Cp complexes

Despite tremendous kinds of Cp complexes have been synthesized as mentioned in **1-1**, Cp complexes showing strong phosphorescence can be hardly found except for some of the Cp carbonyl group 6 bimetallic complexes.[157] For example, ruthenocene (Cp_2Ru) showed very weak

phosphorescence at 560 nm, in less than 3% quantum yield even at 28 K.[158] The nonradiative deactivation of ruthenocene was known to occur partly through the C–H bonds on the Cp ring.[159] It is also reported that ruthenocene changes its structure largely along with electron excitation, in which the metal–Cp bond is elongated.[158–160]

1-3. Helicenes

[*n*]Helicenes are *ortho*-fused aromatic rings with helical chirality (*n* = the number of fused rings). Their beautiful helical structure, due to a distortion of the π-system imposed by an intramolecular steric repulsion, makes them unique in optical properties, chiroptical properties, assembly, and so on. Investigation of the racemization behaviors is also an intriguing topic. Based on the Helicity Rule,[161] enantiomer with clockwise helicity is denoted by *P* ("plus"), while the other enantiomer showing anticlockwise helicity is denoted by *M* ("minus") (Figure 1-10).

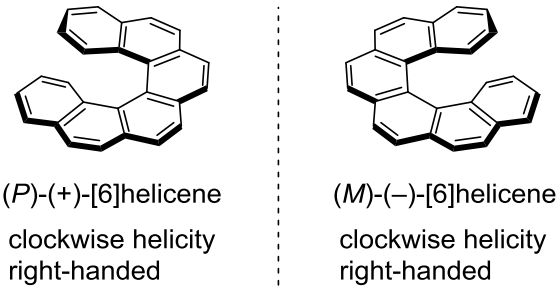

Figure 1-10. Two enantiomers of [6]helicenes

1-3-1. Early examples of helicenes

In 1903, Meisenheimer and Witte reported the first examples of helicenes, which contained nitrogen atom(s) in their skeleton (Figure 1-11a,b).[162] The first example for helicene comprised

of only carbon and hydrogen atoms, [5]helicene, was synthesized by Weitzenböck and Klingler in 1918 (Figure 1-11c).[163] Other than these two examples, only a small number of helicenes had been reported in the first half of the 19th century (Figure 1-11c−e).[164–167] In 1955, Newman *et al.* reported the synthesis of optically pure [6]helicene as the first example of helicene with stable helical chirality, by using diastereomer salt complexation.[167] After this report, contributing to much interest in chiroptical properties of enantiopure helicenes, a variety of helicenes and helicene-like compounds have been synthesized so far.

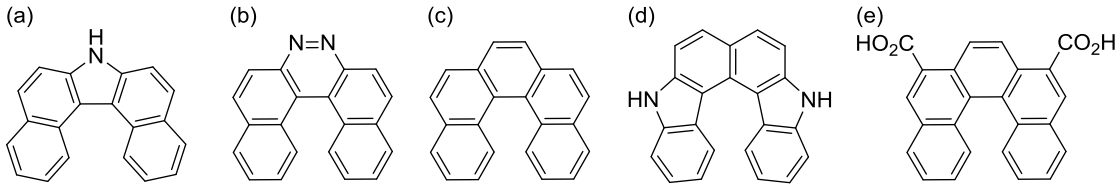

Figure 1-11. Early examples of helicenes

1-3-2. Variety of helicenes

Nowadays, various kinds of helicenes have been synthesized. Selected examples will be mentioned below.

1-3-2-1. Carbo-helicenes[168,169]

With various methods such as Friedel–Crafts reaction,[170] photo-cyclization,[171,172] Diels-Alder reaction,[173] [*n*]helicenes composed of *ortho*-fused *n* benzene rings have been synthesized. The longest helicene reported so far is [16]helicene (Figure 1-12) reported by Fujita *et al.* in 2015, synthesized by photocyclization.[174] When increasing the number of annulated rings, the helicene starts to form additional layers; a double layer at n = 7–12, a triple layer from n = 13.[175]

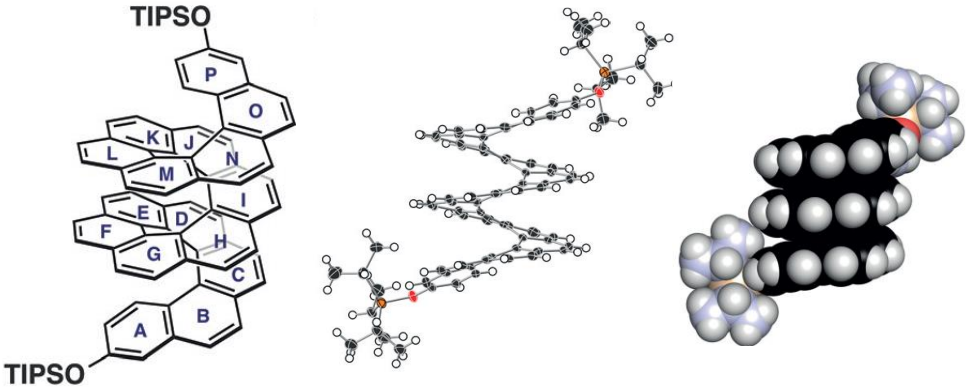

Figure 1-12. The longest carbo-helicene, [16]helicene[174]

1-3-2-2. Hetero-helicenes[176]

In addition to helicenes whose aromatic rings consist of only carbon atoms, a number examples were reported for hetero-helicenes containing hetero atom(s) in their skeletons (Figure 1-13). The major family is composed of helicenes in which aromatic heterocycle(s), such as thiophene,[177] pyrrole,[178,179] furan,[178] phosphole,[180] pyridine,[181–183] lactam,[184,185] and so on, are fused between or at the edge of *ortho*-fused arene rings. Other than this family, the synthesis of a [7]helicene comprised of only fused thiophene rings was reported by Rajca *et al*.[186,187]

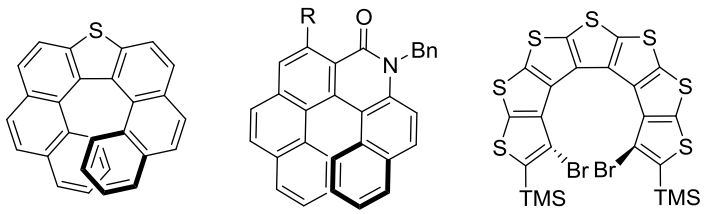

Figure 1-13. Selected examples of hetero-helicenes

1-3-2-3. Multi-helicenes

Aromatic compounds possessing more than one helicene moiety are difficult to be synthesized.

Recently, synthesis of double helicenes[188–190] were achieved (Figure 1-14). There are also examples of double-helicenes[191] and a quadruple helicene[192] in which hetero-atoms were incorporated. Such kind of multi-helicenes have diastereomers, whose kinetic and thermodynamic stabilities and isomerization behavior are intriguing.[193]

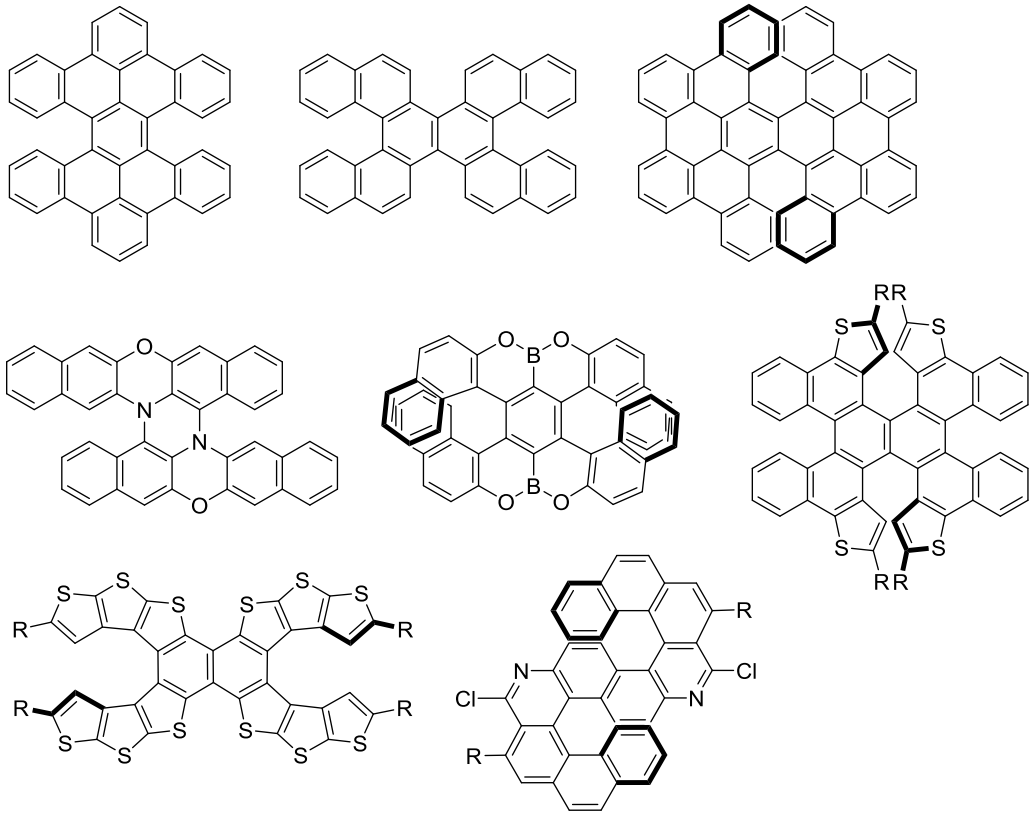

Figure 1-14. Selected examples of multi-helicenes

1-3-2-4. Helicene-like compounds

There are several examples of helical-shaped molecules comprised of ortho-fused rings, but not fully conjugated (Figure 1-15). They are often called "helicene-like compounds" because they are not helicenes on the basis of the definition. Teplý *et al.* synthesized a family of cationic partially-hydrogenated helicenes in which nitrogen atoms are incorporated in their skeleton at the fused points (Figure 1-15a).[194–197] Chen *et al.* synthesized tetrahydrogenated[5]helicenes (Figure 1-

15b).[198,199] Nozaki *et al.* synthesized [7]helicene-like compounds possessing either a fluorene unit[200] or silole moiety.[201] Helical molecules with silole rings were synthesized also by other groups.[202,203] There are several reports on asymmetric catalytic reactions generating new helicene-like compounds (Figure 1-15c,d).[203–208]

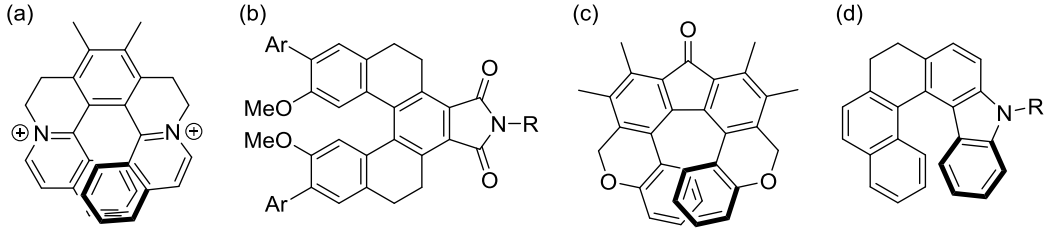

Figure 1-15. Selected examples of helicene-like molecules

1-3-3. Properties of helicenes

Because of their unique structures, with helical chirality and extended π-conjugated system, helicenes show intriguing properties. In this section, properties of only normal carbo[*n*]helicenes (*n* = 5–13) will be mentioned.

1-3-3-1. Inversion behavior of helicenes

Racemization behaviors of helicenes were investigated based on both experimental and theoretical ways. In 1956, experimental study on the thermal racemization of [6]helicene was reported by Newman and Lednicer.[170] [5]-,[209] [7]-, [8]-, and [9]helicenes were investigated by Martin *et al*. in 1974.[210] Comparing the estimated activation energies for their racemization (Table 1-1), they were enlarged as the number of aromatic rings increased from 5 to 7, however, the values were very similar from [7]- to [9]helicene, around 42 kcal mol^{-1}. Martin *et al.* commented on this fact that "the helicenes are in fact much more 'flexible' than is generally believed." This trend of the racemization energies well matched with the result of theoretical calculations.[211]

Table 1-1. Experimental and calculated activation barriers for racemization of carbo[*n*]helicene (*n* = 5–9)[211]

helicene	ΔΔ*H*[a] [kcal mol⁻¹]	AM1 GS[b] [kcal mol⁻¹]	AM1 TS[b] [kcal mol⁻¹]	AM1 TS-GS [kcal mol⁻¹]	B3LYP/3-21G TS-GS[c] [kcal mol⁻¹]	B3LYP/3-21G TS-GS[d] [kcal mol⁻¹]
1	22.9[28]	104.5	127.4	22.9	28.02	25.65
2	35.0[11,29]	126.8	158.2	31.4	40.50	38.16
3	40.5[11]	151.1	185.8	34.7	44.31	42.04
4	41.0[11]	175.9	210.8	34.9	43.38	41.76
5	41.7[11]	200.6	234.6	34.0	40.80	39.72

[a] Experimental results. [b] Heat of formation. [c] B3LYP/3-21G//AM1. [d] B3LYP/3-21G//B3LYP/3-21G.

For the mechanism of the isomerization, there were three possible pathways; C-C bond breaking, retro Diels–Alder reaction and Diels–Alder reaction, and reversible inversion of the helical structure. Martin *et al.* denied the first two pathways from the experimental results.[212] Haufe *et al.* and Peyerimhoff *et al.* independently reported theoretical studies on inversion pathway of helicenes.[211,213] In each report, it was suggested that the transition state of the racemization of helicenes has C_s symmetry with the terminal rings bending to the same side (Figure 1-16). The following reports supported this mechanism.[214]

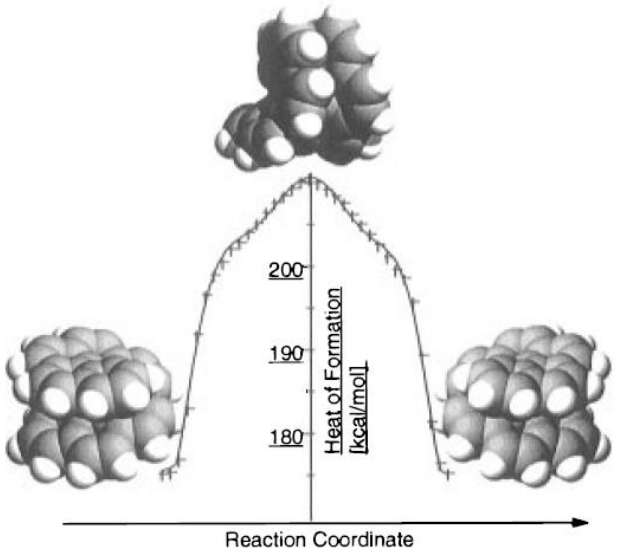

Figure 1-16. Mechanism of inversion of a helicene

1-3-3-2. Chiroptical properties

Because of their helical shapes, helicenes show large optical rotations and intense responses in circularly dichroism (CD). There is a general relationship between the absolute structure and optical rotation; (*P*)-helicenes are dextrorotatory and (*M*)-forms are levorotatory.[215] The value of specific rotation increases as the number of the aromatic rings becomes larger (Table 1-2).[169]

Table 1-2. Optical rotation of (*M*)-carbo[*n*]helicene (*n* = 4–13)[169]

n	**[α] (°)**	***n***	**[α] (°)**
4	Low barrier of racemization	9	−8150
5	−1670	10	−8940
6	−3570	11	−9310
7	−5900	12	Not available
8	−7170	13	−9620

In CD spectra, each enantiomer of carbo-helicenes shows two strong Cotton effects (Figure 1-17). There is a general relation also between the absolute conformation and the shape of spectrum; (*P*)-helicenes show a negative cotton effect at higher-energy region and a positive one at lower-energy region, while (*M*)-forms exhibit the opposite pattern.[210] A number of theoretical studies were conducted to predict the CD spectra of helicenes. In earlier studies, empirical and semiempirical methods were used because of the large size of helicenes, but recently, TD-DFT calculations were performed.[216,217] More precise studies by the coupled cluster method were also reported, in which the calculated CD intensity and the wavelength well-matched with the experimental results.[218] It is also noted that the substitution on helicene was predicted to have both electronic and steric effect on the CD spectra.[219,220]

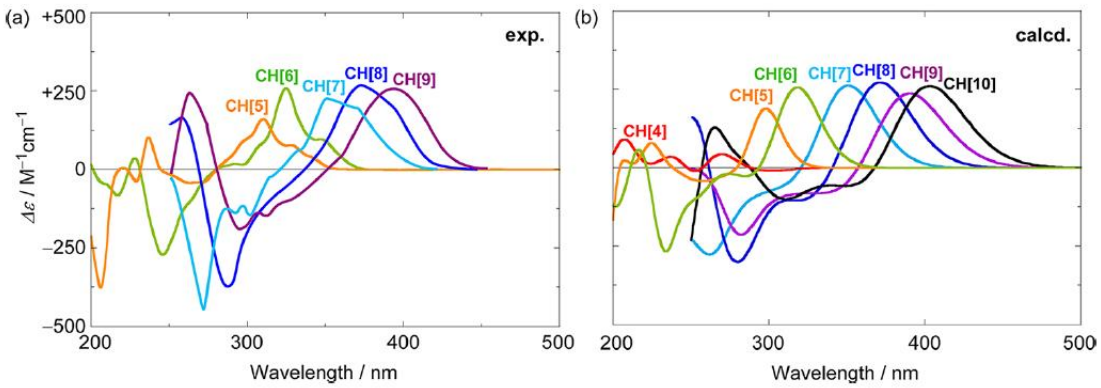

Figure 1-17. Experimental and calculated CD spectra of carbo[*n*]helicene (*n* = 4–10)[218]

1-3-4. The use of helicenes[221]

1-3-4-1. Chiral recognition

Several helicene derivatives interact with one enantiomer of a chiral compound selectively. The first example of chiral recognition by a helicene was reported by Nakazaki *et al.* in 1983, in which they reported the synthesis of crown ethers incorporating a methyl-substituted helicene moiety (Figure 1-18).[222,223] They selectively transported one enantiomer of chiral amino acids through a bulk organic solvent membranes. Interestingly, crown ether with (*P*)-[5]helicene and one with (*P*)-[6]helicene showed the opposite selectivity to each other although they possessed the same helical chirality. Chiral recognition by helicene derivatives using hydrogen bonds,[224–226] and stereoselective complexation of helicene derivatives with β-cyclodextrin[227,228] are also known.

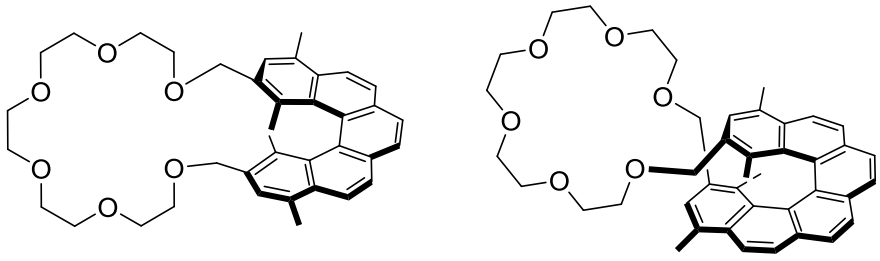

Figure 1-18. Crown ethers possessing a helicene moiety for chiral recognition

Recently, chiral molecular recognitions by helicenes have been studied in the field of chemical-biology. In most of the research, DNA is the target molecules, and usually it favors a helicene derivative possessing the same helical configuration.[229]

1-3-4-2. Asymmetric reactions[176,230]

There are some studies on stereoselective reactions performed with helicenes. In 1980's, Martin *et al.* developed diastereoselective reactions using helicene derivatives as substrates.[176] The first example of asymmetric catalysts possessing a helicene moiety was reported by Reetz *et al.* in 1997 (Scheme 1-6).[231] After that, several catalytic reactions were reported in which helicenes with either hydroxy, phosphine, or phosphite moiety were used as a ligand for organometallic catalyst.[232] There are also examples of organocatalytic reactions performed with a helicene possessing amine or nitroxide group.[233] Non-functionalized carbo-helicenes are able to be used as a chiral-induced reagent for autocatalytic reactions developed by Soai *et al*.[234]

Scheme 1-6. Asymmetric hydrogenation reaction by catalysts possessing a helicene part

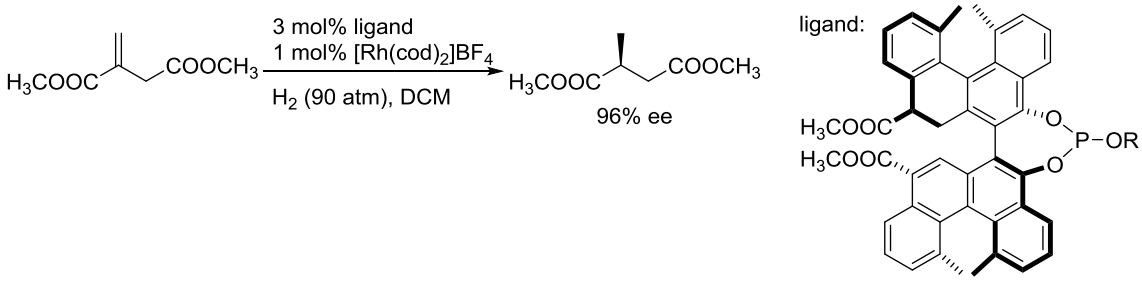

1-3-4-3. Optical materials

Although the normal carbo-helicenes do not show strong fluorescence because of their rapid intersystem crossing,[235] some of the hetero-helicenes and helicene-like compounds exhibit intense

emission. Especially circularly polarized luminescence (CPL) are notable, originating from their helically chiral structures. In 2006, Barnes *et al.* succeeded in observation CPL of an individual helicene molecule deposited on the surface of a polymer film.[236] [7]Helicene-like compounds reported by Nozaki *et al.*[200,201] and Tanaka *et al.*[184,203,208,237] exhibited strong CPL in high asymmetric factor. Hasbe *et al.* found that the quinoxaline-fused thia-helicenes with electron-withdrawing groups showed good CPL property.[238] Chen *et al.* developed a series of tetrahydro[5]helicene derivatives with various substituents and achieved full-color fluorescence,[199,239] which were applied to cell imaging[240] and sensing of mercury.[241]

1-3-4-4. Liquid crystals

Katz *et al.* made great contribution in construction of helicene-based liquid crystals. In 1998, they synthesized a helicene-bisquinone with long alkyl chains, which formed an anisotropic liquid-crystalline phase at room temperature, and turned to an isotropic phase by heating at 85 °C.[242] Applying an electric field to this material made it aggregated into helical columns, whose orientation could be changed by the electric field, generating discotic nematic liquid-crystalline phases.[243–245]

Some helicenes were also used as chiral dopants to convert a nematic liquid crystal to a twisted nematic (cholesteric) phase.[246]

1-3-4-5. Nonlinear optics

Nonlinear optical (NLO) effect is defined as "effect brought about by electromagnetic radiation the magnitude of which is not proportional to the irradiance."[247] One of the concepts to increase the NLO properties is self-assembly of multiple molecules leading to an enhancement of the properties beyond the sum of the individual molecular property. In this point of view, helicene-

bisquinones, developed by Katz's group as was mentioned in the previous paragraph, was studied as a candidate for nonlinear optics. Verbiest and Katz *et al.* made Langmuir–Blodgett film with a non-racemic helicene-bisquinone derivatives and found that it showed second-order NLOs.[248,249] The NLO susceptibility of the material composed of optically-pure helicene was 30 times larger than that of racemic material, because of the longer columnar assembled structure observed in AFM images (Figure 1-19).

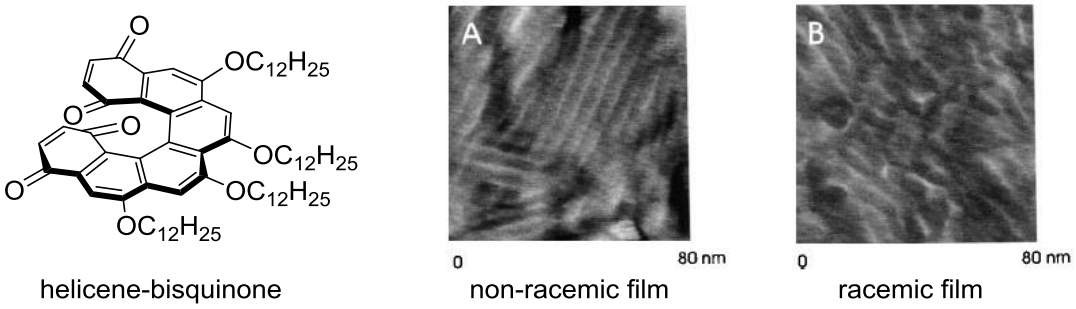

Figure 1-19. AFM images of assembled optically-pure and racemic helicene-bisquinone[248]

1-3-4-6. Molecular ratchet

Kelly *et al.* tried to build a molecular motor which rotates unidirectionally.[250] In this challenge, they designed a molecular ratchet by employing a triptycene as the toothed wheel and a [4]helicene as the pawl. According to Scheme 1-7, they succeeded in one-directional rotation by 120 ° around the C–C bond between the two units.[251]

Scheme 1-7. One-directional rotation of a molecular ratchet incorporating [4]helicene moiety

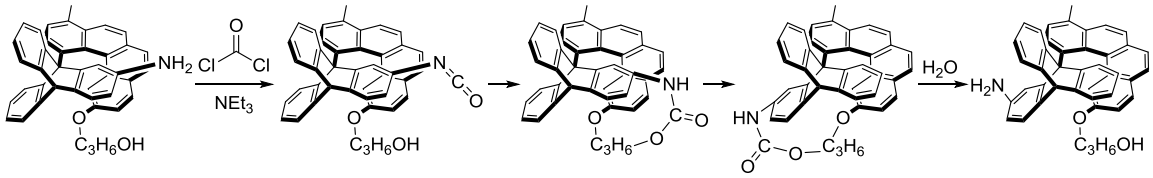

1-4. Helicene organometallic complexes[252]

Helicene is sometimes used as a ligand for metal complexes. In this part, representative examples of helicene organometallic compounds possessing carbon–metal bond(s) will be mentioned.

1-4-1. Cp complexes

Katz *et al.* developed a family of helicene metallocenes with cobalt or iron as a central metal (Figure 1-20). The complexes had Cp moiety(ies) at the edge of the helicene ligands. In 1979, the authors reported synthesis of bimetallic complexes with two of [4]helicene or [5]helicene ligands, which did not have rigid helical chirality.[253] Three years later, they reported [7]helicene metallocene, in which the central metal was sandwiched by two Cp moieties at the both edges of the same [7]helicene (Figure 1-20a).[254] These [7]helicene metallocenes could be synthesized in their optically pure forms.[255] Furthermore, in 1993, Katz's group reported cobaltocene with one [8]helicene ligand (Figure 1-20b), with two [8]helicene ligands (c), and bimetallic cobaltocene with a [9]helicene ligand (d).[256] They also succeeded in synthesis of metallo-polymer with [9]helicene ligands (Figure 1-20e).[257] This polymer showed reversible reduction and oxidation in solution, which made significant changes in the CD spectrum.[258] It can be thought as a redox-triggered CD switching system.

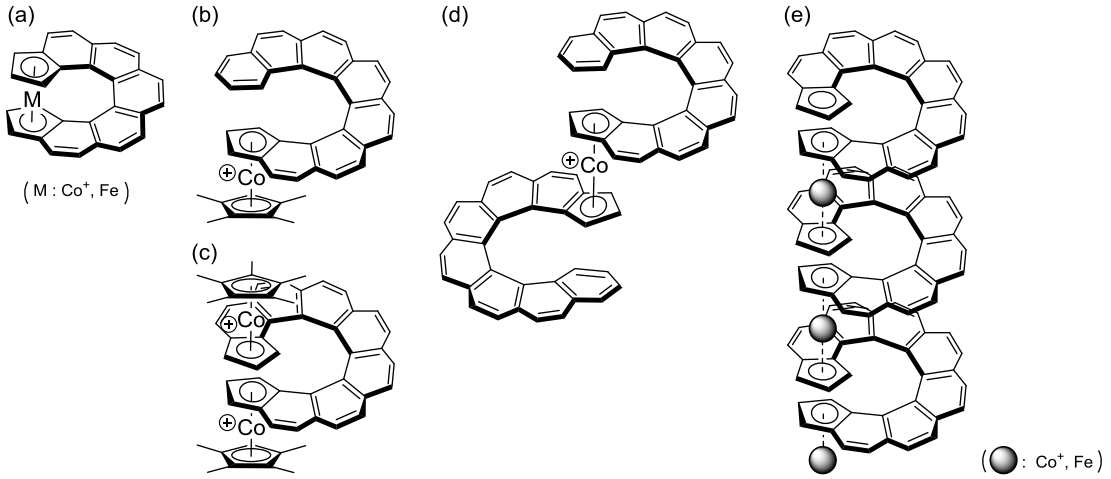

Figure 1-20. Family of helicene Cp complexes developed by Katz *et al.*

Thiel *et al*. synthesized metal complexes with dibenzo[*c*,*g*]fluorenyl anion, [5]helicene possessing a Cp moiety at the middle of its skeleton (Figure 1-21). They reported the complexes with various metals as a central metal, such as cobalt,[259] iron,[260,261] ruthenium,[262] manganese,[261] molybdenum,[263] and tungsten.[263] Although the [5]helicene ligand in these complexes showed a helical-chiral conformation in the crystal state due to the axial-chirality of the binaphthyl backbone, racemization proceeded rapidly at room temperature in solution.[261]

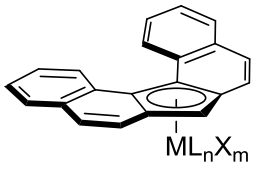

Figure 1-21. Family of [5]helicene Cp complexes developed by Thiel *et al.*

Carreno *et al.* reported the synthesis of enantiopure ferrocen[4]helicenequinone by a kinetic resolution using a stereoselective Diels-Alder reaction in 2011.[264]

1-4-2. Arene complexes

In 2011, Alvarez *et al.* reported the synthesis of metal complexes with a [6]helicene composed of only 6-membered rings (Fiigure 1-22).[265] They identify the three regioisomers of the iridium [6]helicene complex **A**, **B**, and **C**, generated as a result of reaction of [6]helicene and the iridium precursor. The metal on the ligand migrated over the helicene rings, and these isomers converted to the most thermodynamically stable isomer **C** after several days in solution. Also in the case of bimetallic [6]helicene complexes with iridium or ruthenium atoms, three isomers generated at first, then they converged into the most stable isomer, in which each of two metals bound to the arene ring at the edge of the helicene ligand.

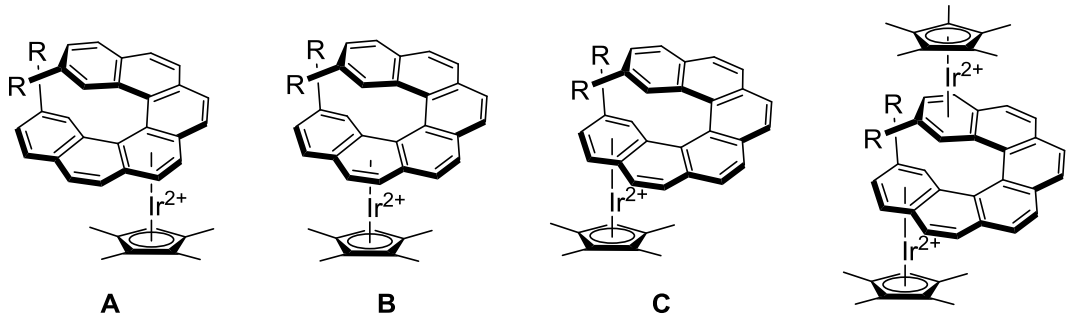

Figure 1-22. Arene complexes with a [6]helicene ligand

1-4-3. Cyclometalated complexes

Crassous *et al.* made grate contributions in synthesizing helicenes with a metal atom incorporated in their skeleton, through cyclometalation reaction of phenylpyridine derivatives (Figure 1-23).[266] The authors used mainly platinum as a coordinated metal, and synthesized monometallic- and bimetallic complexes (Figure 1-23a,b).[266] They also developed diplatinum complex with two helicene ligands, in which a Pt–Pt bond exists (Figure 1-23c).[267,268] The complexes with bearing helicene ligands possess two diastereomers; homochiral isomer and heterochiral isomer.

Homochiral isomer of complex was found to convert to heterochiral one under 80 °C in toluene solution, which suggested that the latter isomer was more thermodynamically stable. It was notable that these platinum complexes showed circularly polarized luminescence (CPL) in high g_{lum} value (~10^{-2}),[269] with which circularly polarized phosphorescent OLED was constructed.[270] Cyclometalated helicenes possessing iridium and osmium as a coordinated metal were also synthesized.[266,271,272]

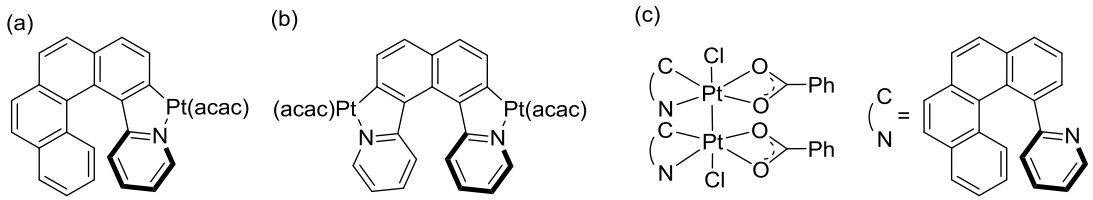

Figure 1-23. Helicene cyclometalated complexes

1-4-4. Alkenyl and alkynyl complexes

There are several reports on synthesizing helicene metal complexes in which each helicene ligand has alkenyl or alkynyl substituent(s) on the aromatic ring to coordinate to a metal. Crassous *et al.* synthesized monometallic and bimetallic [6]helicene alkenyl complexes with either ruthenium[273] or osmium[272] atom through hydrometallation of ethynyl[6]helicene (Figure 1-24a). With these alkenyl complexes, reversible CD switching systems, which are like the metallo polymer reported by Katz *et al.*,[258] were developed: Reversible oxidation and reduction triggered a change in the CD spectra of the ruthenium complex. In the case of the osmium complex, CD spectra changed by reversible isomerization between alkenyl complex and carbene complex by addition of acid and base (Figure 1-24b).[272] Most recently, Crassous and Autschbach *et al.* reported the synthesis of a [6]helicene alkynyl bimetallic complex with iron, which led to redox-triggered chiroptical switching system active in the IR and near-IR regions.[274]

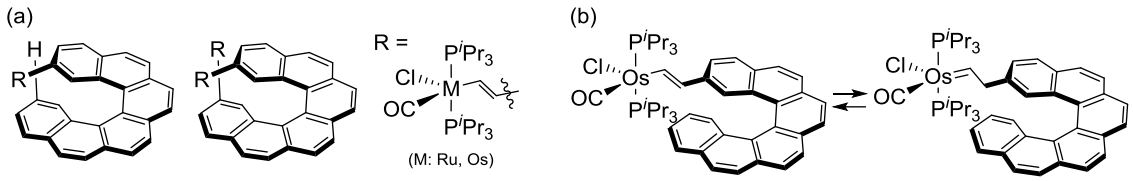

Figure 1-24. Helicene alkenyl metal complexes

Meanwhile, Licandro *et al.* reported the synthesis of tetrathia[7]helicene complexes substituted with either a ferrocenylethynyl group or a {(η^5-cyclohexadienyl)tricarbonylmanganese}ethynyl group (Figure 1-25).[275] It was suggested in the report that the helicene-substituted ferrocene was more difficult to be oxidized comparing to non-substituted ferrocene (Cp_2Fe).

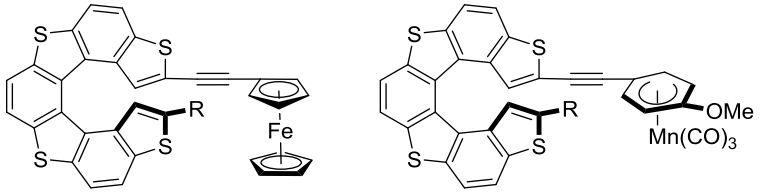

Figure 1-25. Synthesis of tetrathia[7]helicene metal complexes

1-5. Metal complexes with other curved π-conjugated molecules

There are some important examples of organometallic complexes in which the metal coordinated to curved π-conjugated molecules other than helicenes.

1-5-1. Bucky metallocenes

Nakamura *et al.* developed "bucky metallocenes", in which [60] or [70]fullerene and ferrocene were combined.[276] Because the five-membered ring in fullerene has only 5π-electrons, the authors developed methods to functionalize fullerene at first.[277,278] With a penta-substituted fullerene,

bucky ferrocene and ruthenocene were synthesized, in which the fullerene was coordinated to a metal in an η^5-manner (Scheme 1-8).[279,280] They also synthesized rhenium and rhodium complexes with the substituted fullerene.[281]

Scheme 1-8. Synthesis of bucky metallocenes

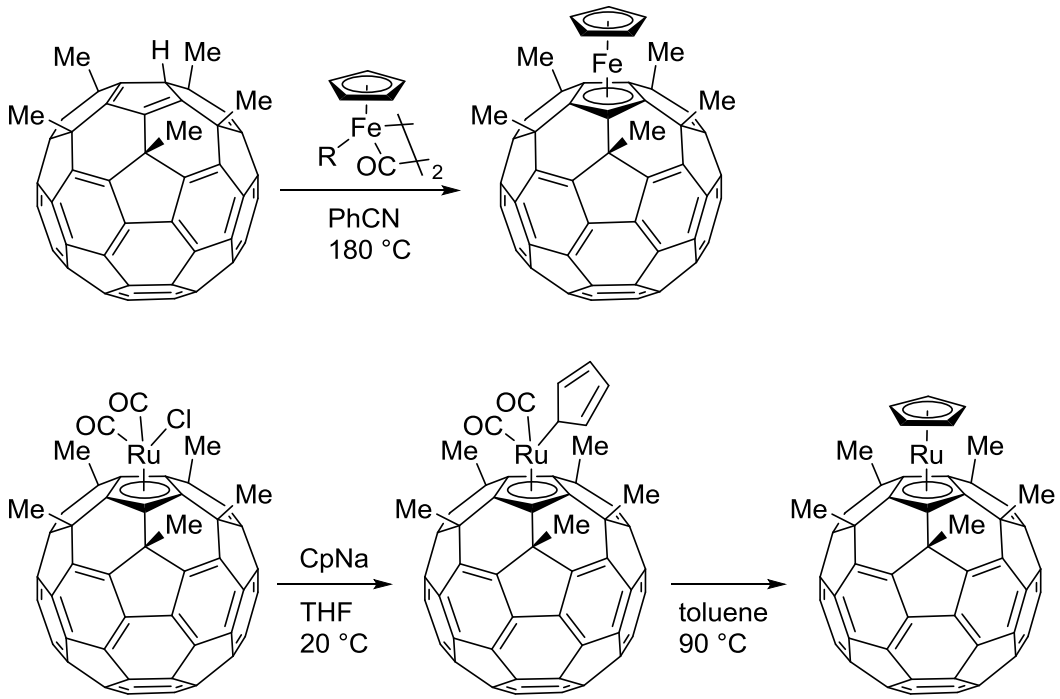

1-5-2. Complexes with bowl-shaped molecule[282]

Bowl-shaped hydrocarbon molecules, corannulene and sumanene,[283] are also able to form organometallic complexes. In the coordination chemistry of such bowl-shaped molecules, there are two intriguing selectivities; surface selectivity (concave or convex) and coordination-site selectivity. Change in the depth of the bowl structure is also notable.

In 1997, Siegel *et al.* reported the first corannulene metal complex, in which the corannulene was coordinated to a ruthenium atom in an η^6 manner.[284] The metal bound to concave site in the crystal state, as predicted by theoretical calculations. The group 9 metal complexes,

with rhodium and iridium, were also synthesized.[285] It was found that the metal on the corannulene migrated over the corannulene rings.[286] Angelici *et al.* synthesized a bis-ruthenium complex with corannulene.[287] Each of the two ruthenium atoms bound onto the opposite surface to each other. It was found from the comparison of free-corannulene, monometallic corannulene complex, and bimetallic one, that the coordination to the metal made the bowl-structure flatter.[288]

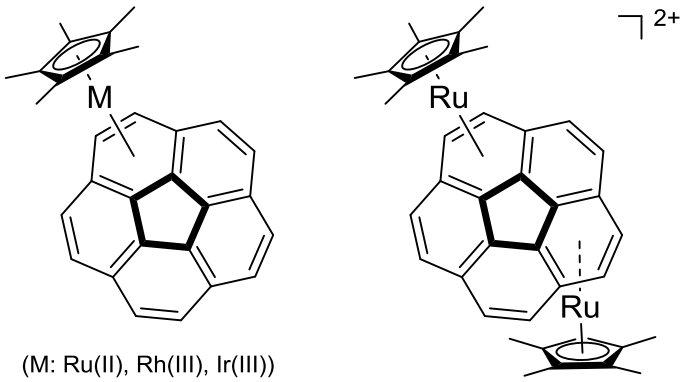

Figure 1-26. Corannulene metal complexes

There are also several examples of η^2-corannulene metal complexes. In 2003, Petrukhina *et al.* synthesized η^2-corannulene rhodium complexes.[289] In their packing structure of in crystal, 1D polymer and 2D network structure were observed depending on the conditions of complexation[290–293] In the case of η^2-corannulene silver complexes reported by Siegel *et al.*, the crystal packing motif was changed by the counter anion.[294] With regards to both of the examples, the depth of the bowl was not changed by the metal-coordination, although the bond length of the metal-bound C=C bond was slightly elongated.

A family of organometallic complexes with sumanene as a ligand was developed by Amaya and Hirao *et al.*[295,296] The first sumanene complex reported in 2007 was cationic η^6-sumanene iron complex.[297] In contrast to the corannulene complex, the iron bound onto the

concave surface of the sumanene, and the bowl-depth was hardly changed by the coordination. The surface-selective coordination of the iron atom was investigated also by theoretical calculations.[298] Regarding to its ruthenium analogue, showing a longer metal-sumanene bond, both concave and convex conformation were observed.[299] There were an equilibrium between them, and the dynamic bowl-inversion behavior was studied. The authors also synthesized an iron complex possessing a chiral substituent on the Cp ligand, and investigated its dynamic behavior and chiroptical properties.[300]

Most recently, a zirconium complex possessing an η^5-sumanenyl ligand, and its trinuclear version were synthesized.[301] The zirconium atom(s) in the both mono- and trimetallic complexes bound to the convex surface of the sumanene. The bowl-depth got larger than free-sumanene.

1-6. The purpose of this study

A Cp ligand forms a stable metal–ligand bond with various metals (**1-1**). Meanwhile, helicene shows characteristic properties because of its large helical aromatic structure (**1-3**). A Cp complex bearing a helicene skeleton is expected to be a unique functional molecule involving an interaction between the metal's d-orbitals and the helical π-orbitals. However, the isolated optically-active helicene Cp complexes are limited to be the ones reported by Katz *et al.*, who pursued the research concentrating on the CD spectra and developed a redox-triggered switching system (**1-4-1**). There must be other possibilities of helicene Cp complexes with different structures. As seen in the case with organometallic complexes with other curved-π molecules (**1-5**), coordination-site-selectivity, structural change in the ligand caused by the complexation, and dynamic behaviors are also intriguing.

This PhD study focuses on the synthesis of organometallic complexes with [7]helicene

ligand(s) possessing a Cp moiety at the middle of its skeleton, aiming at development of novel functional molecules. A helicene Cp complex with a Cp ring incorporated in the central part of fused rings has never been isolated in an enantiopure form. In comparison with the inseparable [5]helicene metal complexes reported by Thiel *et al.* (**1-4-1**), [7]helicene metal complexes have extended helical structure, which will lead to more rigid chirality. In addition, not only the Cp moiety but also arene parts can act as coordination sites (**1-4-2**). Here in this thesis, three kinds of compounds are synthesized and their properties are investigated (Figure 1-27); complex **1** possesses one [7]helicene ligand and one iron or ruthenium atom, complex **2** is a monometallic bis-helicene complex, and complex **3** has two ruthenium atoms on one [7]helicene ligand. It is most notable in this thesis that the bimetallic complex **3** was found to exhibit strong phosphorescence. This is the first example of phosphorescent Cp complex (**1-2-3**), which shows a new direction of the Cp complexes serving as a photoluminescence material.

Figure 1-27. Synthesis of three kinds of [7]helicene metallocenes synthesized in this PhD study

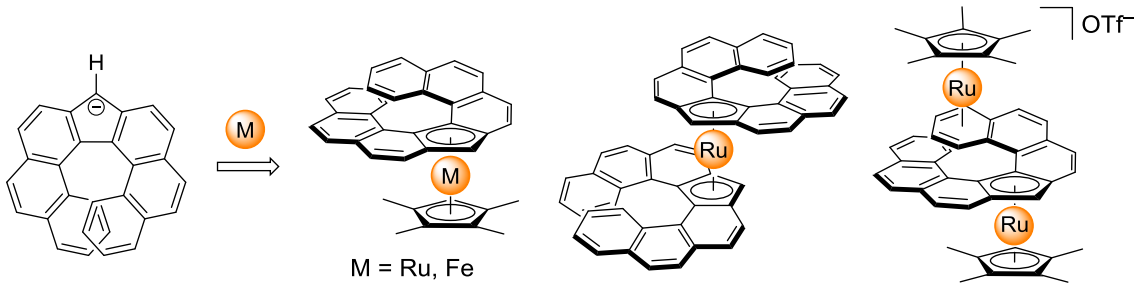

In the chapter 2, the synthesis of these complexes and resolution of their enantiomers are described. Their helical structures are discussed based on the x-ray single crystal structural analysis. The chapter 3 focuses on the isomerization behavior especially for bis-helicene complex

2. The kinetic and thermodynamic parameters are estimated, and the mechanism is investigated. In the chapter 4, electronic, optical, and chiroptical properties of the complexes are discussed based on both experimental and theoretical ways. The chapter 5 describes the unique phosphorescent property of bimetallic complex **3**.

1-7. References

(1) Kealy, T. J.; Pauson, P. L. *Nature* **1951**, *168*, 1039–1040.

(2) Wilkinson, G.; Rosenblum, M.; Whiting, M. C.; Woodward, R. B. *J. Am. Chem. Soc.* **1952**, *74*, 2125–2126.

(3) Fischer, E. O.; Pfab, W. *Z. Naturforsch. B* **1952**, *7b*, 377–379.

(4) Eiland, P. F.; Pepinsky, R. *J. Am. Chem. Soc.* **1952**, *74*, 4971–4971.

(5) DUNITZ, J. D.; ORGEL, L. E. *Nature* **1953**, *171*, 121–122.

(6) Dunitz, J. D.; Orgel, L. E. *J. Chem. Phys.* **1955**, *23*, 954.

(7) Jutzi, P.; Burford, N. *Chem. Rev.* **1999**, *99*, 969–990.

(8) Sapunov, V. N.; Kirchner, K.; Schmid, R. *Coord. Chem. Rev.* **2001**, *214*, 143–185.

(9) Arndt, S.; Okuda, J. *Chem. Rev.* **2002**, *102*, 1953–1976.

(10) Togni, A.; Hayashi, T. *Ferrocenes: Homogeneous Catalysis, Organic Synthesis, Materials Science*; Togni, A., Hayashi, T., Eds.; Wiley-VCH Verlag GmbH: Weinheim, Germany, 1994.

(11) Kaminsky, W. *Catal. Today* **1994**, *20*, 257–271.

(12) Crabtree, R. H. *The Organometallic Chemistry of the Transition Metals, 6th Edition*; WILEY-VCH Verlag, 2014.

(13) Hartwig, J. F. *Organotransition Metal Chemistry*; University Science Books: Sausalito, CA., 2010.

(14) Conley, B. L.; Pennington-Boggio, M. K.; Boz, E.; Williams, T. J. *Chem. Rev.* **2010**, *110*, 2294.

(15) Kusumoto, S.; Akiyama, M.; Nozaki, K. *J. Am. Chem. Soc.* **2013**, *135*, 18726–18729.

(16) Connelly, N. G.; Geiger, W. E. *Chem. Rev.* **1996**, *96*, 877–910.

(17) Muraoka, T.; Kinbara, K.; Aida, T. *Nature* **2006**, *440*, 512–515.

(18) Fukino, T.; Joo, H.; Hisada, Y.; Obana, M.; Yamagishi, H.; Hikima, T.; Takata, M.; Fujita, N.; Aida, T. *Science* **2014**, *344*, 499–504.

(19) Bunting, H. E.; Green, M. L. H.; Marder, S. R.; Thompson, M. E.; Bloor, D.; Kolinsky, P. V.; Jones, R. J. *Polyhedron* **1992**, *11*, 1489–1499.

(20) Biot, C.; Nosten, F.; Fraisse, L.; Ter-Minassian, D.; Khalife, J.; Dive, D. *Parasite* **2011**, *18*, 207.

(21) Debreczeni, J. É.; Bullock, A. N.; Atilla, G. E.; Williams, D. S.; Bregman, H.; Knapp, S.; Meggers, E. *Angew. Chem. Int. Ed.* **2006**, *45*, 1580–1585.

(22) Meggers, E.; Atilla-Gokcumen, G. E.; Bregman, H.; Maksimoska, J.; Mulcahy, S. P.; Pagano, N.; Williams, D. S. *Synlett* **2007**, No. 8, 1177–1189.

(23) Halterman, R. L. *Chem. Rev.* **1992**, *92*, 965–994.

(24) Moise, C.; Leblanc, J. C.; Tirouflet, J. *J. Am. Chem. Soc.* **1975**, *97*, 6272–6274.

(25) Leblanc, J. C.; Moise, C. *J. Organomet. Chem.* **1977**, *131*, 35–42.

(26) Couturier, S.; Gautheron, B. *J. Organomet. Chem.* **1978**, *157*, C61–C63.

(27) Cesarotti, E.; Kagan, H. B.; Goddard, R.; Krüger, C. *J. Organomet. Chem.* **1978**, *162*, 297–309.

(28) Cesarotti, E.; Chiesa, A.; Ciani, G. F.; Sironi, A.; Vefghi, R.; White, C. *J. Chem. Soc., Dalt. Trans.* **1984**, 653–661.

(29) Halterman, R. L.; Vollhardt, K. P. C. *Organometallics* **1988**, *7*, 883–892.

(30) Gutnov, A.; Drexler, H. J.; Spannenberg, A.; Oehme, G.; Heller, B. *Organometallics* **2004**, *23*, 1002–1009.

(31) Halterman, R. L.; Crow, L. D. *Tetrahedron Lett.* **2003**, *44*, 2907–2909.

(32) Gutnov, A.; Heller, B.; Drexler, H.-J.; Spannenberg, A.; Oehme, G. *Organometallics* **2003**, *22*, 1550–1553.

(33) Turner, Z. R.; Buffet, J.-C.; O'Hare, D. *Organometallics* **2014**, *33*, 3891–3903.

(34) McGlacken, G. P.; O'Brien, C. T.; Whitwood, A. C.; Fairlamb, I. J. S. *Organometallics* **2007**, *26*, 3722–3728.

(35) Colletti, S. L.; Halterman, R. L. *Tetrahedron Lett.* **1989**, *30*, 3513–3516.

(36) Colletti, S. L.; Halterman, R. L. *Organometallics* **1991**, *10*, 3438–3448.

(37) Colletti, S. L.; Halterman, R. L. *Organometallics* **1992**, *11*, 980–983.

(38) Schnutenhaus, H.; Brintzinger, H. H. *Angew. Chem. Int. Ed.* **1979**, *18*, 777–778.

(39) Wild, F. R. W. P.; Zsolnai, L.; Huttner, G.; Brintzinger, H. H. *J. Organomet. Chem.* **1982**, *232*, 233–247.

(40) LEDNICER, D.; HAUSER, C. R. *J. Org. Chem.* **1959**, *24*, 43–46.

(41) Thomson, J. *Tetrahedron Lett.* **1959**, *43*, 3–4.

(42) Aratani, T.; Gonda, T.; Nozaki, H. *Tetrahedron* **1970**, *26*, 5453–5464.

(43) Aratani, T.; Gonda, T.; Nozaki, H. *Tetrahedron Lett.* **1969**, *10*, 2265–2268.

(44) Marquarding, D.; Klusacek, H.; Gokel, G.; Hoffmann, P.; Ugi, I. *J. Am. Chem. Soc.* **1970**, *92*, 5389–5393.

(45) Price, D.; Simpkins, N. S. *Tetrahedron Lett.* **1995**, *36*, 6135–6136.

(46) Nishibayashi, Y.; Arikawa, Y.; Ohe, K.; Uemura, S. *J. Org. Chem.* **1996**, *61*, 1172–1174.

(47) Tsukazaki, M.; Tinkl, M.; Roglans, A.; Chapell, B. J.; Taylor, N. J.; Snieckus, V. *J. Am. Chem. Soc.* **1996**, *118*, 685–686.

(48) Arae, S.; Ogasawara, M. *Tetrahedron Lett.* **2015**, *56*, 1751–1761.

(49) Yamazaki, Y.; Uebayasi, M.; Hosono, K. *Eur. J. Biochem.* **1989**, *184*, 671–680.

(50) Siegel, S.; Schmalz, H. *... Chemie Int. Ed. English* **1997**, No. 22, 2456–2458.

(51) Bueno, A.; Rosol, M.; García, J.; Moyano, A. *Adv. Synth. Catal.* **2006**, *348*, 2590–2596.

(52) Ogasawara, M.; Watanabe, S.; Fan, L.; Nakajima, K.; Takahashi, T. *Organometallics* **2006**, *25*, 5201–5203.

(53) Ogasawara, M.; Watanabe, S.; Nakajima, K.; Takahashi, T. *Pure Appl. Chem.* **2008**, *80*, 1109.

(54) Ogasawara, M.; Watanabe, S.; Nakajima, K.; Takahashi, T. *J. Am. Chem. Soc.* **2010**, *132*, 2136.

(55) Ogasawara, M.; Arae, S.; Watanabe, S.; Nakajima, K.; Takahashi, T. *Chem. - Eur. J.* **2013**, *19*, 4151–4154.

(56) Tseng, Y.-Y.; Kamikawa, K.; Wu, Q.; Takahashi, T.; Ogasawara, M. *Adv. Synth. Catal.* **2015**, *357*, 2255–2264.

(57) Arae, S.; Nakajima, K.; Takahashi, T.; Ogasawara, M. *Organometallics* **2015**, *34*, 1197–1202.

(58) Ogasawara, M.; Arae, S.; Watanabe, S.; Nakajima, K.; Takahashi, T. *ACS Catal.* **2016**, *6*, 1308.

(59) Duan, W. L.; Imazaki, Y.; Shintani, R.; Hayashi, T. *Tetrahedron* **2007**, *63*, 8529–8536.

(60) Patti, A.; Pedotti, S. *Tetrahedron Asymmetry* **2010**, *21*, 2631–2637.

(61) Steffen, P.; Unkelbach, C.; Christmann, M.; Hiller, W.; Strohmann, C. *Angew. Chem. Int. Ed.* **2013**, *52*, 9836–9840.

(62) Pi, C.; Li, Y.; Cui, X.; Zhang, H.; Han, Y.; Wu, Y. *Chem. Sci.* **2013**, *4*, 2675.

(63) Gao, D.-W.; Shi, Y.-C.; Gu, Q.; Zhao, Z. Le; You, S.-L. *J. Am. Chem. Soc.* **2012**, *135*, 86–89.

(64) Alba, A. N.; Gómez-Sal, P.; Rios, R.; Moyano, A. *Tetrahedron Asymmetry* **2009**, *20*, 1314–1318.

(65) Akiyama, M.; Akagawa, K.; Seino, H.; Kudo, K. *Chem. Commun.* **2014**, *50*, 7893–7896.

(66) Akagawa, K.; Akiyama, M.; Kudo, K. *Eur. J. Org. Chem.* **2015**, *2015*, 3894–3898.

(67) Brunner, H. *Angew. Chem. Int. Ed.* **1969**, *8*, 382–383.

(68) Brunner, H.; Schindler, H.-D. *J. Organomet. Chem.* **1970**, *24*, C7–C10.

(69) Brunner, H. *Angew. Chem. Int. Ed.* **1999**, *38*, 1194–1208.

(70) Slugovc, C.; Simanko, W.; Mereiter, K.; Schmid, R.; Kirchner, K.; Xiao, L.; Weissensteiner, W. *Organometallics* **1999**, *18*, 3865–3872.

(71) Standfest-Hauser, C.; Slugovc, C.; Mereiter, K.; Schmid, R.; Kirchner, K.; Xiao, L.; Weissensteiner, W. *J. Chem. Soc. Dalt. Trans.* **2001**, *108*, 2989–2995.

(72) Evans, S.; Faller, J. W.; Parr, J. *J. Organomet. Chem.* **2003**, *674*, 56–62.

(73) Kataoka, Y.; Saito, Y.; Nagata, K.; Kitamura, K.; Shibahara, A.; Tani, K. *Chem. Lett.* **1995**, *24*, 833–834.

(74) Kataoka, Y.; Saito, Y.; Shibahara, A.; Tani, K. *Chem. Lett.* **1997**, *26*, 621–622.

(75) Kataoka, Y.; Shibahara, A.; Saito, Y.; Yamagata, T.; Tani, K. *Organometallics* **1998**, *17*, 4338.

(76) Kataoka, Y.; Iwato, Y.; Shibahara, A.; Yamagata, T.; Tani, K. *Chem. Commun.* **2000**, *428*, 841.

(77) Onitsuka, K.; Ajioka, Y.; Matsushima, Y.; Takahashi, S. *Organometallics* **2001**, *20*, 3274–3282.

(78) Kataoka, Y.; Nakagawa, Y.; Shibahara, A.; Yamagata, T.; Mashima, K.; Tani, K.

Organometallics **2004**, *23*, 2095–2099.

(79) Brunner, H.; Herrmann, W. A. *Chem. Ber.* **1972**, *105*, 3600–3610.

(80) Brunner, H.; Herrmann, W. A. *Angew. Chem. Int. Ed.* **1972**, *11*, 418–419.

(81) Resconi, L. *Angew. Chem. Int. Ed.* **2008**, *47*, 8155–8155.

(82) Kaminsky, W.; Külper, K.; Brintzinger, H. H.; Wild, F. R. W. P. *Angew. Chem. Int. Ed.* **1985**, *24*, 507–508.

(83) Liu, Z.; Somsook, E.; White, C. B.; Rosaaen, K. A.; Landis, C. R. *J. Am. Chem. Soc.* **2001**, *123*, 11193–11207.

(84) Brull, R.; Pasch, H.; Raubenheimer, H. G.; Sanderson, R.; Wahner, U. M. *J. Polym. Sci. Part A Polym. Chem.* **2000**, *38*, 2333–2339.

(85) Kaminsky, W.; Bark, A.; Spiehl, R.; Möller-Lindenhof, N.; Niedoba, S. In *Transition Metals and Organometallics as Catalysts for Olefin Polymerization*; Kaminsky, W., Sinn, H., Eds.; Springer Berlin Heidelberg: Berlin, Heidelberg, 1988; pp 291–301.

(86) Collins, S.; Kelly, W. M. *Macromolecules* **1992**, *25*, 233–237.

(87) Kelly, W. M.; Taylor, N. J.; Collins, S. *Macromolecules* **1994**, *27*, 4477–4485.

(88) Mark Kelly, W.; Wang, S.; Collins, S. *Macromolecules* **1997**, *9297*, 3151–3158.

(89) Kim, I.; Shin, Y. S.; Lee, J. K.; Won, M. S. *J. Polym. Sci. Part A Polym. Chem.* **2000**, *38*, 1520.

(90) Rodrigues, A.-S.; Kirillov, E.; Roisnel, T.; Razavi, A.; Vuillemin, B.; Carpentier, J.-F. *Angew. Chem. Int. Ed.* **2007**, *46*, 7240–7243.

(91) Gutnov, A.; Heller, B.; Fischer, C.; Drexler, H. J.; Spannenberg, A.; Sundermann, B.; Sundermann, C. *Angew. Chem. Int. Ed.* **2004**, *43*, 3795–3797.

(92) Hapke, M.; Kral, K.; Fischer, C.; Spannenberg, A.; Gutnov, A.; Redkin, D.; Heller, B. *J. Org. Chem.* **2010**, *75*, 3993–4003.

(93) Ye, B.; Cramer, N. *Science* **2012**, *338*, 504–506.

(94) Sortais, J. B.; Darcel, C. *ChemCatChem* **2013**, *5*, 1067–1068.

(95) Ye, B.; Cramer, N. *J. Am. Chem. Soc.* **2013**, *135*, 636–639.

(96) Newton, C. G.; Kossler, D.; Cramer, N. *J. Am. Chem. Soc.* **2016**, *138*, 3935–3941.

(97) Ye, B.; Cramer, N. *Angew. Chem. Int. Ed.* **2014**, *53*, 7896–7899.

(98) Ye, B.; Cramer, N. *Acc. Chem. Res.* **2015**, *48*, 1308–1318.

(99) Ye, B.; Cramer, N. *Synlett* **2015**, *26*, 1490–1495.

(100) Zheng, J.; Cui, W. J.; Zheng, C.; You, S. L. *J. Am. Chem. Soc.* **2016**, *138*, 5242–5245.

(101) Pham, M. V.; Cramer, N. *Chemistry* **2016**, *22*, 2270–2273.

(102) Reddy Chidipudi, S.; Burns, D. J.; Khan, I.; Lam, H. W. *Angew. Chem. Int. Ed.* **2015**, *54*, 13975–13979.

(103) Dieckmann, M.; Jang, Y. S.; Cramer, N. *Angew. Chem. Int. Ed.* **2015**, *54*, 12149–12152.

(104) Kossler, D.; Cramer, N. *J. Am. Chem. Soc.* **2015**, *137*, 12478–12481.

(105) Song, G.; O, W. W. N.; Hou, Z. *J. Am. Chem. Soc.* **2014**, *136*, 12209–12212.

(106) Hayashi, T.; Kumada, M. *Acc. Chem. Res.* **1982**, *15*, 395–401.

(107) Barbaro, P.; Bianchini, C.; Giambastiani, G.; Parisel, S. L. *Coord. Chem. Rev.* **2004**, *248*, 2131–2150.

(108) Gómez Arrayás, R.; Adrio, J.; Carretero, J. C. *Angew. Chem. Int. Ed.* **2006**, *45*, 7674–7715.

(109) Hierso, J. C.; Smaliy, R.; Amardeil, R.; Meunier, P. *Chem. Soc. Rev.* **2007**, *36*, 1754–1769.

(110) Miyake, Y.; Nishibayashi, Y.; Uemura, S. *Synlett* **2008**, No. 12, 1747–1758.

(111) Shintani, R.; Lo, M. M.; Fu, G. C. *Tetrahedron* **2000**, No. 5, 1997–1999.

(112) Ruble, J. C.; Latham, H. A.; Fu, G. C. *J. Am. Chem. Soc.* **1997**, *119*, 1492–1493.

(113) Evans, R. C.; Douglas, P.; Winscom, C. J. *Coord. Chem. Rev.* **2006**, *250*, 2093–2126.

(114) Lowry, M. S.; Bernhard, S. *Chem. - Eur. J.* **2006**, *12*, 7970–7977.

(115) Chou, P.-T.; Chi, Y. *Chemistry* **2007**, *13*, 380–395.

(116) Zhao, J.; Wu, W.; Sun, J.; Guo, S. *Chem. Soc. Rev.* **2013**, *42*, 5323.

(117) Thompson, M. *MRS Bull.* **2007**, *32*, 694–701.

(118) Lees, A. J. *Chem. Rev.* **1987**, *87*, 711–743.

(119) Vogler, A.; Kunkely, H. *Coord. Chem. Rev.* **2001**, *211*, 223–233.

(120) Yam, V. W.-W.; Lo, K. K.-W. *Chem. Soc. Rev.* **1999**, *28*, 323–334.

(121) Strohmeier, W. *Angew. Chem. Int. Ed.* **1964**, *3*, 730–737.

(122) Wrighton, M. *Chem. Rev.* **1974**, *74*, 401–430.

(123) Sacksteder, L.; Lee, M. *J. Am. Chem. Soc.* **1993**, *115*, 8230–8238.

(124) Yam, V. W.; Lau, V. C.-Y.; Cheung, K.-K. *Organometallics* **1995**, *14*, 2749–2753.

(125) Adamson, A. W.; Demas, J. N. *J. Am. Chem. Soc.* **1971**, *93*, 1800–1801.

(126) Gafney, H.; Adamson, A. *J. Am. Chem. Soc.* **1972**, *94*, 8238–8239.

(127) Juris, A.; Balzani, V.; Barigelletti, F.; Campagna, S.; Belser, P.; von Zelewsky, A. *Coord. Chem. Rev.* **1988**, *84*, 85–277.

(128) Fanni, S.; Keyes, T. E.; O'Connor, C. M.; Hughes, H.; Wang, R.; Vos, J. G. *Coord. Chem. Rev.* **2000**, *208*, 77–86.

(129) Shan, B. Z.; Zhao, Q.; Goswami, N.; Eichhorn, D. M.; Rillema, D. P. *Coord. Chem. Rev.* **2001**, *211*, 117–144.

(130) Kim, H. B.; Kitamura, N.; Tazuke, S. *J. Phys. Chem.* **1990**, *94*, 1414–1418.

(131) Cannizzo, A.; Van Mourik, F.; Gawelda, W.; Zgrablic, G.; Bressler, C.; Chergui, M. *Angew. Chem. Int. Ed.* **2006**, *45*, 3174–3176.

(132) Sun, Y.; Hudson, Z. M.; Rao, Y.; Wang, S. *Inorg. Chem.* **2011**, *50*, 3373–3378.

(133) Harrigan, R. W.; Hager, G. D.; Crosby, G. A. *Chem. Phys. Lett.* **1973**, *21*, 487–490.

(134) Felix, F.; Ferguson, J.; Güdel, H. U.; Ludi, A. *Chem. Phys. Lett.* **1979**, *62*, 153–157.

(135) Islam, A.; Ikeda, N.; Nozaki, K.; Ohno, T. *Chem. Phys. Lett.* **1996**, *263*, 209–214.

(136) Kober, E. M.; Meyer, T. J. *Inorg. Chem.* **1982**, *21*, 3967–3977.

(137) Kober, E. M.; Meyer, T. J. *Inorg. Chem.* **1984**, *23*, 3877–3886.

(138) Daul, C.; Baerends, E. J.; Vernooijs, P. *Inorg. Chem.* **1994**, *33*, 3538–3543.

(139) Xu, L.-C.; Li, J.; Shi, S.; Zheng, K.-C.; Ji, L.-N. *J. Mol. Struct.: THEOCHEM* **2008**, *855*, 77–81.

(140) Chi, Y.; Chou, P.-T. *Chem. Soc. Rev.* **2007**, *36*, 1421.

(141) Tung, Y.-L.; Lee, S.-W.; Chi, Y.; Chen, L.-S.; Shu, C.-F.; Wu, F.-I.; Carty, A. J.; Chou, P.-T.; Peng, S.-M.; Lee, G.-H. *Adv. Mater.* **2005**, *17*, 1059–1064.

(142) Tung, Y.-L.; Chen, L.-S.; Chi, Y.; Chou, P.-T.; Cheng, Y.-M.; Li, E. Y.; Lee, G.-H.; Shu, C.-F.; Wu, F.-I.; Carty, A. J. *Adv. Funct. Mater.* **2006**, *16*, 1615–1626.

(143) Kober, E. M.; Sullivan, B. P.; Dressick, W. J.; Caspar, J. V; Meyer, T. J. *J. Am. Chem. Soc.* **1980**, *102*, 7383–7385.

(144) Vogler, L. M.; Jones, S. W.; Jensen, G. E.; Gary Brewer, R.; Brewer, K. J. *Inorg. Chim. Acta* **1996**, *250*, 155–162.

(145) Carlson, B.; Phelan, G. D.; Kaminsky, W.; Dalton, L.; Jiang, X.; Liu, S.; Jen, A. K. Y. *J. Am. Chem. Soc.* **2002**, *124*, 14162–14172.

(146) Flynn, C. M.; Demas, J. N. *J. Am. Chem. Soc.* **1974**, *96*, 1959–1960.

(147) Watts, R. J.; Harrington, J. S.; Houten, J. Van. *J. Am. Chem. Soc.* **1977**, *99*, 2179–2187.

(148) Lamansky, S.; Djurovich, P.; Murphy, D.; Abdel-Razzaq, F.; Lee, H. E.; Adachi, C.; Burrows, P. E.; Forrest, S. R.; Thompson, M. E. *J. Am. Chem. Soc.* **2001**, *123*, 4304–4312.

(149) Nozaki, K.; Takamori, K.; Nakatsugawa, Y.; Ohno, T. *Inorg. Chem.* **2006**, *45*, 6161–6178.

(150) Wallace, L.; Heath, G. A.; Krausz, E.; Moran, G. *Inorg. Chem.* **1991**, *30*, 347–349.

(151) Hwang, F. M.; Chen, H. Y.; Chen, P. S.; Liu, C. S.; Chi, Y.; Shu, C. F.; Wu, F. I.; Chou, P. T.; Peng, S. M.; Lee, G. H. *Inorg. Chem.* **2005**, *44*, 1344–1353.

(152) Nozaki, K. *J. Chin. Chem. Soc.* **2006**, *53*, 101–112.

(153) Zelewsky, A. Von. *J. Am. Chem. Soc.* **1987**, *109*, 7720–7724.

(154) Barigelletti, F.; Sandrini, D.; Maestri, M.; Balzani, V.; Von Zelewsky, A.; Chassot, L.; Jolliet, P.; Maeder, U. *Inorg. Chem.* **1988**, *27*, 3644–3647.

(155) Barbieri, A.; Accorsi, G.; Armaroli, N. *Chem. Commun.* **2008**, No. 19, 2185.

(156) Krylova, V. A.; Djurovich, P. I.; Aronson, J. W.; Haiges, R.; Whited, M. T.; Thompson, M. E. *Organometallics* **2012**, *31*, 7983–7993.

(157) Morgante, C. G.; Struve, W. S. *Chem. Phys. Lett.* **1980**, *69*, 56–60.

(158) Wrighton, M. S.; Pdungsap, L.; Morse, D. L. *J. Phys. Chem.* **1975**, *79*, 66–71.

(159) Riesen, H.; Krausz, E.; Luginbühl, W.; Biner, M.; Güdel, H. U.; Ludi, A. *J. Chem. Phys.* **1992**, *96*, 4131.

(160) Hollingsworth, G. J.; Shin, K. S. K.; Zink, J. I. *Inorg. Chem.* **1990**, *29*, 2501–2506.

(161) Cahn, R. S.; Ingold, C.; Prelog, V. *Angew. Chem. Int. Ed.* **1966**, *5*, 385–415.

(162) Meisenheimer, J.; Witte, K. *Ber. Dtsch. Chem. Ges.* **1903**, *36*, 4153–4164.

(163) Weitzenbock, R.; Klingler, A. *Monatshefte für Chemie* **1918**, *39*, 315–323.

(164) Dischendorfer, O. *Monatshefte für Chemie* **1939**, *73*, 45–56.

(165) Newman, M. S. *J. Am. Chem. Soc.* **1940**, *62*, 1683–1687.

(166) Newman, M. S.; Wheatley, W. B. *J. Am. Chem. Soc.* **1948**, *70*, 1913–1916.

(167) Newman, M. S.; Lutz, W. B.; Lednicer, D. *J. Am. Chem. Soc.* **1955**, *77*, 3420–3421.

(168) Gingras, M. *Chem. Soc. Rev.* **2013**, *42*, 968–1006.

(169) Gingras, M.; Felix, G.; Peresutti, R.; Félix, G.; Peresutti, R.; Felix, G.; Peresutti, R. *Chem. Soc. Rev.* **2013**, *42*, 1007–1050.

(170) Newman, M. S.; Lednicer, D. *J. Am. Chem. Soc.* **1956**, *78*, 4765–4770.

(171) Scholz, F. D. M. *Tetrahedron* **1968**, *24*, 6845–6849.

(172) Scholz, M.; Mühlstädt, M.; Dietz, F. *Tetrahedron Lett.* **1967**, *7*, 665–668.

(173) Liu, L.; Katz, T. J. *Tetrahedron Lett.* **1990**, *31*, 3983–3986.

(174) Mori, K.; Murase, T.; Fujita, M. *Angew. Chem. Int. Ed.* **2015**, *54*, 6847–6851.

(175) Schulman, J. M.; Disch, R. L. *J. Phys. Chem. A* **1999**, *103*, 6669–6672.

(176) Shen, Y.; Chen, C.-F. *Chem. Rev.* **2012**, *112*, 1463–1535.

(177) Dova, D.; Cauteruccio, S.; Prager, S.; Dreuw, A.; Graiff, C.; Licandro, E. *J. Org. Chem.* **2015**, *80*, 3921–3928.

(178) Nakano, K.; Hidehira, Y.; Takahashi, K.; Hiyama, T.; Nozaki, K. *Angew. Chem. Int. Ed.* **2005**, *44*, 7136–7138.

(179) Goto, K.; Yamaguchi, R.; Hiroto, S.; Ueno, H.; Kawai, T.; Shinokubo, H. *Angew. Chem. Int. Ed.* **2012**, *51*, 10333–10336.

(180) Nakano, K.; Oyama, H.; Nishimura, Y.; Nakasako, S.; Nozaki, K. *Angew. Chem. Int. Ed.* **2012**, *51*, 695–699.

(181) Staab, H. A.; Diehm, M.; Krieger, C. *Tetrahedron Lett.* **1994**, *35*, 8357–8360.

(182) Takenaka, N.; Sarangthem, R. S.; Captain, B. *Angew. Chem. Int. Ed.* **2008**, *47*, 9708–9710.

(183) Míšek, J.; Teplý, F.; Stará, I. G.; Tichý, M.; Šaman, D.; Císařová, I.; Vojtíšek, P.; Starý, I. *Angew. Chem. Int. Ed.* **2008**, *47*, 3188–3191.

(184) Nakamura, K.; Furumi, S.; Takeuchi, M.; Shibuya, T.; Tanaka, K. *J. Am. Chem. Soc.* **2014**, *136*, 5555–5558.

(185) Tanaka, M.; Shibata, Y.; Nakamura, K.; Teraoka, K.; Uekusa, H.; Nakazono, K.; Takata, T.; Tanaka, K. *Chem. - Eur. J.* **2016**, *22*, 9537–9541.

(186) Rajca, A.; Rajca, S. *Angew. Chem. Int. Ed.* **2000**, *39*, 4481–4483.

(187) Rajca, A.; Miyasaka, M.; Pink, M.; Wang, H.; Rajca, S. *J. Am. Chem. Soc.* **2004**, *126*, 15211.

(188) Shen, Y.; Chen, C.; Reactions, D. À. A.; Reactions, F. À. C.; Cyclizations, M. *Chem. Rev.* **2012**, *112*, 1463–1535.

(189) Kashihara, H.; Asada, T.; Kamikawa, K. *Chem. - Eur. J.* **2015**, *21*, 6523–6527.

(190) Takao Fujikawa; Yasutomo Segawa; Kenichiro Itami. *J. Am. Chem. Soc.* **2015**, *137*, 7763–7768.

(191) Wang, X.-Y.; Wang, X.-C.; Narita, A.; Wagner, M.; Cao, X.-Y.; Feng, X.; Müllen, K. *J. Am. Chem. Soc.* **2016**, *138*, 12783–12786.

(192) Fujikawa, T.; Segawa, Y.; Itami, K. *J. Am. Chem. Soc.* **2016**, *138*, 3587–3595.

(193) Bachrach, S. M. *Chem. Phys. Lett.* **2016**, *666*, 13–18.

(194) Severa, L.; Adriaenssens, L.; Vávra, J.; Šaman, D.; Císařová, I.; Fiedler, P.; Teplý, F. *Tetrahedron* **2010**, *66*, 3537–3552.

(195) Vávra, J.; Severa, L.; Císařová, I.; Klepetářová, B.; Šaman, D.; Koval, D.; Kašička, V.; Teplý, F. *J. Org. Chem.* **2013**, *78*, 1329–1342.

(196) Čížková, M.; Šaman, D.; Koval, D.; Kašička, V.; Klepetářová, B.; Císařová, I.; Teplý, F. *Eur. J. Org. Chem.* **2014**, *2014*, 5681–5685.

(197) Pospíšil, L.; Bednárová, L.; Štěpánek, P.; Slavíček, P.; Vávra, J.; Hromadová, M.; Dlouhá, H.; Tarábek, J.; Teplý, F. *J. Am. Chem. Soc.* **2014**, *136*, 10826–10829.

(198) Li, M.; Niu, Y.; Zhu, X.; Peng, Q.; Lu, H.-Y.; Xia, A.; Chen, C.-F. *Chem. Commun.* **2014**, *50*.

(199) Li, M.; Yao, W.; Chen, J.-D.; Lu, H.-Y.; Zhao, Y.; Chen, C.-F. *J. Mater. Chem. C* **2014**, *2*, 8373.

(200) Oyama, H.; Akiyama, M.; Nakano, K.; Naito, M.; Nobusawa, K.; Nozaki, K. *Org. Lett.* **2016**, *18*, 3654–3657.

(201) Oyama, H.; Nakano, K.; Harada, T.; Kuroda, R.; Naito, M.; Nobusawa, K.; Nozaki, K. *Org. Lett.* **2013**, *15*, 2104–2107.

(202) Shibata, T.; Uchiyama, T.; Yoshinami, Y.; Takayasu, S.; Tsuchikama, K.; Endo, K. *Chem. Commun.* **2012**, *48*, 1311.

(203) Murayama, K.; Oike, Y.; Furumi, S.; Takeuchi, M.; Noguchi, K.; Tanaka, K. *Eur. J. Org. Chem.* **2015**, *2015*, 1409–1414.

(204) Sehnal, P.; Stara, I. G.; David, S.; Chocholous, J. *Proc. Natl. Acad. Sci. U. S. A.* **2009**, *106*, 17605–17605.

(205) Tanaka, K.; Fukawa, N.; Suda, T.; Noguchi, K. *Angew. Chem. Int. Ed.* **2009**, *48*, 5470–5473.

(206) Kimura, Y.; Fukawa, N.; Miyauchi, Y.; Noguchi, K.; Tanaka, K. *Angew. Chem. Int. Ed.* **2014**, *53*, 8480–8483.

(207) Kötzner, L.; Webber, M. J.; Martínez, A.; De Fusco, C.; List, B. *Angew. Chem. Int. Ed.* **2014**, *53*, 5202–5205.

(208) Sawada, Y.; Furumi, S.; Takai, A.; Takeuchi, M.; Noguchi, K.; Tanaka, K. *J. Am. Chem. Soc.* **2012**, *134*, 4080–4083.

(209) Goedicke, C.; Stegemeyer, H. *Tetrahedron Lett.* **1970**, *11*, 937–940.

(210) Martin, R. H.; Marchant, M. J. *Tetrahedron* **1974**, *30*, 343–345.

(211) Janke, R. H.; Haufe, G.; W??rthwein, E. U.; Borkent, J. H. *J. Am. Chem. Soc.* **1996**, *118*, 6031.

(212) Martin, R. H.; Marchant, M. J. J. *Tetrahedron* **1974**, *30*, 347–349.

(213) Grimme, S.; Peyerimhoff, S. D. *Chem. Phys.* **1996**, *204*, 411–417.

(214) Lebon, F.; Longhi, G.; Gangemi, F.; Abbate, S.; Priess, J.; Juza, M.; Bazzini, C.; Caronna, T.; Mele, A. *J. Phys. Chem. A* **2004**, *108*, 11752–11761.

(215) M. B. Groen H. Wynberg, H. S. *J. Org. Chem.* **1971**, *36*, 2968–2974.

(216) Furche, F.; Ahlrichs, R.; Wachsmann, C.; Weber, E.; Sobanski, A.; Vogtle, F.; Grimme, S. *J. Am. Chem. Soc.* **2000**, *122*, 1717–1724.

(217) Grimme, S.; Harren, J.; Sobanski, A.; Vögtle, F. *Eur. J. Org. Chem.* **1998**, *1998*, 1491–1509.

(218) Nakai, Y.; Mori, T.; Inoue, Y. *J. Phys. Chem. A* **2012**, *116*, 7372–7385.

(219) Nakai, Y.; Mori, T.; Inoue, Y. *J. Phys. Chem. A* **2013**, *117*, 83–93.

(220) Nakai, Y.; Mori, T.; Sato, K.; Inoue, Y. *J. Phys. Chem. A* **2013**, *117*, 5082–5092.

(221) Gingras, M. *Chem. Soc. Rev.* **2013**, *42*, 1051–1095.

(222) Nakazaki, M.; Yamamoto, K.; Ikeda, T.; Kitsuki, T.; Okamoto, Y. *J. Chem. Soc., Chem. Commun.* **1983**, No. 7, 787–788.

(223) Yamamoto, K.; Ikeda, T.; Kitsuki, T.; Okamoto, Y.; Chikamatsu, H.; Nakazaki, M. *J. Chem. Soc. Perkin Trans. 1* **1990**, No. 2, 271.

(224) Deshayes, K.; Broene, R. D.; Chao, I.; Knobler, C. B.; Diederich, F. *J. Org. Chem.* **1991**, *56*, 6787–6795.

(225) Owens, L.; Thilgen, C.; Diederich, F.; Knobler, C. B. *Helv. Chim. Acta* **1993**, *76*, 2757–2774.

(226) Chemie, O.; Zürich, C.-. *J. Chem. Soc., Perkin Trans. 2* **1998**, 747–761.

(227) Kano, K.; Negi, S.; Kamo, H.; Kitae, T.; Yamaguchi, M.; Okubo, H.; Hirama, M. *Chem. Lett.* **1998**, *27*, 151–152.

(228) Kano, K.; Kamo, H.; Negi, S.; Kitae, T.; Takaoka, R.; Yamaguchi, M.; Okubo, H.; Hirama, M. *J. Chem. Soc. Perkin Trans. 2* **1999**, No. 1, 15–22.

(229) Amemiya, R.; Yamaguchi, M. *Org. Biomol. Chem.* **2008**, *6*, 26–35.

(230) Aillard, P.; Voituriez, A.; Marinetti, A. *Dalton Trans.* **2014**, *43*, 15263–15278.

(231) Reetz, M. T.; Beuttenm̈ller, E. W.; Goddard, R. *Tetrahedron Lett.* **1997**, *38*, 3211–3214.

(232) Marinetti, A.; Aillard, P.; Voituriez, A.; Marinetti, A. *Dalton Trans.* **2014**, *43*, 15263–15278.

(233) Šámal, M.; Míšek, J.; Stará, I. G.; Starý, I. *Collect. Czech. Chem. Commun.* **2009**, *74*, 1151–1159.

(234) Sato, I.; Yamashima, R.; Kadowaki, K.; Yamamoto, J.; Shibata, T.; Soai, K. *Angew. Chem. Int. Ed.* **2001**, *40*, 1096–1098.

(235) Sapir, M.; Donckt, E. V. *Chem. Phys. Lett.* **1975**, *36*, 108–110.

(236) Hassey, R.; Swain, E. J.; Hammer, N. I.; Venkataraman, D.; Barnes, M. D. *Science* **2006**, *314*, 1437–1439.

(237) Kaseyama, T.; Furumi, S.; Zhang, X.; Tanaka, K.; Takeuchi, M. *Angew. Chem. Int. Ed.* **2011**, *50*, 3684–3687.

(238) Yamamoto, Y.; Sakai, H.; Yuasa, J.; Araki, Y.; Wada, T.; Sakanoue, T.; Takenobu, T.; Kawai, T.; Hasobe, T. *Chem. - Eur. J.* **2016**, 4263–4273.

(239) Li, M.; Lu, H.-Y.; Zhang, C.; Shi, L.; Tang, Z.; Chen, C.-F. *Chem. Commun.* **2016**, *5*, 4–7.

(240) Li, M.; Feng, L.-H.; Lu, H.-Y.; Wang, S.; Chen, C.-F. *Adv. Funct. Mater.* **2014**, *24*, 4405–4412.

(241) Li, M.; Li, X.-J.; Lu, H.-Y.; Chen, C.-F. *Sens. Actuators, B* **2014**, *202*, 583–587.

(242) Nuckolls, C.; Katz, T. J. *J. Am. Chem. Soc.* **1998**, *120*, 9541–9544.

(243) Vyklický, L.; Eichhorn, S. H.; Katz, T. J. *Chem. Mater.* **2003**, *15*, 3594–3601.

(244) Verbiest, T.; Sioncke, S.; Persoons, A.; Vyklický, L.; Katz, T. J. *Angew. Chem. Int. Ed.* **2002**, *41*, 3882–3884.

(245) Nuckolls, C.; Shao, R.; Jang, W. G.; Clark, N. A.; Walba, D. M.; Katz, T. J. *Chem. Mater.* **2002**, *14*, 773–776.

(246) Pieraccini, S.; Ferrarini, A.; Spada, G. P. *Chirality* **2008**, *20*, 749–759.

(247) Gold, V. *Compendium of Chemical Terminology Gold Book*; Wilkinson, A., McNaught, A. D., Eds.; IUPAC: Research Triagle Park, NC, 2014.

(248) Verbiest, T.; Elshocht, S. Van; Kauranen, M.; Hellemans, L.; Snauwaert, J.; Nuckolls, C.; Katz, T. J.; Persoons, A. *Science* **1998**, *282*, 913–915.

(249) Fox, J. M.; Katz, T. J.; Van Elshocht, S.; Verbiest, T.; Kauranen, M.; Persoons, A.; Thongpanchang, T.; Krauss, T.; Brus, L. *J. Am. Chem. Soc.* **1999**, *121*, 3453–3459.

(250) Kelly, T. R.; Merkert, E. F. *Acc. Chem. Res.* **2001**, *34*, 514–522.

(251) Kelly, T. R.; De Silva, H.; Silva, R. a. *Nature* **1999**, *401*, 150–152.

(252) Saleh, N.; Shen, C.; Crassous, J. *Chem. Sci.* **2014**, *5*, 3680.

(253) Katz, T. J.; Slusarek, W. *J. Am. Chem. Soc.* **1979**, *101*, 4259–4267.

(254) Katz, T. J.; Pesti, J. *J. Am. Chem. Soc.* **1982**, *104*, 346–347.

(255) Sudhakar, A.; Katz, T. J. *J. Am. Chem. Soc.* **1986**, *108*, 179–181.

(256) Gilbert, A. M.; Katz, T. J.; Geiger, W. E.; Robben, M. P.; Rheingold, A. L. *J. Am. Chem. Soc.* **1993**, *115*, 3199–3211.

(257) Sudhakar, A.; Katz, T. J.; Yang, B. W. *J. Am. Chem. Soc.* **1986**, *108*, 2790–2791.

(258) Katz, T. J.; Sudhakar, A.; Teasley, M. F.; Gilbert, A. M.; Geiger, W. E.; Robben, M. P.; Wuensch, M.; Ward, M. D. *J. Am. Chem. Soc.* **1993**, *115*, 3182–3198.

(259) Pammer, F.; Sun, Y.; Sieger, M.; Fiedler, J.; Sarkar, B.; Thiel, W. R. *Organometallics* **2010**, *29*, 6165–6168.

(260) Pammer, F.; Sun, Y.; Pagels, M.; Weismann, D.; Sitzmann, H.; Thiel, W. R. *Angew. Chem. Int. Ed.* **2008**, *47*, 3271–3274.

(261) Pammer, F.; Sun, Y.; May, C.; Wolmershäuser, G.; Kelm, H.; Krüger, H.-J.; Thiel, W. R. *Angew. Chem. Int. Ed.* **2007**, *46*, 1270–1273.

(262) Pammer, F.; Sun, Y.; Thiel, W. R. *Inorg. Chim. Acta* **2011**, *374*, 205–210.

(263) Pammer, F.; Sun, Y.; Thiel, W. R. *Organometallics* **2008**, *27*, 1015–1018.

(264) Latorre, A.; Urbano, A.; Carreño, M. C. *Chem. Commun.* **2011**, *47*, 8103–8105.

(265) Álvarez, C. M.; Barbero, H.; García-Escudero, L. A.; Martín-Alvarez, J. M.; Martínez-Pérez, C.; Miguel, D. *Inorg. Chem.* **2012**, *51*, 8103–8111.

(266) Norel, L.; Rudolph, M.; Vanthuyne, N.; Gareth Williams, J. A.; Lescop, C.; Roussel, C.; Autschbach, J.; Crassous, J.; Réau, R. *Angew. Chem. Int. Ed.* **2010**, *49*, 99–102.

(267) Anger, E.; Rudolph, M.; Shen, C.; Vanthuyne, N.; Toupet, L. L.; Roussel, C.; Autschbach, J.; Crassous, J.; Réau, R.; Réau, R. *J. Am. Chem. Soc.* **2011**, *133*, 3800–3803.

(268) Anger, E.; Rudolph, M.; Norel, L.; Zrig, S.; Shen, C.; Vanthuyne, N.; Toupet, L.; Williams, J. A. G.; Roussel, C.; Autschbach, J.; Crassous, J.; Réau, R. *Chem. - Eur. J.* **2011**, *17*, 14178–14198.

(269) Shen, C.; Anger, E.; Srebro, M.; Vanthuyne, N.; Deol, K. K.; Jefferson, T. D.; Muller, G.; Williams, J. A. G.; Toupet, L.; Roussel, C.; Autschbach, J.; Réau, R.; Crassous, J. *Chem. Sci.* **2014**, *5*, 1915.

(270) Brandt, J. R.; Wang, X.; Yang, Y.; Campbell, A. J.; Fuchter, M. J. *J. Am. Chem. Soc.* **2016**, *138*, 9743–9746.

(271) Crespo, O.; Eguillor, B.; Esteruelas, M. a; Fernández, I.; García-Raboso, J.; Gómez-Gallego, M.; Martín-Ortiz, M.; Oliván, M.; Sierra, M. a. *Chem. Commun.* **2012**, *48*, 5328–5330.

(272) Anger, E.; Srebro, M.; Vanthuyne, N.; Roussel, C.; Toupet, L.; Autschbach, J.; Réau, R.; Crassous, J. *Chem. Commun.* **2014**, *50*, 2854.

(273) Anger, E.; Srebro, M.; Vanthuyne, N.; Toupet, L.; Rigaut, S.; Roussel, C.; Autschbach, J.; Crassous, J.; Réau, R. *J. Am. Chem. Soc.* **2012**, *134*, 15628–15631.

(274) Shen, C.; Loas, G.; Srebro-Hooper, M.; Vanthuyne, N.; Toupet, L.; Cador, O.; Paul, F.; López Navarrete, J. T.; Ramírez, F. J.; Nieto-Ortega, B.; Casado, J.; Autschbach, J.; Vallet, M.; Crassous, J. *Angew. Chem. Int. Ed.* **2016**, *55*, 8062–8066.

(275) Rose-Munch, F.; Li, M.; Rose, E.; Daran, J. C.; Bossi, A.; Licandro, E.; Mussini, P. R. *Organometallics* **2012**, *31*, 92–104.

(276) Nakamura, E. *J. Organomet. Chem.* **2004**, *689*, 4630–4635.

(277) Sawamura, M.; Iikura, H.; Ohama, T.; Hackler, U. E.; Nakamura, E. *J. Organomet. Chem.* **2000**, *599*, 32–36.

(278) Sawamura, M.; Toganoh, M.; Kuninobu, Y.; Kato, S.; Nakamura, E. *Chem. Lett.* **2000**, *29*, 270.

(279) Sawamura, M.; Kuninobu, Y.; Toganoh, M.; Matsuo, Y.; Yamanaka, M.; Nakamura, E. *J. Am. Chem. Soc.* **2002**, *124*, 9354–9355.

(280) Matsuo, Y.; Kuninobu, Y.; Ito, S.; Nakamura, E. *Chem. Lett.* **2004**, *33*, 68–69.

(281) Toganoh, M.; Matsuo, Y.; Nakamura, E. *J. Organomet. Chem.* **2003**, *683*, 295–300.

(282) Petrukhina, M. a; Scott, L. T. *Dalton Trans.* **2005**, No. 18, 2969–2975.

(283) Wu, Y.-T.; Siegel, J. S. *Chem. Rev.* **2006**, *106*, 4843–4867.

(284) Seiders, T. J.; Baldridge, K. K.; O'Connor, J. M.; Siegel, J. S. *J. Am. Chem. Soc.* **1997**, *119*, 4781–4782.

(285) Siegel, J. S.; Baldridge, K. K.; Linden, A.; Dorta, R. *J. Am. Chem. Soc.* **2006**, *128*, 10644–10645.

(286) Alvarez, C. M.; Angelici, R. J.; Sygula, A.; Sygula, R.; Rabideau, P. W. *Organometallics* **2003**, *22*, 624–626.

(287) Vecchi, P. A.; Alvarez, C. M.; Ellern, A.; Angelici, R. J.; Sygula, A.; Sygula, R.; Rabideau, P. W. *Angew. Chem. Int. Ed.* **2004**, *43*, 4497–4500.

(288) Vecchi, P. A.; Alvarez, C. M.; Ellern, A.; Angelici, R. J.; Sygula, A.; Sygula, R.; Rabideau, P. W. *Organometallics* **2005**, *24*, 4543–4552.

(289) Petrukhina, M. A.; Andreini, K. W.; Mack, J.; Scott, L. T. *Angew. Chem. Int. Ed.* **2003**, *42*, 3375.

(290) Petrukhina, M. A.; Andreini, K. W.; Tsefrikas, V. M.; Scott, L. T. *Organometallics* **2005**, *24*, 1394–1397.

(291) Petrukhina, M. A.; Andreini, K. W.; Peng, L.; Scott, L. T. *Angew. Chem. Int. Ed.* **2004**, *43*, 5477.

(292) Petrukhina, M. A.; Sevryugina, Y.; Rogachev, A. Y.; Jackson, E. A.; Scott, L. T. *Angew. Chem. Int. Ed.* **2006**, *45*, 7208–7210.

(293) Petrukhina, M. A.; Sevryugina, Y.; Rogachev, A. Y.; Jackson, E. A.; Scott, L. T. *Organometallics* **2006**, *25*, 5492–5495.

(294) Elliott, E. L.; Hernández, G. A.; Linden, A.; Siegel, J. S. *Org. Biomol. Chem.* **2005**, *3*, 407–413.

(295) Amaya, T.; Hirao, T. *Chem. Commun.* **2011**, *47*, 10524–10535.

(296) Amaya, T.; Hirao, T. *Chem. Rec.* **2014**, 310–321.

(297) Amaya, T.; Sakane, H.; Hirao, T. *Angew. Chem. Int. Ed.* **2007**, *46*, 8376–8379.

(298) Okumura, M.; Nakanishi, Y.; Kinoshita, K.; Yamada, S.; Kitagawa, Y.; Kawakami, T.; Yamanaka, S.; Amaya, T.; Hirao, T. *Int. J. Quantum Chem.* **2013**, *113*, 437–442.

(299) Amaya, T.; Wang, W. Z.; Sakane, H.; Moriuchi, T.; Hirao, T. *Angew. Chem. Int. Ed.* **2010**, *49*, 403–406.

(300) Sakane, H.; Amaya, T.; Moriuchi, T.; Hirao, T. *Angew. Chem. Int. Ed.* **2009**, *48*, 1640–1643.

(301) Spisak, S. N.; Wei, Z.; O'Neil, N. J.; Rogachev, A. Y.; Amaya, T.; Hirao, T.; Petrukhina, M. A. *J. Am. Chem. Soc.* **2015**, *137*, 9768–9771.

Chapter 2.

Synthesis and Structural Analysis of [7]Helicene Metallocenes

2-1. Introduction

In this chapter, synthesis of group 8 metallocenes possessing [7]helicene ligand **L** will be described. Structure of each complex will be discussed based on X-ray diffraction analysis of a single crystal.

When there are multiple numbers of coordination sites exist in a large π-conjugated ligand, selectivity of the coordination site should be considered. For example, in monometallic and bimetallic complexes with a [6]helicene composed of only 6-membered rings, the metal first bound to any ring of [6]helicene, and then migrated to the arene ring at the edge to afford the most thermodynamically stable isomer.[1] As mentioned in **1**-**5**-**2**, corannulene coordinates to metals both in η^6- and η^2-manners depending on the kind of metal and other ligands.[2] In most examples of sumanene complexes, the metals bound on arene rings of the sumanene ligand,[3,4] except that zirconium complexes showed coordination on the Cp rings.[5] The [7]helicene ligand used in this study can serve one Cp moiety at the middle of its skeleton and the other 6 arene rings as coordination sites.

2-2. Synthesis of [7]helicene metallocenes

Three ruthenocene derivatives **1**, **2**, and **3** were synthesized in the procedure described in Scheme 2-1. First, a racemic mixture of **LH**[6] was used as a precursor, which was readily deprotonated after the addition of potassium hydride. The following reaction with an equimolar amount of [Cp*Ru(MeCN)$_3$]OTf afforded a mono-helicene ruthenocene bearing one helicene ligand, *rac*-**1**, in 76% yield. Complex 1 is stable in air and water, and unstable on silica-gel. The purification was done by extraction with dichloromethane and following recrystallization.

When two equivalents of [Cp*Ru(MeCN)$_3$]OTf was added, a bimetallic ruthenium

complex *rac*-**3** was obtained in 49% yield. The structure of the obtained complex was determined by preliminary single crystal X-ray diffraction analysis (see **2**-**3**); one ruthenium atom bound to the Cp moiety in an η^5 manner, and the other to the arene moiety at the edge of the helical ligand in an η^6 manner. These two metals were located at the opposite face of the helicene ligand to each other. Although other isomers varying in the metal coordination to other aromatic rings would have been possibly generated,[1] selective formation of **3** soon after the addition of ruthenium precursor was confirmed by ^{1}H NMR analysis. Because complex **3** decomposed in solution in air, it was purified by reprecipitation and recrystallization under inert atmosphere.

The reaction of deprotonated *rac*-**LH** with a half equimolar of $RuCl_2(dmso)_4$ gave bis-helicene ruthenocene **2** as a mixture of (*P*,*P*)- and (*M*,*M*)-**2** (*rac*-**2**), and (*P*,*M*)-**2** (*meso*-**2**) in a 7:3 ratio, in 26% total yield. Two of the diastereomers were separable by the difference of solubility; *meso*-**2** was much less soluble in any organic solvent. The both isomers are so stable even on silica-gel in air that I could isolated them by silica-gel column chromatography. The yield of **2** was much lower than **1** and **3**, and it was confirmed by proton NMR that the starting material **LH** was recovered in 17% yield. This fact suggested that the generated **L** anion was subjected to one-electron oxidation by a metal chloride to afford **L** radical, which abstracted a hydrogen radical from THF.[7]

Scheme 2-1. Synthesis of the [7]helicene ruthenocenes.

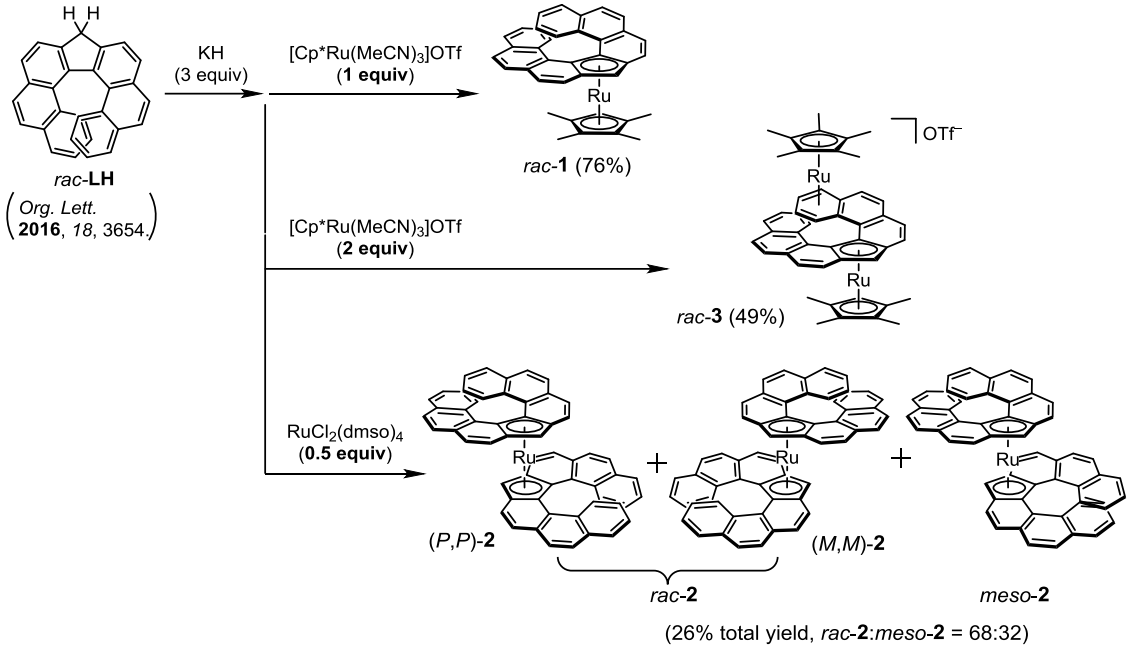

The [7]helicene metallocenes could be synthesized in their optically pure forms (Scheme 2-2). Enantiopure (*P*)-**LH** obtained by separation of a racemic mixture using chiral HPLC was converted to optically pure (*P*)-**1**, (*P,P*)-**2**, and (*P*)-**3** by the same procedure as those for the synthesis of their racemic mixtures. The opposite enantiomers were also prepared from (*M*)-**LH**. It was confirmed that the complexation underwent without any loss of enantiopurity by chiral HPLC for complex **1** and **3**. It is notable that the [7]helicene ligand afforded enantiopure helicene ruthenocenes, while the complexes with [5]helicene reported by Thiel *et al*. could not be separated into enantiomers due to the rapid racemization.[8]

Scheme 2-2. Synthesis of the [7]helicene ruthenocenes in optically-pure forms.

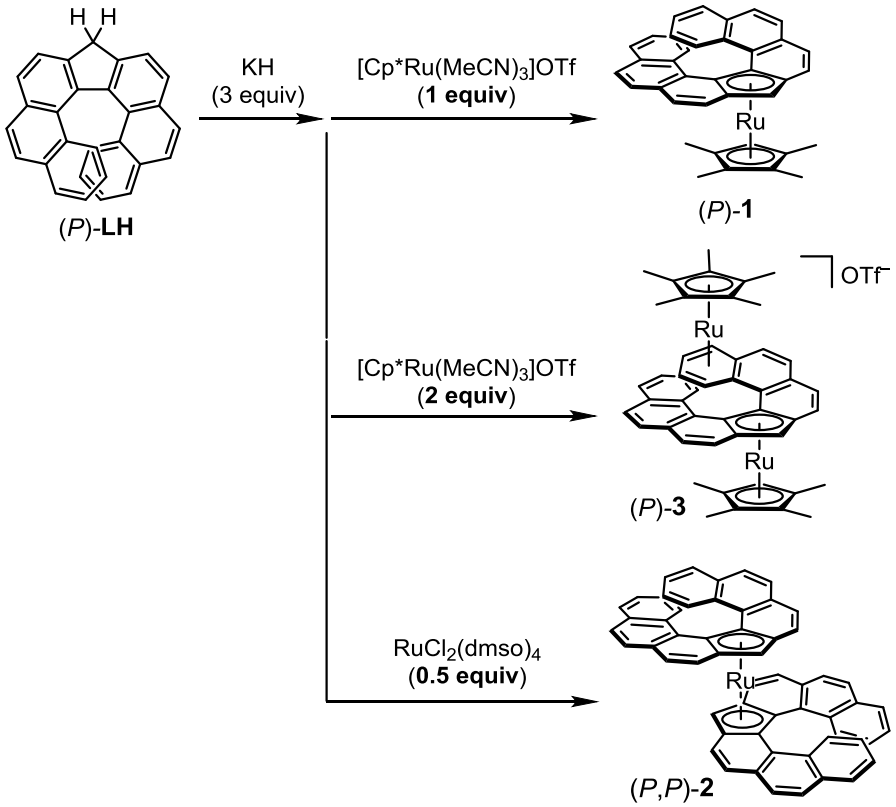

The iron analogue of complex **1** was also synthesized by the similar procedure (Scheme 2-3) in 3% isolated yield. There were several problems in the synthesis of $\mathbf{1_{Fe}}$. The first one was the one-electron oxidation of **L** anion by the iron precursor, suggested by the fact that the resulting mixture after the reaction contained **LH**, as well as the case with the synthesis of complex **2**. It is probably because iron(II) is more likely to be reduced by one-electron than ruthenium(II). The second problem was purification. Because $\mathbf{1_{Fe}}$ is unstable on silica even without oxygen, and very soluble to organic solvents, silica-gel column chromatography and reprecipitation are not available. Finally, it was found that size exclusion column chromatography under inert atmosphere is effective for purification of $\mathbf{1_{Fe}}$, and the desired [7]helicene ferrocene was successfully isolated although the yield was very low.

Scheme 2-3. Synthesis of [7]helicene ferrocene $\mathbf{1_{Fe}}$.

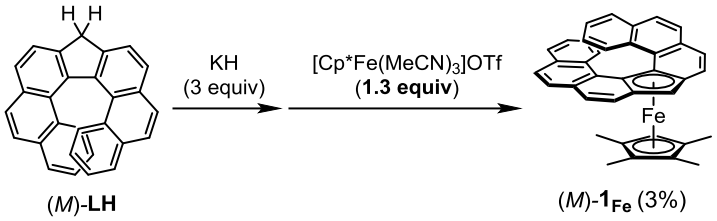

2-3. X-ray structural analysis

Single crystals of the obtained complexes were analyzed by X-ray diffraction (Figure 2-1, Table 2-1).

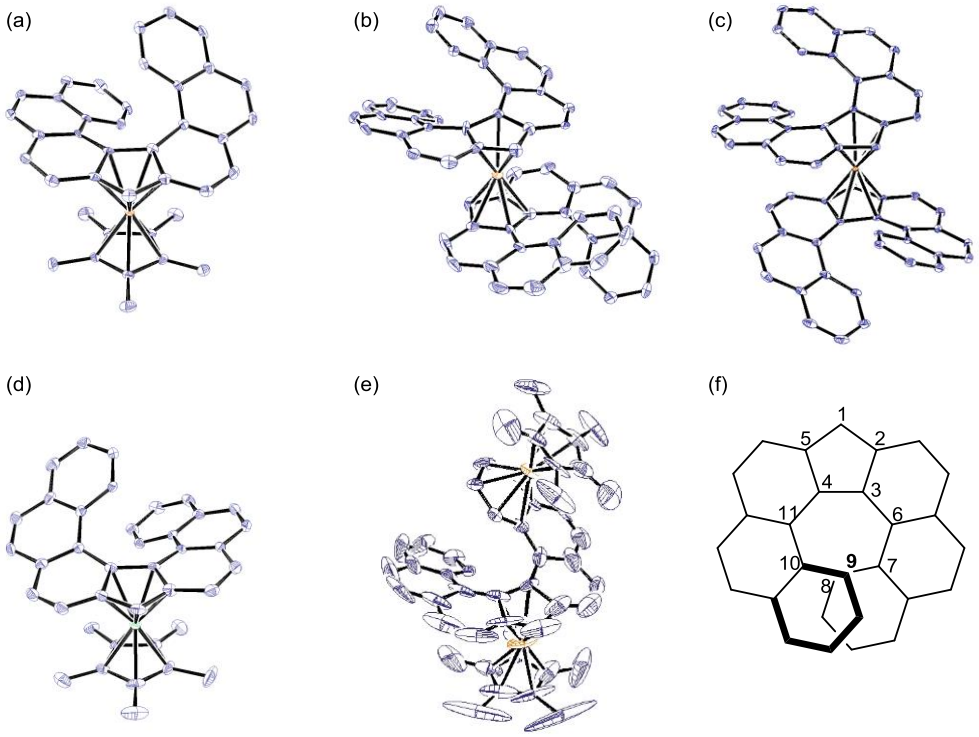

Figure 2-1. X-ray structures of *rac*-**1** (a), *rac*-**2** (b), and *meso*-**2** (c), (*M*)-$\mathbf{1_{Fe}}$ (d), *rac*-**3** (e), and the carbon numbering of **L** (f).

Table 2-1. Crystal structure data.

	rac-**1**	*rac*-**2**	*meso*-**2**	(*M*)-**1**$_{Fe}$	(*M*)-**LH**
C1-C2 (Å)	1.412(7)	1.42(2) 1.43(2)	1.426(4) 1.430(5)	1.416(6)	1.495(5)
C2-C3 (Å)	1.452(8)	1.45(2) 1.48(2)	1.469(5) 1.459(4)	1.463(6)	1.408(4)
C3-C4 (Å)	1.474(6)	1.50(1) 1.49(1)	1.463(4) 1.466(4)	1.483(6)	1.494(4)
C4-C5 (Å)	1.463(7)	1.45(2) 1.47(2)	1.458(5) 1.461(6)	1.462(6)	1.408(4)
C5-C1 (Å)	1.424(7)	1.43(2) 1.42(1)	1.423(5) 1.405(5)	1.414(7)	1.492(5)
M-Cp(**L**) (Å)	1.850	1.846 1.832	1.848 1.840	1.689	-
M-Cp* (Å)	1.793	-	-	1.665	-
sum of five dihedral angles (º) [a]	77.0	83.6	79.6	77.6	86.5

[a] The sum of ∠C9-C10-C11-C4, ∠C10-C11-C4-C3, ∠C11-C4-C3-C6, ∠C4-C3-C6-C7, and ∠C3-C6-C7-C8.

Focusing on the bond length of the five-membered ring, it was found that the cyclopentadiene moiety of **LH** was aromatized to Cp anion from the shorter C1–C2, C3–C4, and C5–C1 bonds, and the longer C2–C3 and C4–C5 bonds in the complexes. The ruthenium atom coordinated to the Cp moiety in an η^5 manner. Taking a closer look at the bond lengths however, these five bond lengths are not equal; C1–C2 and C5–C1 bonds are the shortest, and the C3–C4 bond is the longest. The bond lengths in fused aromatic rings can be explained by

their resonance structures. For example, the indenyl ligand on Ru(ind)Cp* showed two of the shortest C–C bonds,[9] which could originate from the large contribution of resonance structure **A** and **A'** in Figure 2-3a, stabilized by the aromatic ring. In the case of fluorenyl ligand in Ru(flu)Cp*, the bond lengths of the five-membered ring are almost uniform.[9] In dibenzofluorenyl ligand reported by Thiel *et al*.,[10] the resonance structure **D**, **E**, and **E'** in Figure 2-3b, containing one or two aromatic benzene ring(s), seem to contribute largely. It was implied by the crystal structure of *rac*-**1** that **E** and **E'** more contributed to the [7]helicene ligand than to dibenzofluorenyl anion, which might be because the anion generated on C3 or C4 was stabilized by the extended π-conjugated system.

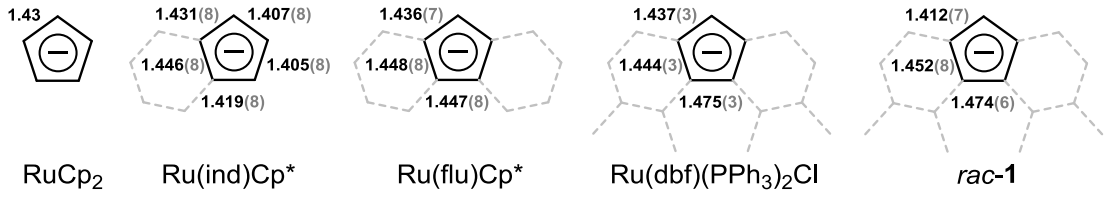

Figure 2-2. Bond length of the five-membered rings in ruthenium complexes.[9–11]

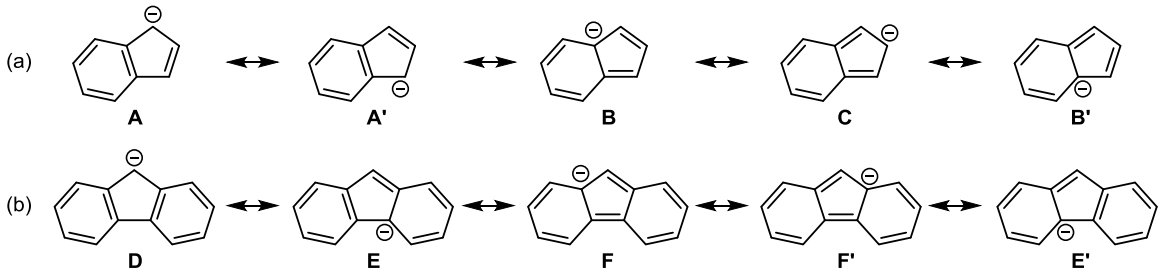

Figure 2-3. Resonance structures of indenyl (a) and fluorenyl (b) anion

The distortion of the helical structure is one of the important factors in the structural analysis of helicenes and helicene-like compounds, because it largely affects the stability of the helical chirality and chiroptical properties. In the case with hetero[7]helicene and helicene-like

compounds reported by Nozaki *et al.*,[6,12–14] possessing a five-membered ring at the middle in their skeleton, the helical distortions was assessed by sum of the five dihedral angles that are derived from the seven C–C bonds (∠C9-C10-C11-C4, ∠C10-C11-C4-C3, ∠C11-C4-C3-C6, ∠C4-C3-C6-C7, and ∠C3-C6-C7-C8 in Figure 2-1f). According to this values, all of the [7]helicene metallocenes obtained in this study showed less-distorted structure than that **LH** (Table 2-1). The bis-helicene ruthenocene **2** were slightly more twisted than **1**, which can be caused by the steric repulsion between the two helicene ligands. The data of *rac*-**3** was not suitable for discussing its precise structure because of the bad R factor.

The distance between the metal and the five-membered ring in complex **1** was almost the same as that of unsubstituted ruthenocene (Cp_2Ru) (Figure 2-4).[11] On the other hand, the metal-Cp bond in $\mathbf{1_{Fe}}$ was slightly longer than Cp_2Fe.[15] In the crystal structure of metallocenes with a group 8 metal, there are two possible conformations; staggered and eclipsed. Although unsubstituted ferrocene (Cp_2Fe) is eclipsed according to the gas phase electron diffraction analysis[16] and theoretical studies in the gas phase,[17] it shows staggered configuration in its crystal state,[15,18] and most of the other ferrocene derivatives as well.[19,20] As one of the exceptions, 1,1'-ferrocenedicarboxylic acid showed eclipsed conformation in the crystal as a result of forming intermolecular hydrogen bonds.[21] It is notable that [7]helicene ferrocene $\mathbf{1_{Fe}}$ showed eclipsed conformation in its crystal state Given that the iron complex with [5]helicene and tetraisopropylcyclopentadienyl ligand reported by Thiel *et al.* showed staggered conformation,[22] the eclipsed $\mathbf{1_{Fe}}$ is probably because of the steric repulsion between the benzene ring at the edge of the [7]helicene ligand and the methyl group.

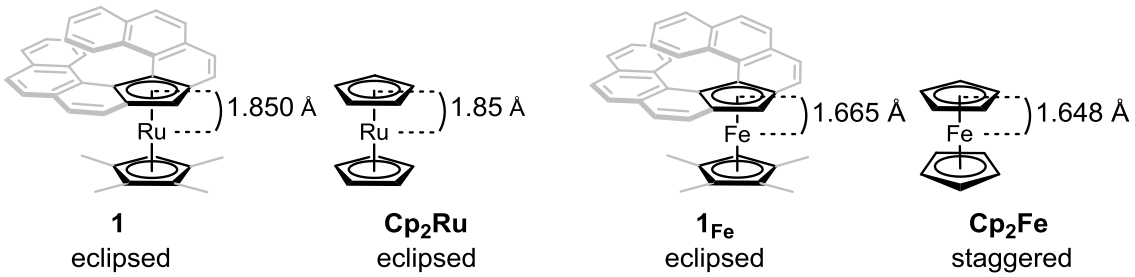

Figure 2-4. Comparison of the [7]helicene metallocenes **1** and $\mathbf{1_{Fe}}$ with the corresponding unsubstituted metallocenes.

According to the crystal packing structure of each complex, any intermolecular interaction other than C–H-π was not observed (Figure 2-5). Unlike the case of some of other helicenes,[13,23] columnar structure was not formed.

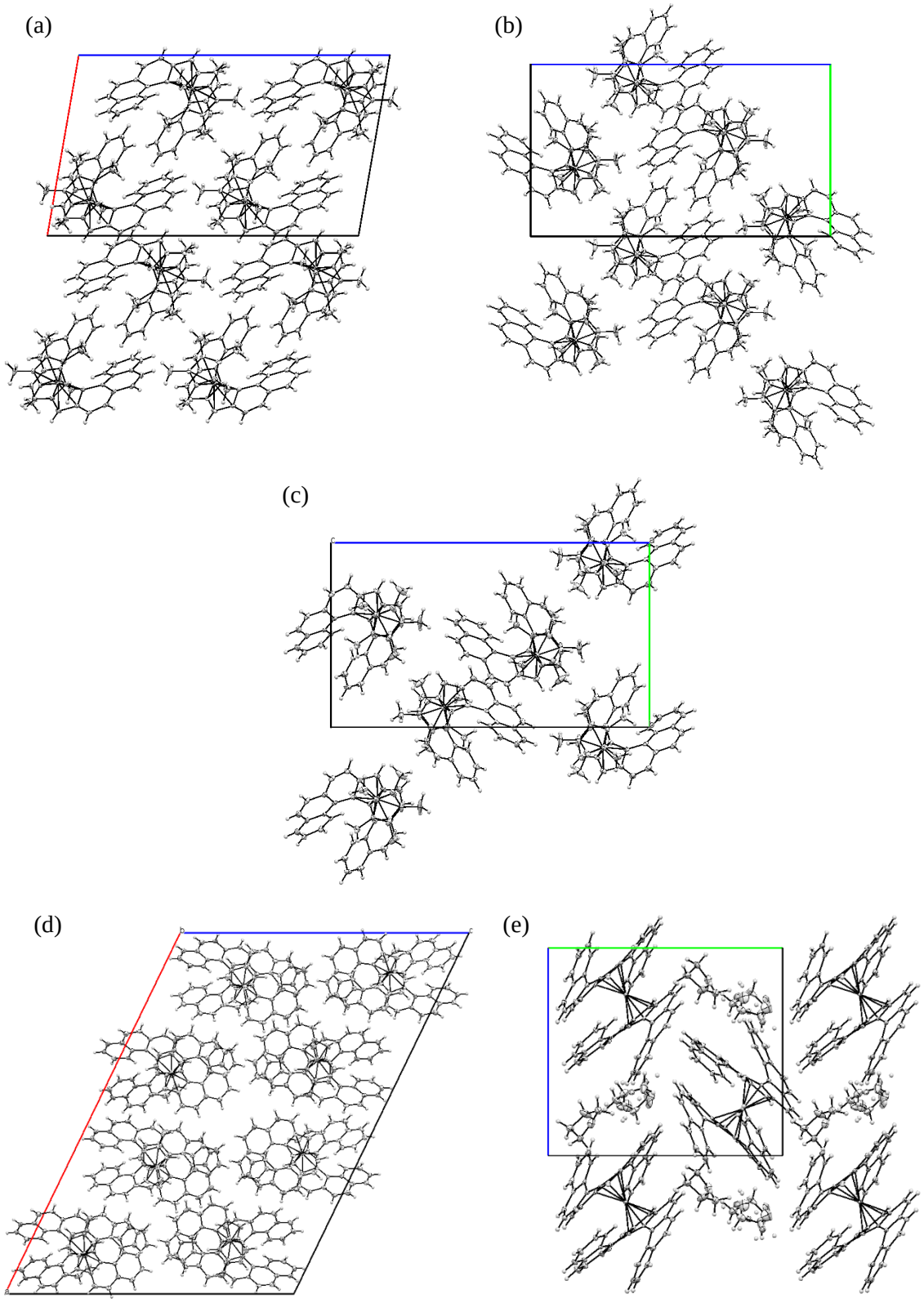

Figure 2-5. Packing structures of *rac*-**1** (a), (*M*)-**1** (b), (*M*)-**1**$_{Fe}$ (c), *rac*-**2** (d), and *meso*-**2** (e).

2-4. Conclusions

[7]Helicene metallocenes **1**, **2**, **3**, and $\mathbf{1_{Fe}}$ were successfully synthesized not only in racemic mixture but also in their optically pure forms. Each of their structure was analyzed and discussed especially focused on the distortion of the helical structure, the metal-ligand distance, and the conformation of the metallocene moiety.

2-5. References

(1) Álvarez, C. M.; Barbero, H.; García-Escudero, L. A.; Martín-Alvarez, J. M.; Martínez-Pérez, C.; Miguel, D. *Inorg. Chem.* **2012**, *51*, 8103–8111.

(2) Petrukhina, M. a; Scott, L. T. *Dalton Trans.* **2005**, No. 18, 2969–2975.

(3) Amaya, T.; Hirao, T. *Chem. Commun.* **2011**, *47*, 10524–10535.

(4) Amaya, T.; Hirao, T. *Chem. Rec.* **2014**, 310–321.

(5) Amaya, T.; Takahashi, Y.; Moriuchi, T.; Hirao, T. *J. Am. Chem. Soc.* **2014**, *136*, 12794–12798.

(6) Oyama, H.; Akiyama, M.; Nakano, K.; Naito, M.; Nobusawa, K.; Nozaki, K. *Org. Lett.* **2016**, *18*, 3654–3657.

(7) Al-Afyouni, M. H.; Huang, T. A.; Hung-Low, F.; Bradley, C. A. *Tetrahedron Lett.* **2011**, *52*, 3261–3265.

(8) Pammer, F.; Sun, Y.; May, C.; Wolmersh??user, G.; Kelm, H.; Kr??ger, H. J.; Thiel, W. R. *Angew. Chem. Int. Ed.* **2007**, *46*, 1270–1273.

(9) Gassman, P. G.; Winter, C. H. *J. Am. Chem. Soc.* **1988**, *110*, 6130–6135.

(10) Pammer, F.; Sun, Y.; Thiel, W. R. *Inorganica Chim. Acta* **2011**, *374*, 205–210.

(11) Hardgrove, G. L.; Templeton, D. H. *Acta Crystallogr.* **1959**, *12*, 28–32.

(12) Nakano, K.; Hidehira, Y.; Takahashi, K.; Hiyama, T.; Nozaki, K. *Angew. Chem. Int. Ed.* **2005**, *44*, 7136–7138.

(13) Nakano, K.; Oyama, H.; Nishimura, Y.; Nakasako, S.; Nozaki, K. *Angew. Chem. Int. Ed.* **2012**, *51*, 695–699.

(14) Oyama, H.; Nakano, K.; Harada, T.; Kuroda, R.; Naito, M.; Nobusawa, K.; Nozaki, K. *Org. Lett.* **2013**, *15*, 2104–2107.

(15) Seller, P.; Dunitz, J. D. *Acta Crystallogr. Sect. B Struct. Crystallogr. Cryst. Chem.* **1979**, *35*, 2020–2032.

(16) Haaland, A.; Nilsson, J. E.; Olson, T.; Norin, T. *Acta Chem. Scand.* **1968**, *22*, 2653–2670.

(17) Coriani, S.; Haaland, A.; Helgaker, T.; Jørgensen, P. *Chemphyschem* **2006**, *7*, 245–249.

(18) DUNITZ, J. D.; ORGEL, L. E. *Nature* **1953**, *171*, 121–122.

(19) Guo, Y.-F.; Wang, J.-J.; Xu, W.-J.; Sun, D.-H.; Gao, Q. *Acta Crystallogr. Sect. E Crystallogr. Commun.* **2015**, *71*, m213–m214.

(20) Razak, I. A.; Usman, A.; Fun, H.-K.; Yamin, B. M.; Kasim, N. A. M. *Acta Crystallogr. Sect. C Cryst. Struct. Commun.* **2002**, *58*, m225–m227.

(21) Palenik, G. J. *Inorg. Chem.* **1969**, *8*, 2744–2749.

(22) Pammer, F.; Sun, Y.; Pagels, M.; Weismann, D.; Sitzmann, H.; Thiel, W. R. *Angew. Chem. Int. Ed.* **2008**, *47*, 3271–3274.

(23) Nuckolls, C.; Katz, T. J.; Castellanos, L. *J. Am. Chem. Soc.* **1996**, *118*, 3767–3768.

Chapter 3.

Isomerization Behavior of the Metal-Bound [7]Helicene

3-1. Introduction

In this chapter, the isomerization behavior of the metal-bound [7]helicene will be discussed based on the experimental results using bis-helicene metallocene **2**.

Racemization behavior of simple carbo-helicenes was well-studied by both experimental and theoretical ways, as mentioned in **1-3-3-1**. Other reports on synthesizing helicenes or helicene-like compounds (mentioned in **1-3-3-2**~**1-3-3-4**) described the racemization barrier of the compounds.[1–12] For example, racemization behavior of the hetero[7]helicenes with a five-membered ring at the middle of their skeleton (Figure 3-1), which have similar structure with the [7]helicene ligand **L**, was experimentally investigated. For oxa- and aza[7]helicenes,[9] racemization was observed at higher temperature than 100 °C, and the each activation energy was estimated to be 31.5 kcal mol^{-1} for oxa[7]helicene, 32.7 kcal mol^{-1} for aza[7]helicene, and 33.7 kcal mol^{-1} for aza[7]helicene with a phenyl group on nitrogen.[13] On the other hand, the enantiopurity of λ^5-phospha[7]helicenes remained intact after heating at 150 °C,[10] and the helicene-like molecules with a dimethylsilole moiety did not lost its optical purity at all even at 220 °C.[11]

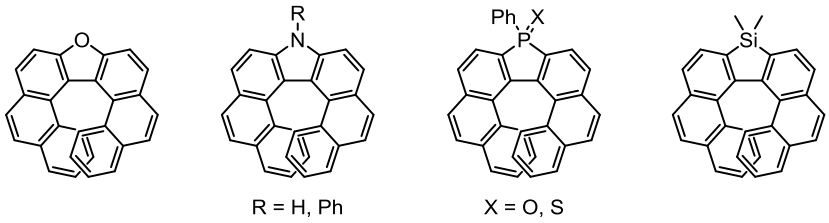

Figure 3-1. Hetero[7]helicenes with a five-membered ring at the middle of their skeleton

Inversion of one helicene moiety in multiple-helicenes[3–6,12] or multiple-helicene metal complexes[8] with multiple chiral centers results in conversion from one diastereomer to the other. In such cases, not only the activation barrier but also the energy difference between the

diastereomers is intriguing topics when discussing about dynamic behavior of helicenes. For example, when synthesizing a quadruple helicene reported by Itami *et al.*, only (*P*,*P*)-(*P*,*P*)-form and its enantiomer were generated, which isomerized to (*P*,*P*)-(*M*,*M*)-form under 80 °C within 2 days (Scheme 3-1).[4] Theoretical calculations also showed that the (*P*,*P*)-(*M*,*M*)-form was the most stable of the possible nine stereoisomers. With regard to the Crassous' bis-helicene diplatinum complex, its heterochiral isomer fully converted into its homochiral form after heating at 80 ºC for 3 days.[8]

Scheme 3-1. Synthesis and thermal isomerization of a quadruple helicene

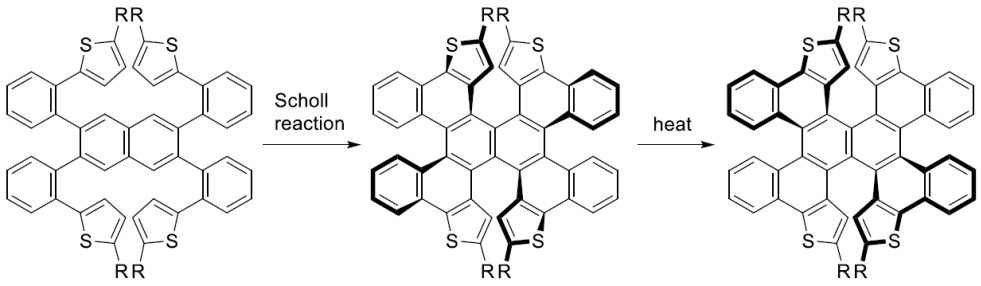

3-2. Estimation of the isomerization barrier of the bis-helicene ruthenocene

The thermal behavior of *rac*-**2** in solution was investigated at 100, 110, 122, and 150 ºC, monitoring the ratio of the two isomers by ^{1}H NMR (Scheme 3-2). It was found that *rac*-**2** slowly converted to *meso*-**2** in solution at higher temperature than 100 ºC, and the ratio of *rac*- and *meso*-**2** converged into a specific value depending on temperature. There should be an equilibrium between the two isomers (Figure 3-3). The determined equilibrium constant (K) at each temperature was plotted to Van't Hoff plot (Figure 3-2a), from which the racemic form was

estimated to be more stable than its meso form by 2.3 kcal mol^{-1} at 400 K. Arrhenius plot[] was also generated from the kinetic constants (k) at the various temperature (Figure 3-2b) calculated within the frame of reversible first-order kinetics ($\ln([rac\text{-}\mathbf{2}]/[rac\text{-}\mathbf{2}]_0) = -kt+C$), and the activation energy of isomerization from *rac*-**2** to *meso*-**2** was determined to be 33.9 kcal mol^{-1} at 400 K.

Scheme 3-2. Heating experiments of *rac*-**2**

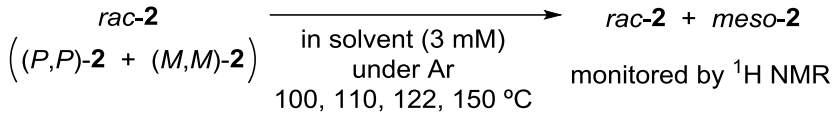

(a)

T (°C)	K	k (h^{-1})
100	0.35	0.0014
110	0.38	0.0034
122	0.42	0.0237
150	0.50	0.3619

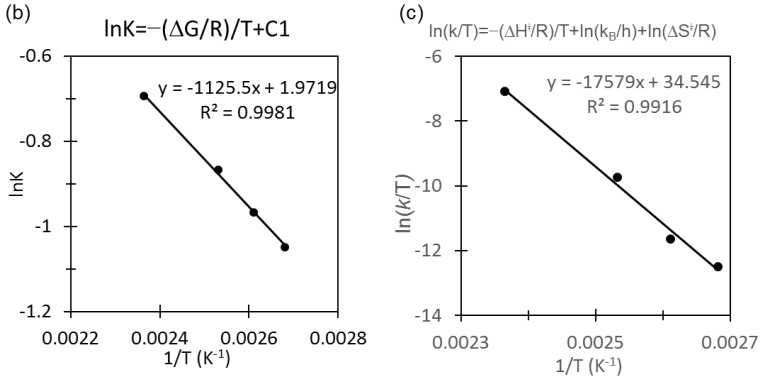

Figure 3-2. The equilibrium constants and the kinetic constants at various temperature (a), Van't Hoff plot (b), Arrhenius plot (c) based on the heating experiments

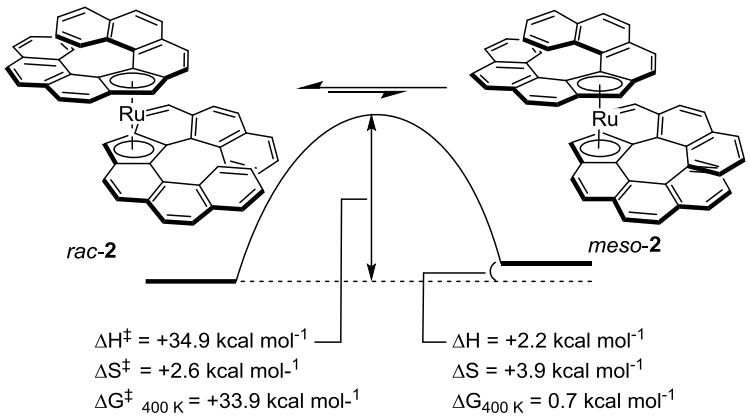

Figure 3-3. Equilibrium between *rac*-**2** and *meso*-**2**

The estimated activation energy from *rac*-**2** to *meso*-**2** was close to the racemization barrier of [6]helicene composed of only 6-membered rings (36.2 kcal mol^{-1}),[14] and much higher than the theoretically calculated value for the [5]helicene ligand reported by Thiel *at al*. (18.8 kcal mol^{-1}).[15] The $\Delta G^{\ddagger}$ for the isomerization was comparable also to that of the previously-reported oxa- and aza[7]helicenes possessing the similar structure with the [7]helicene ligand.[13] However, it should be noted that the isomerization behavior of [7]helicene metallocenes is different from hetero[7]helicenes, implied by the positive $\Delta S^{\ddagger}$ values in isomerization from *rac*-**2** to *meso*-**2**. Not only the inversion of helicene ligand, but also the other factors in the transition state, such as intramolecular interaction between two ligands and change in M-Cp bond length, should be considered. The racemization barriers of complexes **1** and **3** could not be determined because of their unstability at high temperature in solution.

3-3. Mechanism of the isomerization of the bis-helicene ruthenocene

For the conversion from *rac*-**2** to *meso*-**2**, two pathways are considerable; a flip of one of the helicene units, and/or exchange of ligands between (*P*,*P*)- and (*M*,*M*)-**2** (Figure 3-4). To clarify

the mechanism, the author tested if the thermal isomerization could occur with enantiopure **2** (Scheme 3-3). If the isomerization of *rac*-**2** to *meso*-**2** took place via the ligand exchange, there would be no isomerization starting from (*P*,*P*)-isomer. Upon heating (*P*,*P*)-**2** at 122 ºC, however, *meso*-**2** and (*M*,*M*)-**2** were generated, suggesting that the epimerization occurred through the helical inversion of the ligand.

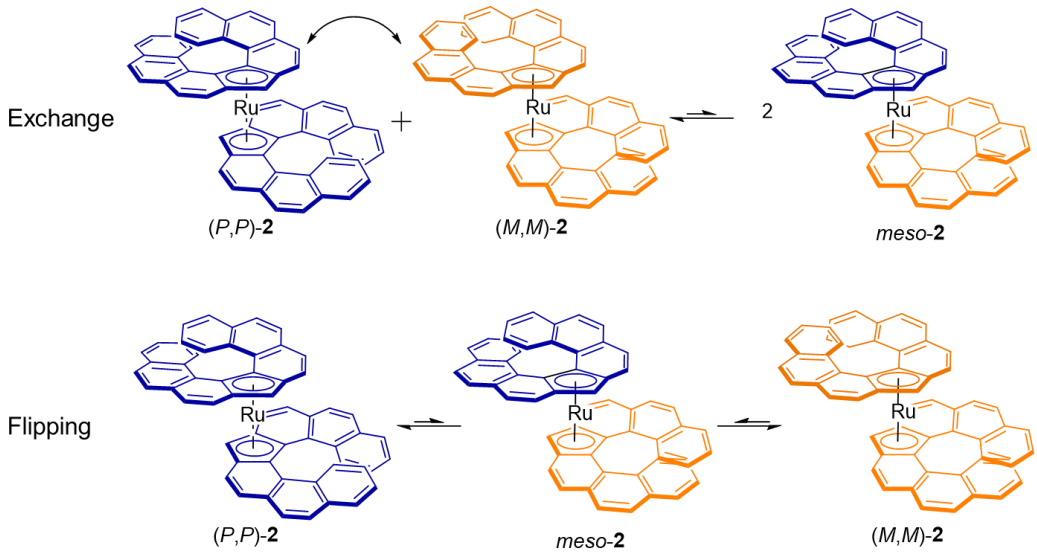

Figure 3-4. Two possible pathways for isomerization of the bis-helicene ruthenocene

Scheme 3-3. Heating experiments of (*P*,*P*)-**2**

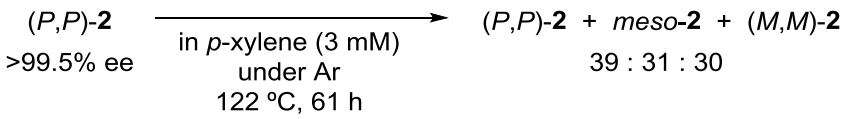

3-4. Conclusions

Because of its stable helical chirality, the isomerization barrier of the [7]helicene bound to a metal was able to be estimated from heating experiments. The isomerization of the bis-helicene

ruthenocene was confirmed to occur through the flipping of the helicene ligand.

3-5. References

(1) Jančařík, A.; Rybáček, J.; Cocq, K.; Chocholoušová, J. V.; Vacek, J.; Pohl, R.; Bednárová, L.; Fiedler, P.; Císařová, I.; Stará, I. G.; Starý, I. *Angew. Chem. Int. Ed.* **2013**, *52*, 9970–9975.

(2) Rajca, A.; Miyasaka, M.; Pink, M.; Wang, H.; Rajca, S. *J. Am. Chem. Soc.* **2004**, *126*, 15211–15222.

(3) Takao Fujikawa; Yasutomo Segawa; Kenichiro Itami. *J. Am. Chem. Soc.* **2015**, *137*, 7763–7768.

(4) Fujikawa, T.; Segawa, Y.; Itami, K. *J. Am. Chem. Soc.* **2016**, *138*, 3587–3595.

(5) Luo, J.; Xu, X.; Mao, R.; Miao, Q. *J. Am. Chem. Soc.* **2012**, *134*, 13796–13803.

(6) Kashihara, H.; Asada, T.; Kamikawa, K. *Chem. - Eur. J.* **2015**, *21*, 6523–6527.

(7) Li, M.; Lu, H.-Y.; Zhang, C.; Shi, L.; Tang, Z.; Chen, C.-F. *Chem. Commun.* **2016**, *5*, 4–7.

(8) Anger, E.; Rudolph, M.; Shen, C.; Vanthuyne, N.; Toupet, L. L.; Roussel, C.; Autschbach, J.; Crassous, J.; Réau, R.; Réau, R. *J. Am. Chem. Soc.* **2011**, *133*, 3800–3803.

(9) Nakano, K.; Hidehira, Y.; Takahashi, K.; Hiyama, T.; Nozaki, K. *Angew. Chem. Int. Ed.* **2005**, *44*, 7136–7138.

(10) Nakano, K.; Oyama, H.; Nishimura, Y.; Nakasako, S.; Nozaki, K. *Angew. Chem. Int. Ed.* **2012**, *51*, 695–699.

(11) Oyama, H.; Nakano, K.; Harada, T.; Kuroda, R.; Naito, M.; Nobusawa, K.; Nozaki, K. *Org. Lett.* **2013**, *15*, 2104–2107.

(12) Wang, X.-Y.; Wang, X.-C.; Narita, A.; Wagner, M.; Cao, X.-Y.; Feng, X.; Müllen, K. *J. Am. Chem. Soc.* **2016**, *138*, 12783–12786.

(13) Hidehira, Y. Master thesis, The University of Tokyo.

(14) Martin, R. H.; Marchant, M. J. J. *Tetrahedron* **1974**, *30*, 347–349.

(15) Pammer, F.; Sun, Y.; May, C.; Wolmershäuser, G.; Kelm, H.; Krüger, H.-J.; Thiel, W. R. *Angew. Chem. Int. Ed.* **2007**, *46*, 1270–1273.

Chapter 4.

Electronic, Optical, and Chiroptical Properties

4-1. Introduction

In this chapter, physical properties, such as electronic, optical, and chiroptical properties of the [7]helicene ruthenocenes will be discussed based on both experimental and theoretical studies.

When paying attention to the central metal, it is intriguing to know how the electronic property changes by the coordination to a large aromatic molecule. Especially for group 8 metallocenes, redox potentials are often studied compared to the corresponding unsubstituted metallocenes, which are typical redox reagents.[1] Licandro *et al.* reported that the tetrathia[7]helicene complexes substituted with a ferrocenylethynyl group showed higher oxidation potential than non-substituted ferrocene (Cp_2Fe).[2] The cobaltocenium complexes with a helicene ligand reported by Katz *et al.*[3] and Thiel *et al.*[4] was found to show reduction potential which is close to that of unsubstituted cobaltocenium ion (Cp_2Co^+) and lower than that of bisindenylcobalt ion.

Taking a look at the helicene ligand, optical and chiroptical properties are attractive to argue. Helicenes themselves show unique optical and chiroptical properties due to their extended π-conjugated system and helical shape, which can be changed by the coordination of metal(s).[5] Crassous *et al.* found that optical rotations of the ethynyl helicenes got much higher after the complexation with ruthenium[3] or iron atom.[6] CD spectra also changed by the coordination of the metal especially for the bimetallic complex. These chiroptical properties further changed by reversible oxidation of the bound metal species.

4-2. Electronic properties

Cyclic voltammetry measurements of helicene ruthenocenes *rac*-**1**, *rac*-**2**, and *rac*-**3** were performed (Figure 4-1). The oxidation potentials of the two mono-helicene ruthenocenes *rac*-**1**

and *rac*-**2** were nearly the same, $E_{ox1/2}$ = 0.08 V for *rac*-**1**, 0.07 V for *rac*-**2**, vs Fc/Fc^+, respectively. It is reported that decamethylruthenocene shows a much lower oxidation potential (0.11 V)[7] than that of ruthenocene (0.49 V)[8] because of the high electron-donating ability of pentamethylcyclopentadienyl anion (Table 4-1). When the indenyl anion was used as one of the ligand, the oxidation potential (0.12 V) was almost the same as that of decamethylruthenocene, and the fluorenyl anion made the oxidation potential much lower (0.03 V),[7] which was probably because the cation generated after oxidation was stabilized by delocalization over the conjugated ligand. Compared to these examples, the oxidation potentials of [7]helicene complexes **1** (0.08 V) and *rac*-**2** (0.07 V) are between those of ruthenocene with an indenyl anion and the one possessing a fluorenyl anion. This fact implied that the expansion of the p-conjugated system does not contribute to further stabilization by delocalization. Compared to these monometallic [7]helicene ruthenocenes, bis-ruthenium [7]helicene complex *rac*-**3** showed higher oxidation potential. This can be because of the lower electron density of the π-conjugated system with the cationic ruthenium atom on the arene moiety.[3]

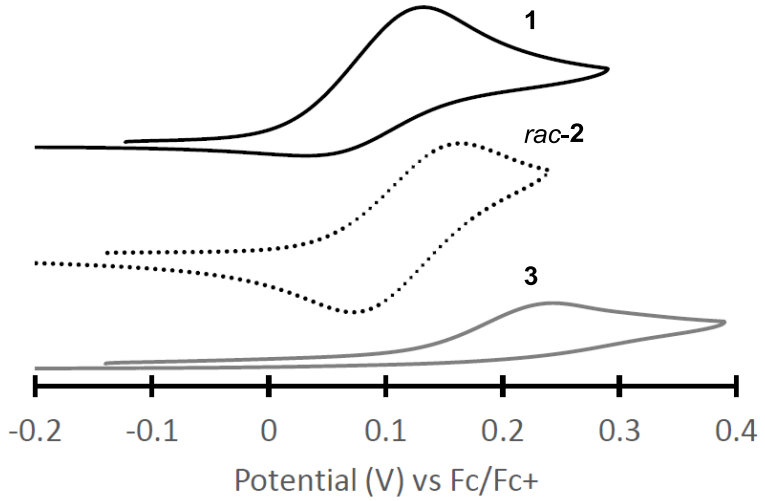

Figure 4-1. Cyclic voltammograms of **1**, *rac*-**2**, and **3** (10 mM in CH_2Cl_2 containing 0.1 M of Bu_4NBF_4 as supporting electrolyte, 100 mV s^{-1})

Table 4-1. Oxidation potentials of reported ruthenocene derivatives[7] and the [7]helicene ruthenocenes

	$E_{1/2}$ (V) vs Fc/Fc^+
Cp_2Ru	0.49
Cp^*_2Ru	0.11
Cp*(ind)Ru	0.12
Cp*(flu)Ru	0.03
1	0.08
rac-**2**	0.07

While *rac*-**1** and *rac*-**3** exhibited irreversible oxidation like most ruthenocene derivatives,[7] *rac*-**2** showed a quasi-reversible wave like decamethylruthenocene.[9,10] For complex *rac*-**2**, the disproportionation of Ru(III) species to Ru(II) and Ru(IV), which is usually the cause of the irreversible oxidation of ruthenocene derivatives,[11] was probably suppressed by the steric hindrance of the helicene ligands.

4-3. UV-vis absorption spectra

In each UV-vis absorption spectrum of the obtained [7]helicene ruthenocenes, a weak broad peak was observed at longer wavelength than 400 nm, while the ligand precursor **LH** did not show any peak at the low-energy range (Figure 4-2). When comparing the three complexes, the absorption edge was red-shifted in the spectra of *rac*-**2** and **3** than in that of complex **1**.

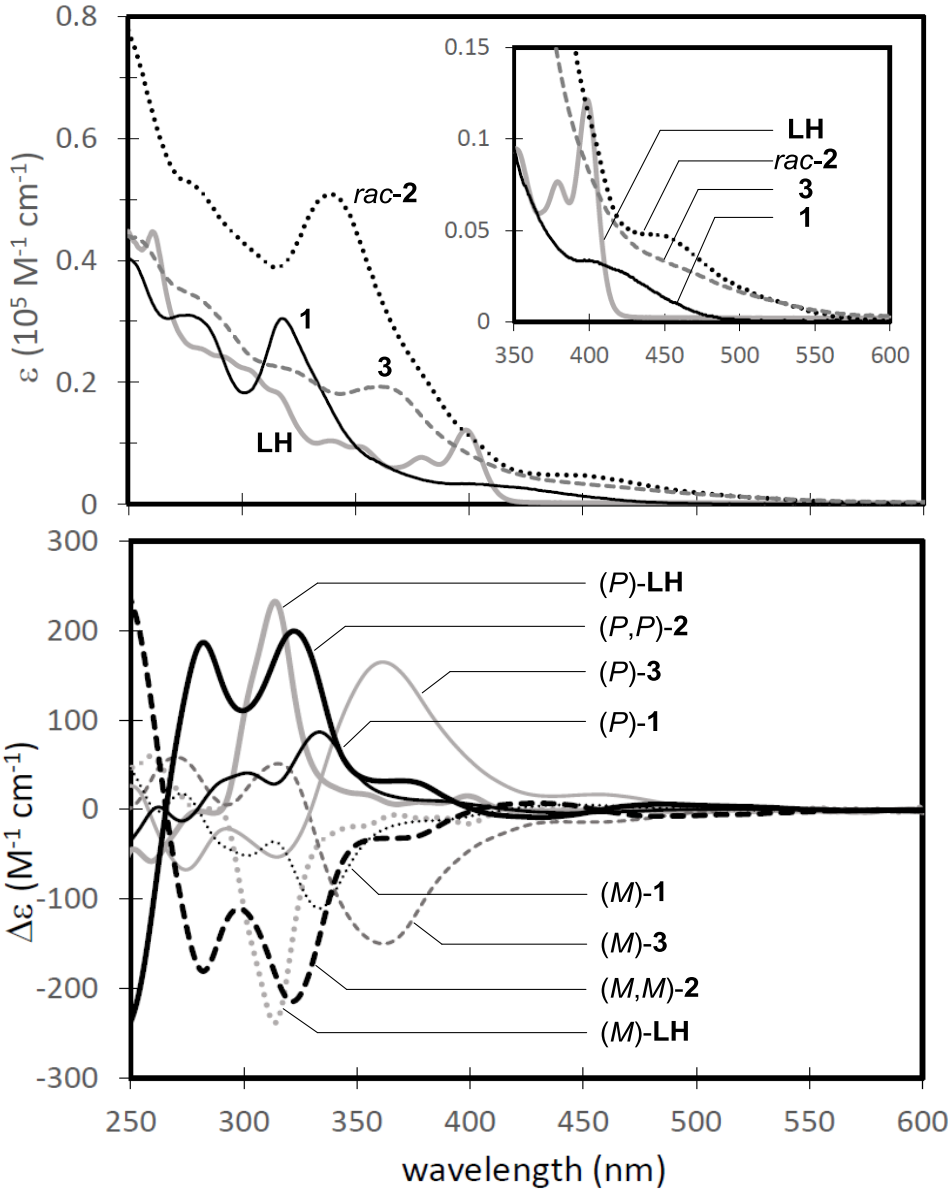

Figure 4-2. UV-vis absorption spectra of [7]helicene ruthenocenes and the ligand precursor **LH**.

4-4. Chiroptical properties

Specific rotation of (*M*)-**1** showed $[\alpha]_D^{23}$ of -1.0×10^3 (c = 0.1, $CHCl_3$, the same hereinafter), whose absolute value was smaller than that of enantiopure **LH** (2.7×10^3), which could be attributed to the less distorted structure of helical moieties in the complexes than in **LH**, as

mentioned in **2-3**. As was the case with the complexes possessing two helicene ligands reported by Katz[3] and Crassous,[12] (*M*,*M*)-**2** exhibited larger optical rotation than (*M*)-**1**, -2.8×10^3. Optical rotation of (*M*)-**3** was -2.9×10^3, which was also greater than that of (*M*)-**1**.

The CD spectra of the complexes were mirror images to each enantiomer. All of the [7]helicene ruthenocenes showed large cotton effect in the shorter wavelength range, and small one at longer wavelength area than 400 nm (Figure 4-3).

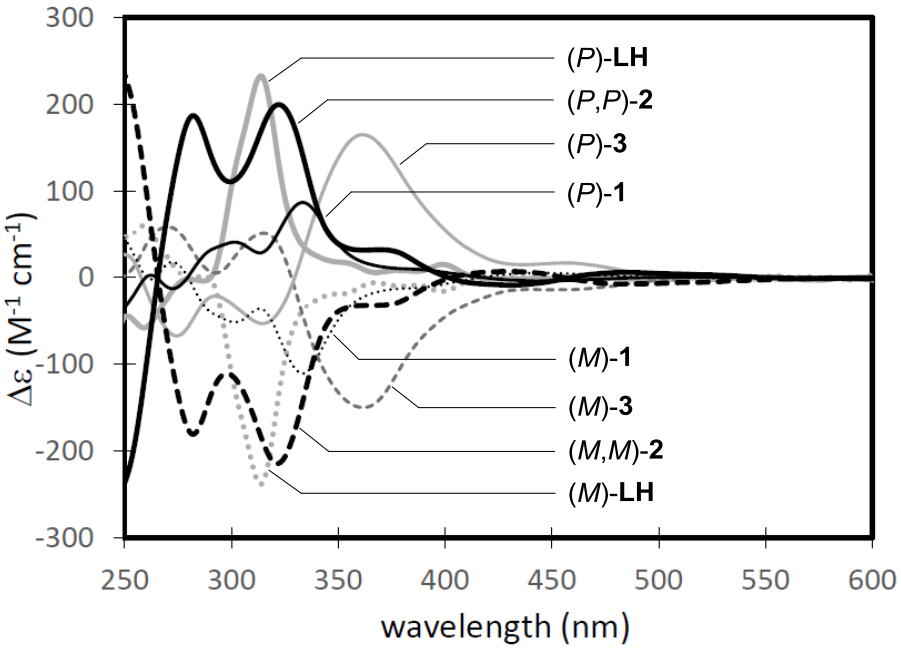

Figure 4-3. CD spectra of [7]helicene ruthenocenes and the ligand precursor **LH**.

4-5. Theoretical investigations

The experimental results mentioned above could be explained by theoretical calculations (M06/LANL2DZ for Ru, 6-31G* for others). First, the frontier orbitals of each complex were depicted (Figure 4-4). The relative energy levels of HOMOs are in good accordance with oxidation potentials estimated by CV (mentioned in **4-2**); monometallic complexes **1** and *rac*-**2**

showed similar values of HOMO levels, and **3** exhibit much lower. The energy difference between HOMO and LUMO of *rac*-**2** (3.3 eV) and **3** (3.1 eV) was narrower than that of **1** (3.9 eV), which well matched with their red-shifted absorption edges. For complex *rac*-**2**, the π-orbitals of the ligands were delocalized over the entire molecule through the central ruthenium atom, and its LUMO was contributed largely by the metal's d-orbital (26%). With regard to complex **3**, the d-orbital of the additional ruthenium on arene moiety was hybridized to the LUMO+1 of complex **1**, which resulted in LUMO of complex **3** with low energy. The d-orbital contributed to LUMO of complex **3** to a considerable extent (17%).

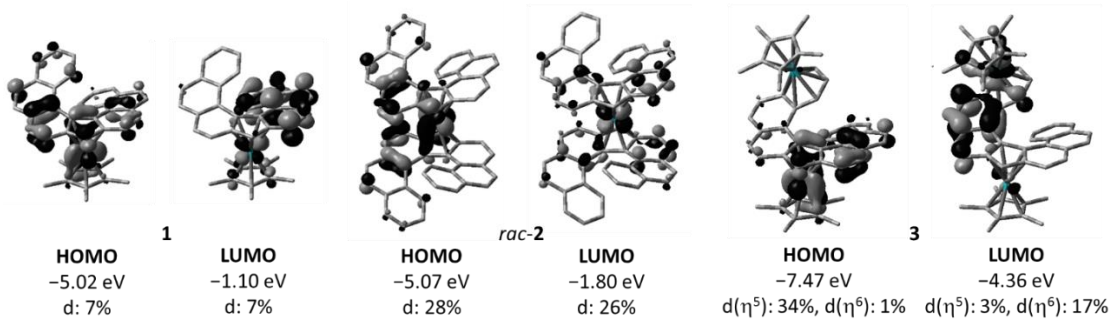

Figure 4-4. Energy levels and the d-orbital percentage of frontier orbitals of [7]helicene ruthenocenes. (Calculated by M06/LANL2DZ (Ru), 6-31G*)

TD-DFT calculations (M06/LANL2DZ for Ru, 6-31G* for others) were also conducted. The computed UV-vis absorption and CD spectra of the helicene complexes well fitted to the experimental data. According to the natural transition orbital analysis,[13] it was found that the metal's d-orbitals significantly contributed to the weak broad peaks at long wavelength range in the absorption and CD spectra, which did not appear in the spectra of **LH**. For complex **1**, the first six excitation states (S_1–S_6) were metal-centered d-d transition mixing with metal-to-ligand charge transfer (MLCT) (Figure 4-5). With regard to complex *rac*-**2**, ligand-to-metal charge

transfer (LMCT) was also found in singlet excited states (S_4, S_7) in addition to MLCT and d-d (Figure 4-6). The LMCT detected for *rac*-**2** was suggested to originate from the larger contribution of the metal's d-orbital to its LUMO (26%) than in the case of complex **1** (7%) (Figure 4-4). In the case of complex **3**, excitation states with low energy (S_1–S_4) were described as charge transfer transitions, in which the ruthenium atom on the five-membered ring worked as an electron donor, and the other ruthenium acted as an acceptor, through the helicene ligand (Figure 4-7). This can be because of the cationic character of the ruthenium on the arene ring. For all complexes, as the energy level of an excited state became higher, the contribution of intra-ligand π-π* transition was enlarged, and the oscillator strength increased.

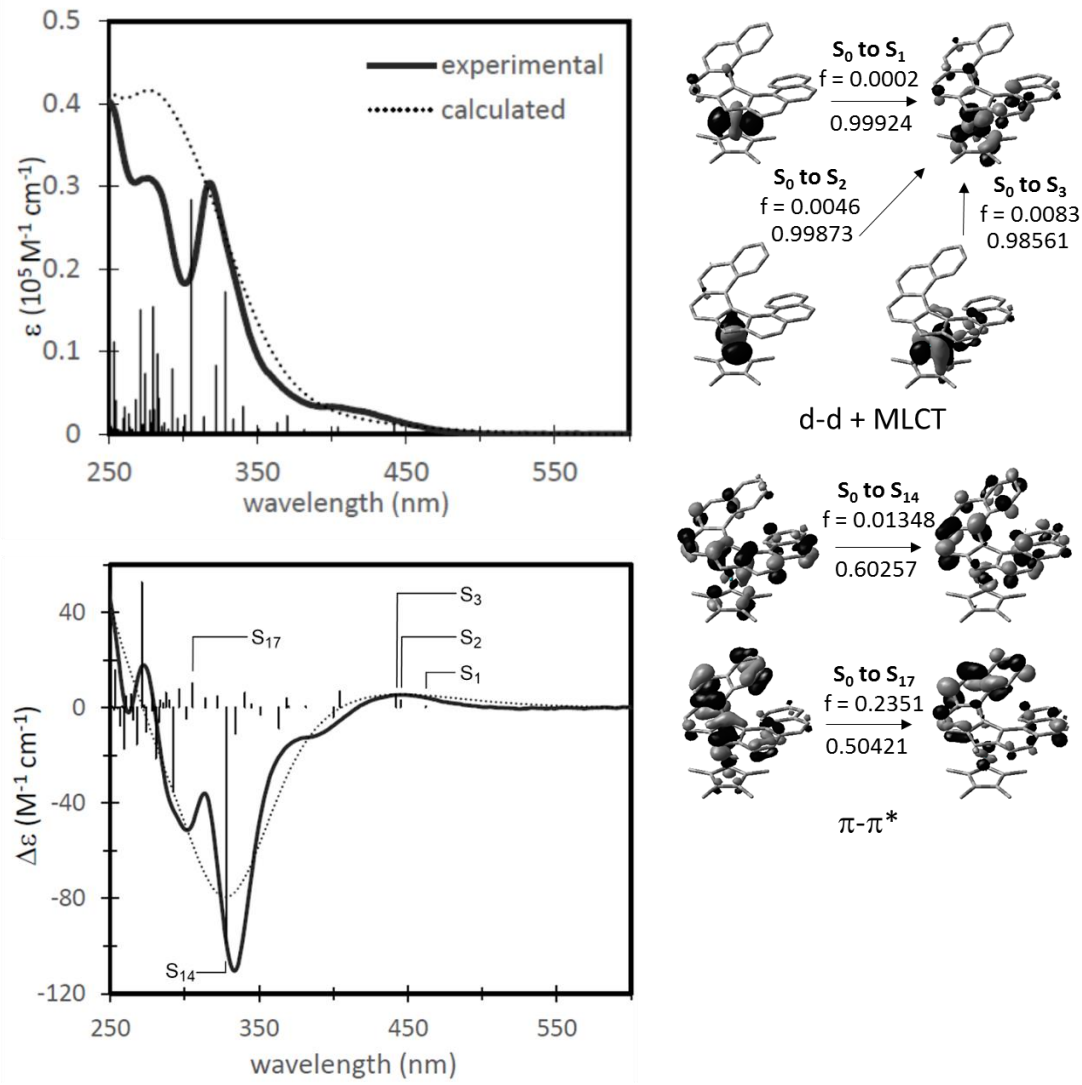

Figure 4-5. Experimental (solid line) and simulated (dotted line) UV-vis absorption and CD spectra, and selected singlet excitations of (*M*)-**1**. (Calculated by M06/LANL2DZ (Ru), 6-31G*)

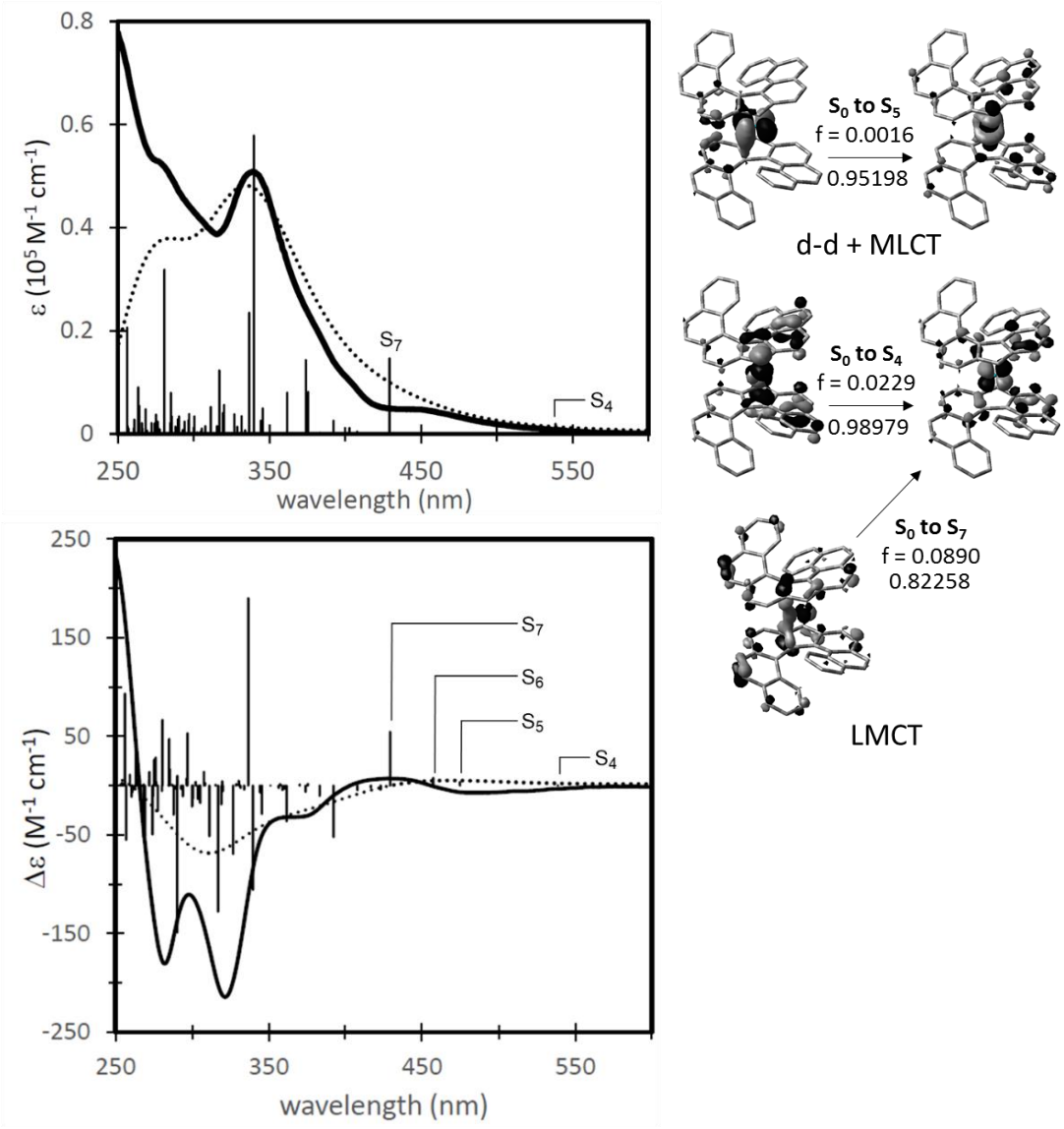

Figure 4-6. Experimental (solid line) and simulated (dotted line) UV-vis absorption and CD spectra, and selected singlet excitations of (*M*,*M*)-**2**. (Calculated by M06/LANL2DZ (Ru), 6-31G*)

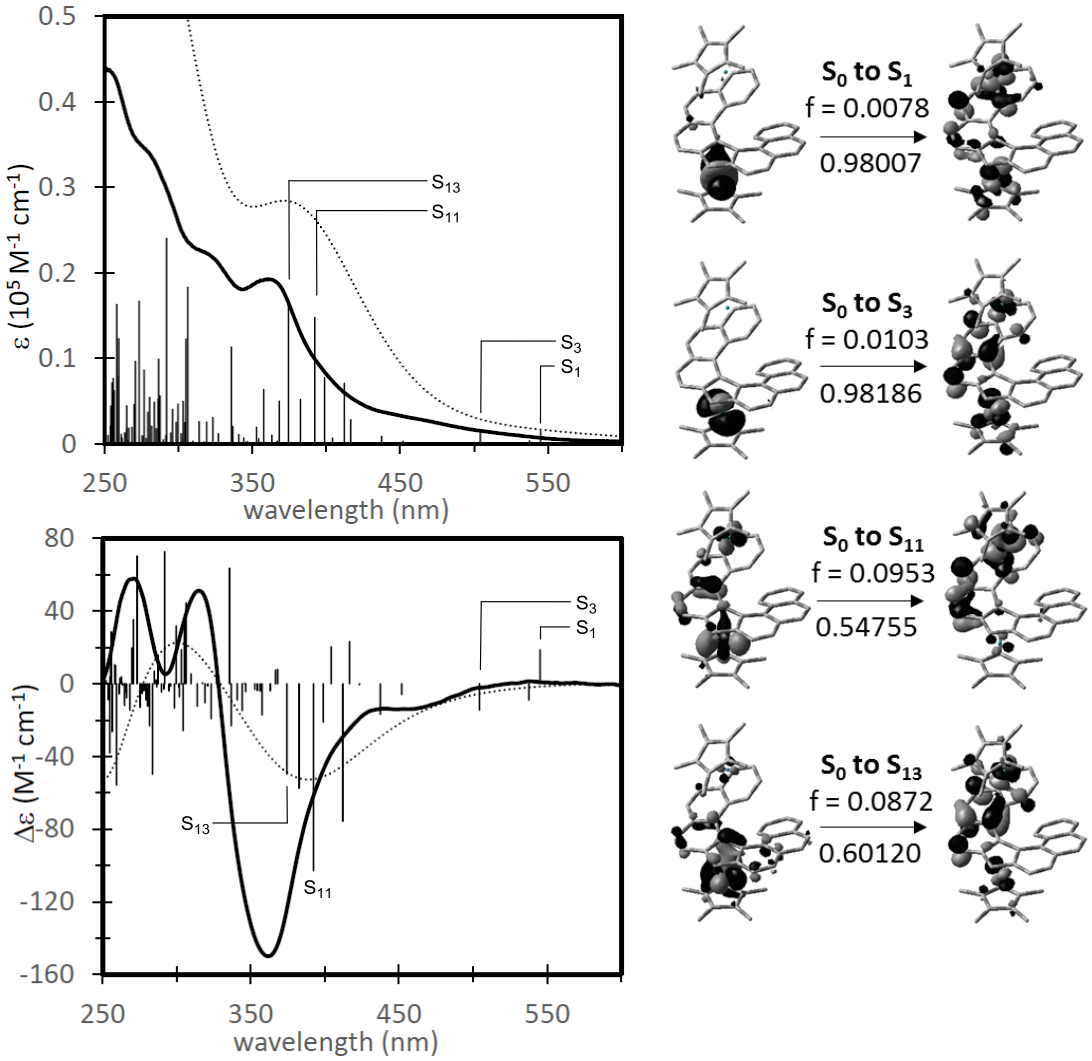

Figure 4-7. Experimental (solid line) and simulated (dotted line) UV-vis absorption and CD spectra, and selected singlet excitations of (*M*)-**3**. (Calculated by M06/LANL2DZ (Ru), 6-31G*)

4-6. Conclusions

Electronic, optical, and chiroptical properties of [7]helicene ruthenocenes were investigated. Experimental data well agree with the result of theoretical calculations. CV measurement showed that the oxidation potential of the ruthenium atom was changed by the coordination of [7]helicene ligand. Meanwhile, optical and chiroptical properties were affected by the interaction between π-

orbitals of [7]helicene and d-orbitals of the metal. In the case of bimetallic complex **3**, the cationic ruthenium atom on the arene moiety has a significant effect on both electronic and optical properties.

4-7. References

(1) Connelly, N. G.; Geiger, W. E. *Chem. Rev.* **1996**, *96*, 877–910.

(2) Rose-Munch, F.; Li, M.; Rose, E.; Daran, J. C.; Bossi, A.; Licandro, E.; Mussini, P. R. *Organometallics* **2012**, *31*, 92–104.

(3) Gilbert, A. M.; Katz, T. J.; Geiger, W. E.; Robben, M. P.; Rheingold, A. L. *J. Am. Chem. Soc.* **1993**, *115*, 3199–3211.

(4) Pammer, F.; Sun, Y.; Sieger, M.; Fiedler, J.; Sarkar, B.; Thiel, W. R. *Organometallics* **2010**, *29*, 6165–6168.

(5) Saleh, N.; Shen, C.; Crassous, J. *Chem. Sci.* **2014**, *5*, 3680.

(6) Shen, C.; Loas, G.; Srebro-Hooper, M.; Vanthuyne, N.; Toupet, L.; Cador, O.; Paul, F.; López Navarrete, J. T.; Ramírez, F. J.; Nieto-Ortega, B.; Casado, J.; Autschbach, J.; Vallet, M.; Crassous, J. *Angew. Chem. Int. Ed.* **2016**, 1–6.

(7) Gassman, P. G.; Winter, C. H. *J. Am. Chem. Soc.* **1988**, *110*, 6130–6135.

(8) Gubin, S. P.; Smirnova, S. A.; Denisovich, L. I.; Lubovich, A. A. *J. Organomet. Chem.* **1971**, *30*, 243–255.

(9) Koelle, U.; Salzer, A. *J. Organomet. Chem.* **1983**, *243*, C27–C30.

(10) Kolle, U.; Grub, J. *J. Organomet. Chem.* **1985**, *289*, 133–139.

(11) Swarts, J. C.; Nafady, A.; Roudebush, J. H.; Trupia, S.; Geiger, W. E. *Inorg. Chem.* **2009**, *48*, 2156–2165.

(12) Anger, E.; Rudolph, M.; Shen, C.; Vanthuyne, N.; Toupet, L. L.; Roussel, C.; Autschbach, J.; Crassous, J.; Réau, R.; Réau, R. *J. Am. Chem. Soc.* **2011**, *133*, 3800–3803.

(13) Martin, R. L. *J. Chem. Phys.* **2003**, *118*, 4775–4777.

Chapter 5.

Phosphorescence from Bimetallic [7]Helicene Ruthenocenes

5-1. Introduction

In this chapter, unexpected phosphorescence emission of [7]helicene bis-ruthenium complex **3** will be described.

As mentioned in **1-2-2**, various kinds of phosphorescent transition-metal complexes have been synthesized so far for the sake of application to optical materials. Although there are a number of ruthenium complexes showing phosphorescence, represented by $Ru(bpy)_3^{2+}$,[1–5] to the best of the author's knowledge, there is no precedents without any sp^2-nitrogen based ligand such as pyridine, phenanthroline, quinoline, and so on. For example, non-substituted ruthenocene showed very weak phosphorescence, in less than 3% quantum yield even at 25 K,[6] partly because the nonradiative deactivation through the stretching vibration of C–H bonds on the Cp ring.[7]

If an optically active compound shows photoluminescence, it is expected to show circularly polarized luminescence (CPL). Indeed, some of helicenes and helicene-like compounds exhibit CPL. Considering about the application of CPL to OLED materials, phosphorescence is better than fluorescence because the theoretical maximum value of quantum efficiency is much higher. Among several reports on circularly polarized phosphorescent OLED (CP-PHOLED) device,[8–10] one of the most successful examples was reported by Fuchter *et al.* in 2016.[10] The authors developed a circularly polarized phosphorescent OLED device using the Crassous' optically chiral platinahelicene complex as a CPL dopant,[11,12] and poly(vinylcarbazole) and 1,3-bis[2-(4-*tert*-butylphenyl)-1,3,4-oxadiazol-5-yl]benzene as hole and electron transport materials. This device showed the large *g*-value of 0.38, although the luminance and the power efficiency was below the current state-of-art. In the end of this report, Fuchter *et al.* stated the potential of helically chiral complexes as CP-PHOLED materials by mentioning as follows: "By developing new helically chiral metal complexes, devices with

different colors and higher efficiencies could be obtained. Additionally, the development of highly thermally stable complexes could allow the fabrication of vacuum sublimed devices. Such improvements, leading to bright and highly dissymmetric CP-PHOLEDS, are likely to have a large impact on future display technologies and other applications employing CP-light."

5-2. Photoluminescence properties

Monometallic complexes **1** and *rac*-**2** showed no luminescence at all even at 77 K like non-substituted ruthenocene.[6] On the other hand, the bimetallic complex **3** was found to exhibit a strong broad emission peak at around 650 nm at 77 K both in a butyronitrile solution and in a solid state (Figure 5-1). The lifetime of this emission was in 10 μs order, which was long enough to be characterized as phosphorescence. The quantum yield was 31% in a butyronitrile solution, and 18% in a solid state, respectively. These values were much higher than that of ruthenocene derivatives which have been reported so far.[6]

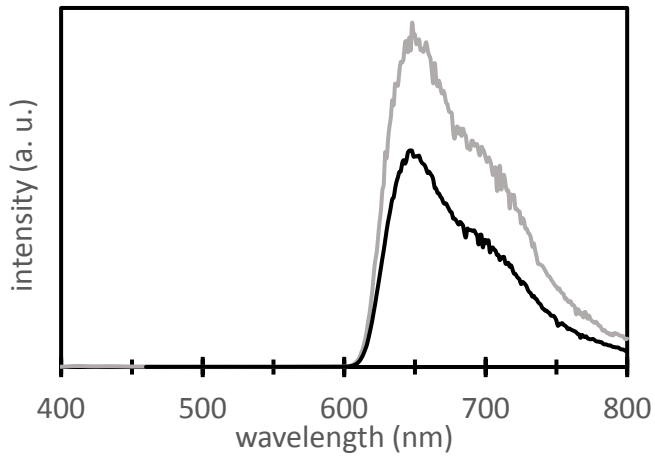

	Φ	life time
in BuCN	31%	71 μs, 43 μs (8:2)
crystal	18%	40 μs,12 μs (6:4)

Figure 5-1. Luminescence spectra of complex **3** (at 77 K, 4.0×10^{-4} M in *n*BuCN, excited at 360 nm (gray line) and 450 nm (black line))

CPL measurement was also conducted. As a result of the measurement using a dichloromethane solution of enantiopure **3** at room temperature, no significant peak was detected, probably because of the low quantum yield the phosphorescence at ambient temperature. Even the measurement with a ground solid of enantiopure **3** at 77 K, no larger peak than the detection limit ($g = 4.0 \times 10^{-4}$) was observed.

5-3. Theoretical investigations

TD-DFT and ΔSCF calculations at triplet state structures were performed to obtain mechanistic insight into the photoluminescent properties. It was suggested that the electron-transition between T_1 and S_0 in both complexes was derived from MLCT excited state of the ruthenium on the Cp moiety, involving the change in angular momentum of the d-orbital (Figure 5-2). In addition, the ruthenium on the arene moiety in complex **3** contributes to the electron-transition some extent. These characters of the electron transition are similar to those of HOMO-LUMO transition in each complex. It is implied that, as the HOMO-LUMO gap of complex **3** is smaller than that of **1**, the energy difference between T_1 and S_0 is smaller in complex **3** because of the contribution of d-orbital of the additional ruthenium on the arene ring. The smaller energy gap possibly prevents the thermal deactivation of an excited electron, leading to phosphorescence. Nonetheless, the magnitude of this contribution was largely dependent on the method used in calculations.

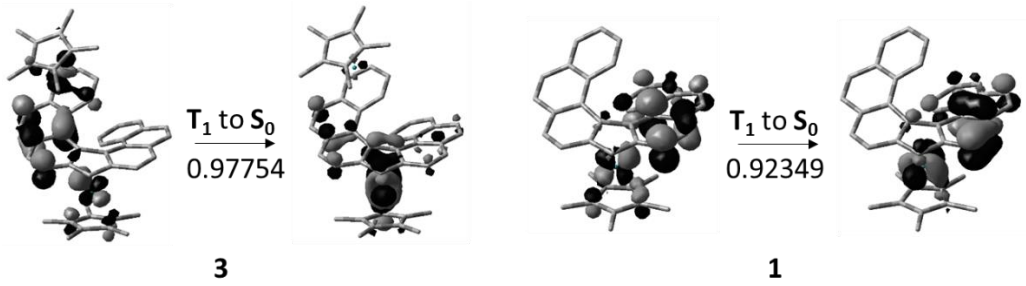

Figure 5-2. Electron transition from T_1 to S_0 in complex **3**, **1**. (Calculated by M06/LANL2DZ (Ru), 6-31G*)

5-4. Conclusions

Bimetallic ruthenium complexes **3** and **4** exhibited strong phosphorescence both in a solution and solid state. These are the first examples of phosphorescent Cp complexes, which show a new direction of Cp complexes serving as photoluminescence materials. Although the quantum yield of the emission and the thermal stability of the complexes were not enough to apply them to optical and chiroptical devices, designing new complexes based on this skeleton will improve the properties (see **7-4**).

5-5. References

(1) Adamson, A. W.; Demas, J. N. *J. Am. Chem. Soc.* **1971**, *93*, 1800–1801.

(2) Gafney, H.; Adamson, A. *J. Am. Chem. Soc.* **1972**, *94*, 8238–8239.

(3) Juris, A.; Balzani, V.; Barigelletti, F.; Campagna, S.; Belser, P.; von Zelewsky, A. *Coord. Chem. Rev.* **1988**, *84*, 85–277.

(4) Fanni, S.; Keyes, T. E.; O'Connor, C. M.; Hughes, H.; Wang, R.; Vos, J. G. *Coord. Chem. Rev.* **2000**, *208*, 77–86.

(5) Striplin, D. .; Crosby, G. . *Coord. Chem. Rev.* **2001**, *211*, 163–175.

(6) Wrighton, M. S.; Pdungsap, L.; Morse, D. L. *J. Phys. Chem.* **1975**, *79*, 66–71.

(7) Riesen, H.; Krausz, E.; Luginbühl, W.; Biner, M.; Güdel, H. U.; Ludi, A. *J. Chem. Phys.* **1992**, *96*, 4131.

(8) Zinna, F.; Giovanella, U.; Bari, L. Di. *Adv. Mater.* **2015**, *27*, 1791–1795.

(9) Li, T.-Y.; Jing, Y.-M.; Liu, X.; Zhao, Y.; Shi, L.; Tang, Z.; Zheng, Y.-X.; Zuo, J.-L. *Sci. Rep.* **2015**, *5*, 14912.

(10) Brandt, J. R.; Wang, X.; Yang, Y.; Campbell, A. J.; Fuchter, M. J. *J. Am. Chem. Soc.* **2016**, *138*, 9743–9746.

(11) Norel, L.; Rudolph, M.; Vanthuyne, N.; Gareth Williams, J. A.; Lescop, C.; Roussel, C.; Autschbach, J.; Crassous, J.; Réau, R. *Angew. Chem. Int. Ed.* **2010**, *49*, 99–102.

(12) Shen, C.; Anger, E.; Srebro, M.; Vanthuyne, N.; Deol, K. K.; Jefferson, T. D.; Muller, G.; Williams, J. A. G.; Toupet, L.; Roussel, C.; Autschbach, J.; Réau, R.; Crassous, J. *Chem. Sci.* **2014**, *5*, 1915.

Chapter 6.

Experimental Details

6-1. General methods

All air- and moisture-sensitive manipulations were carried out with standard Schlenk techniques or in a glove box under argon. NMR spectra were recorded on JEOL JNMECS400 or BRUKER Ascend500 spectrometers. Elemental analyses were performed by the One-stop Sharing Facility Center for Future Drug Discoveries, Department of Chemistry, Graduate School of Pharmaceutical Science, The University of Tokyo. Optical rotations were recorded on JASCO P-1030 polarimeters. UV-VIS spectra were recorded on SHIMADZU UV-3150 spectrometer.

Cyclic voltammetry measurements were performed in CH_2Cl_2 containing 10 m*M* of substrate and 0.1 *M* of Bu_4NBF_4 as supporting electrolyte at a scan rate of 100 mV/s using ALS/CHI 610C or 619Ep electrochemical analyzer. The counter and working electrodes were Pt wires, and the reference electrode was Ag/Ag^+. The potentials were corrected against Fc/Fc^+.

In single crystal X-ray diffraction analysis, a single crystal was mounted with mineral oil on a loop-type mount, and transferred to the goniometer of a Rigaku Saturn CCD diffractometer. The radiation was performed with graphite-monochromated Mo K_α (λ = 0.71075 Å). The structures were solved by direct method with (SHELXT 2014)[1] and refined by full-matrix least-squares techniques against F^2 (SHELXL 2014)[1]. The intensities were corrected for Lorentz and polarization effects. The non-hydrogen atoms were refined anisotropically. Hydrogen atoms were placed using AFIX instructions.

The computations were performed using workstation at Research Center for Computational Science, National Institutes of Natural Sciences, Okazaki, Japan. All the calculations were performed by using Gaussian 09 (revision C.1) program[2] by the B3LYP,[3] the CAM-B3LYP[4] or M06 method[5] with the LANL2DZ basis sets[6] (Ru) and the 6-31G* basis sets[7] (others). All structures were optimized without any symmetry assumptions. Zeropoint energy, enthalpy, and Gibbs free energy at 298.15 K and 1 atm were estimated from the gasphase

studies.

Tetrahydrofuran (THF), hexane and toluene were purified by passing through neutral alumina columns under argon. Potassium hydride was washed with pentane and dried in *vacuo* before use. Pentane (Wako Chemicals), hexanes (Kanto Chemicals), toluene (Wako Chemicals), diethylether (Et_2O, Kanto Chemicals), dichloromethane (DCM, Asahi Glass), and chloroform ($CHCl_3$, Kanto Chemicals) were used as received. [Cp*Ru(MeCN)$_3$]OTf,[8] $RuCl_2(dmso)_4$,[9] **LH**[10] were synthesized following the literature procedures.

6-2. Synthetic procedures

(*M*)-(η^5-Pentamethylcyclopentadienyl)(η^5-9*H*-cyclopenta[1,2-*c*:4,3-*c*']diphenanthrenyl)ruthenium (**1**).

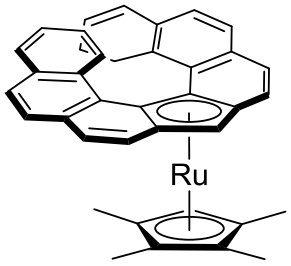

(*M*)-**1**

Potassium hydride (5.5 mg, 137 μmol) was added to a solution of (*M*)-**LH** (>99.5% ee, 15.1 mg, 41 μmol) in THF (0.5 mL). After stirring the mixture at room temperature for 30 min, the remaining solid was filtered off by a syringe filter and washed twice with THF (3 mL). [Cp*Ru(MeCN)$_3$]OTf (20.8 mg, 41 μmol) was added to the resulting solution, and the mixture was stirred for 1 h. Water was added and the solution was extracted with chloroform three times and dried over magnesium sulfonate. The crude mixture was purified by recrystallization from slow diffusion of pentane into a chloroform solution to afford (*M*)-**1** (yellow crystal, >99.5% ee,

19.2 mg, 78% yield). The optical purity of (*M*)-**1** was confirmed by chiral HPLC as written below. A crystal (yellow block) suitable for an X-ray diffraction analysis was obtained by recrystallization from slow evaporation of THF/hexanes solution. ^{1}H NMR (400 MHz, $CDCl_3$) δ 7.90 (brd, *J* = 8 Hz, 1H), 7.83–7.77 (m, 4H), 7.76–7.70 (m, 2H), 7.56 (brd, *J* = 8 Hz, 1H), 7.47 (brd, *J* = 8 Hz, 1H), 7.42–7.38 (m, 2H), 7.16 (brd, *J* = 9 Hz, 1H), 7.10 (brt, *J* = 7 Hz, 1H), 6.98 (brt, *J* = 7 Hz, 1H), 6.27 (brt, *J* = 7 Hz, 1H), 6.15 (brt, *J* = 7 Hz, 1H), 5.43 (brs, 1H), 1.05 (s, 15H); ^{13}C{^{1}H } NMR (100 MHz, $CDCl_3$) δ 132.1, 131.7 , 130.8, 130.7, 130.7, 130.2, 129.7, 128.5, 127.9, 126.6, 126.5, 126.2, 126.1, 125.9, 125.1, 125.0, 124.8, 124.7, 123.5, 122.3, 121.7, 121.4, 96.2, 93.9, 91.6, 82.4, 77.5, 66.3, 9.5; Anal. Calcd for $C_{39}H_{32}Ru$ (%): C, 77.84; H, 5.36. Found: C, 77.57; H, 5.50; Melting point was not observed; decomposition temperature 132 ºC; UV-vis (DCM) $\lambda_{max}(\varepsilon)$=281 (3000), 320 (3000), 400 nm (450); CD (DCM) $\lambda_{max}(\Delta\varepsilon)$= 272 (+18), 303 (−51), 334 (−110), 388 (−12), 446 nm (5.4); $[\alpha]_D^{23}$ = –1044, $[\phi]_D^{23}$ = –6282 (c = 0.1, $CHCl_3$). Synthesis of (*P*)-**1** and *rac*-**1** were accomplished by the same procedure using (*P*)-**LH** and *rac*-**LH** as starting materials. Purification of *rac*-**1** was done by recrystallization from slow evaporation of dichloromethane/hexanes solution, by which a crystal (yellow block) suitable for an X-ray diffraction analysis was obtained. The both enantiomers can be isolated by chiral HPLC; a Daicel Chiralpak IF-3 column with hexanes/DCM = 3/1, flow = 0.75 mL min^{-1}. Retention times: 6.1 min ((*P*)-**1**), 7.3 min ((*M*)-**1**).

(*M*,*M*)-Bis(η^5-9*H*-cyclopenta[1,2-*c*:4,3-*c*']diphenanthrenyl)ruthenium (**2**).

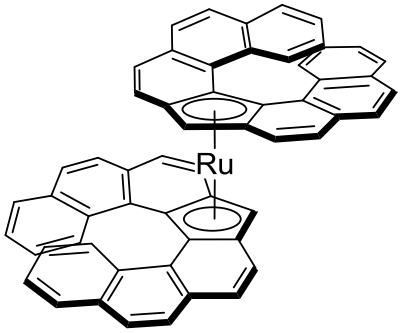

(*M*,*M*)-**2**

Potassium hydride (15.1 mg, 376 μmol) was added to a solution of (*M*)-**LH** (>99.5% ee, 40.1 mg, 109 μmol) in THF (5 mL). After stirring the mixture at room temperature for 30 min, the remaining solid was filtered off by a syringe filter and washed twice with THF (3 mL). The resulting solution was poured into a solution of $RuCl_2(dmso)_4$ (26.5 mg, 55 μmol) in THF (1 mL), and the mixture was stirred for 1 h. The solvent was removed under reduced pressure and the residue was extracted with benzene. The crude product was purified by silica-gel column chromatography using hexanes/dichloromethane (3:1) as the eluent to afford (*M*,*M*)-**2** (red powder, >99.5% ee, 13.1 mg, 29% yield). The optical purity of (*M*,*M*)-**2** was confirmed by chiral HPLC as written below. Further purification can be achieved by recrystallization from slow diffusion of pentane to a chloroform solution. ^{1}H NMR (400 MHz, $CDCl_3$) δ 8.26 (brd, *J* = 9 Hz, 2H), 7.87–7.82 (m, 4H), 7.77 (brd, *J* = 9 Hz, 2H), 7.72–7.66 (m, 4H), 7.41 (brd, *J* = 9 Hz, 2H), 7.22–7.17 (m, 2H), 7.09 (brd, *J* = 9 Hz, 2H), 6.97–9.89 (m, 4H), 6.71 (brd, *J* = 9 Hz, 2H), 6.46 (brd, *J* = 9 Hz, 2H), 6.37–6.29 (m, 4H), 6.12–6.07 (m, 2H), 5.08 (brs, 2H); ^{13}C{^{1}H } NMR (100 MHz, $CDCl_3$) δ 132.0, 131.5, 131.1, 131.0, 130.8, 130.8, 130.3, 129.1, 128.8, 128.3, 126.5, 126.5, 126.4, 125.8, 125.7, 125.4, 124.9, 124.5, 123.1, 122.8, 122.5, 122.2, 92.7, 92.3, 88.5, 74.1, 63.9; Anal. Calcd for $C_{58}H_{34}Ru$ (%): C, 83.73; H, 4.12. Found: C, 83.63; H, 4.51. Melting point was not observed; decomposition temperature 180 ºC; UV-vis (DCM) $\lambda_{max}(\varepsilon)$=339 (5100),

431 nm (490); CD (DCM) $\lambda_{max}(\Delta\varepsilon)$= 241 (+263), 282 (−180), 321 (−214), 370 (−32), 427 (7.1), 481 nm(−7.3); $[\alpha]_D^{23}$ = –1667, $[\phi]_D^{23}$ = –13870 (c = 0.1, $CHCl_3$). Synthesis of (*P*,*P*)-**2** was accomplished by the same procedure using (*P*)-**LH** as a starting material.

rac- and *meso*-**2**.

Potassium hydride (19.4 mg, 483 μmol) was added to a solution of *rac*-**LH** (>99.5% ee, 48.2 mg, 13.1 μmol) in THF (10 mL). After stirring the mixture at room temperature for 30 min, the remaining solid was filtered off by a syringe filter and washed twice with THF (3 mL). The resulting solution was poured into a solution of $RuCl_2(dmso)_4$ (32.2 mg, 6.6 μmol) in THF (1 mL), and the mixture was stirred for 1 hour. The solvent was removed under reduced pressure and the residue was extracted with toluene. The resulting crude mixture contained *rac*-**2**, *meso*-**2**, and **LH** in a 41:19:39 ratio, which was purified by silica-gel column chromatography using hexanes/dichloromethane (3:1) as eluent to afford mixture of *rac*-**2** and *meso*-**2** (red powder, 14.0 mg, 26%). Slow diffusion of Et_2O into a THF solution of the obtained mixture gave red solid mainly containing *meso*-**2** (solid **A**), and orange solution mainly containing *rac*-**2** (solution **B**). A crystal of *meso*-**2** (red block) suitable for an X-ray diffraction analysis was obtained by recrystallization from slow diffusion of diethyl ether into a toluene/THF solution of solid **A**. Solid **A** was further purified by slow reprecipitation from dichloromethane/Et_2O/pentane. The obtained red powder was washed with Et_2O and pentane three times and dried *in vacuo* to afford pure *meso*-**2** (0.8 mg). ^{1}H NMR (500 MHz, acetone-d_6/CS_2 (1:2)) δ 8.61–8.53 (m, 2H), 8.00–7.81 (m, 8H), 7.72–7.54 (m, 6H), 7.27–7.21 (m, 2H), 7.00–6.91 (m, 4H), 6.77–6.71 (m, 2H), 6.61–6.46 (m, 4H), 6.16–6.09 (m, 2H), 5.61–5.55 (m, 2H), 4.80–4.75 (m, 2H); ^{13}C{^{1}H} NMR (126 MHz, acetone-d_6/CS_2 (1:2)) δ 132.2, 131.9, 131.4, 131.0, 130.8, 130.5, 129.9, 129.6, 129.0, 128.2, 127.1, 126.9, 126.8, 126.5, 126.4, 126.4, 125.7, 125.1, 123.7, 123.6, 123.0, 122.4, 122.1,

93.4, 91.0, 87.6, 74.4, 66.0. A crystal of *rac*-**2** (red block) suitable for an X-ray diffraction analysis was obtained by recrystallization from slow diffusion of pentane into a chloroform solution of the concentrated solution **B**. It was possible to separate both enantiomers of *rac*-**2** by chiral HPLC; a Daicel Chiralpak IF-3 column with hexanes/DCM = 3/1, flow = 0.75 mL min^{-1}. Retention times: 9.4 min ((*P*,*P*)-**2**), 13.1 min ((*M*,*M*)-**2**).

(*M*)-(η^5-Pentamethylcyclopentadienyl)(η^5-9*H*-cyclopenta[1,2-*c*:4,3-*c*']diphenanthrenyl)iron (**1$_{Fe}$**).

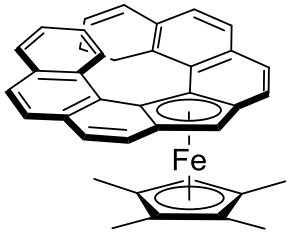

(*M*)-**1$_{Fe}$**

[Cp*Fe(MeCN)$_3$]OTf (156 μmol) was added to a solution of deprotonated (*M*)-**LH** (>99.5% ee, 117 μmol) in Et_2O (2 mL). After stirring the mixture at room temperature for 1 h, the remaining solid was filtered off by a syringe filter and washed twice with Et_2O (3 mL). The remaining solution was concentrated and purified by size exclusion column chromatography (using Bio-Beads S-X1 Support (BIO-RAD), under Ar atmosphere, THF) to afford (*M*)-**1$_{Fe}$** (red solid, 3% NMR yield). Further purification was done by recrystallization from slow evaporation of Et_2O (red crystal). ^{1}H NMR (400 MHz, THF-d8) δ 8.50 (brd, *J* = 9 Hz, 1H), 7.91–7.80 (m, 5H), 7.76–7.71 (m, 3H), 7.66 (brd, *J* = 8 Hz, 1H), 7.62 (brd, *J* = 9 Hz, 1H), 7.17–7.14 (m, 1H), 6.96–6.88 (m, 2H), 6.40–6.36 (m, 1H), 6.08–6.03 (m, 1H), 5.19 (brs, 1H), 1.11 (s, 15H); ^{13}C{^{1}H } NMR (125 MHz, THF-d8) δ 133.7, 133.6, 133.0, 132.8, 132.7, 132.5, 131.8, 131.5, 130.7, 129.1, 128.8, 128.4, 127.6, 127.5, 127.2, 127.1, 126.9, 126.1, 126.0, 125.8, 125.5, 124.2, 122.9, 122.2, 93.0, 90.2, 89.1, 78.1, 74.2, 64.5, 9.5; HRMS-ESI$^+$ (*m*/*z*) calcd for $C_{39}H_{32}Fe$ ([M])

556.1853, found 556.1856.

rac-{μ-[1(1–4,4a,17f-η):2(8a,9,9a,17c,17d-η)]-9*H*-Cyclopenta[1,2-*c*:4,3-*c*']diphenanthrenyl} bis[(η^5-pentamethylcyclopentadienyl)ruthenium(II)] triflate (*rac*-**3**)

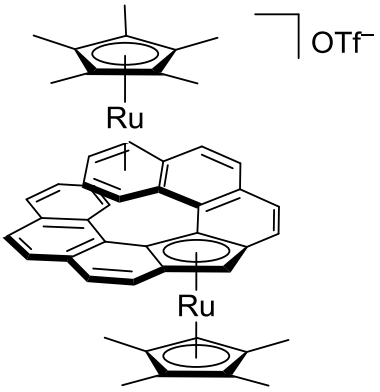

rac-**3**

Potassium hydride (9.5 mg, 237 μmol) was added to a solution of *rac*-**LH** (20.0 mg, 54 μmol) in THF (0.5 mL). After stirring the mixture at room temperature for 1 h, the remaining solid was filtered off by a syringe filter and washed twice with THF (2 mL). [Cp*Ru(MeCN)$_3$]OTf (55.6 mg, 109 μmol) was added to the resulting solution, and the mixture was stirred for 1 h. Hexane (10 mL) was added to the solution and the resulting solid was collected by filtration on Celite®. The solid was extracted with toluene (20 mL) and concentrated to afford *rac*-**3** (39.2 mg, 68% yield). Further purification was done by recrystallization from slow diffusion of pentane into a THF solution (red crystal, 26.6 mg, 49% yield). The obtained crystal was analyzed by x-ray diffraction analysis. Contained solvent molecules were squeezed. 1H NMR analysis showed the crystal contained 0.5 THF and 0.17 pentane for one *rac*-**3**. ^{1}H NMR (500 MHz, CD_3CN) δ 8.16–8.11 (m, 2H), 7.99–7.90 (m, 3H), 7.80 (brd, *J* = 8 Hz, 1H), 7.70 (brd, *J* = 9 Hz, 1H), 7.56–7.53 (m, 2H), 7.50 (brd, *J* = 8 Hz, 1H), 6.50 (brt, *J* = 8 Hz, 1H), 6.30 (brd, *J* = 6 Hz, 1H), 5.69–5.67

(m, 2H), 5.53 (brt, *J* = 6 Hz, 1H), 4.68 (brt, *J* = 6 Hz, 1H), 1.12 (s, 15H), 1.09 (s, 15H); $^{13}C\{^{1}H\}$ NMR (125 MHz, CD_3CN) δ 133.35, 132.80,132.75,132.36, 131.61, 131.16, 130.38, 129.73, 126.59, 126.11, 124.85, 124.56, 123.55, 122.12 (q, *J* = 322 Hz), 121.30, 102.89, 98.51, 94.16, 93.52, 93.30, 92.49, 88.67, 85.17, 84.99, 83.83, 83.54, 77.96, 67.37, 9.61, 9.24; Anal. Calcd for $C_{50}H_{47}Ru_2O_3SF_3$+0.5 THF+0.17 pentane (%): C, 61.31; H, 5.16. Found: C, 61.24; H, 5.22; Melting point was not observed; decomposition temperature 140 ºC; UV-vis (DCM) $\lambda_{max}(\varepsilon)$=360 (19200), 450 (3325).

Synthesis of (*P*)-**3** and (*M*)-**3** was accomplished by the same procedure using (*P*)-**LH** and (*M*)-**LH** as starting materials. Purification of enantiomers of **3** were done by recrystallization from slow evaporation of THF/hexane solution (red block). CD of (*M*)-**3** (DCM) $\lambda_{max}(\Delta\varepsilon)$= 271 (+58), 315 (+51), 363 (−150), 450 (−14); $[\alpha]_D^{23}$ = –2900, $[\phi]_D^{23}$ = –28000 (c = 0.1, $CHCl_3$)

6-3. Estimation of the barrier of isomerization from *rac*-**2** to *meso*-**2**.

A solution of *rac*-**2** (3 mM) in a Schlenk tube was heated at a constant temperature under argon atmosphere (Scheme 6-1). An aliquot was taken in the time course and the *rac*-**2**/*meso*-**2** ratio was analyzed by ^{1}H NMR spectroscopy. The equilibrium constant (K) was determined from the ratio of the isomers converged after the specific time. The experimental variables were treated by regression analysis and the corresponding kinetic constant (k) was calculated within the frame of reversible first-order kinetics: $\ln([rac\text{-}\mathbf{2}]/[rac\text{-}\mathbf{2}]_0) = -kt+C$.

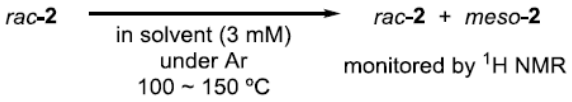

- at 100 °C, in toluene. K = 0.35, k = 0.0014.

t (h)	*rac*	*meso*
0	1	0
24	0.94	0.06
96	0.84	0.16
192	0.74	0.26
264	0.77	0.23

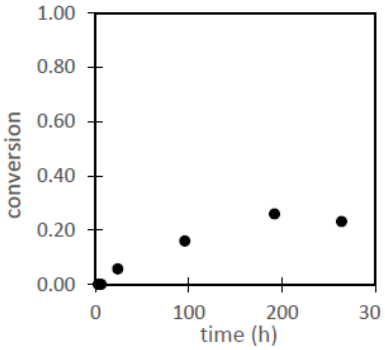

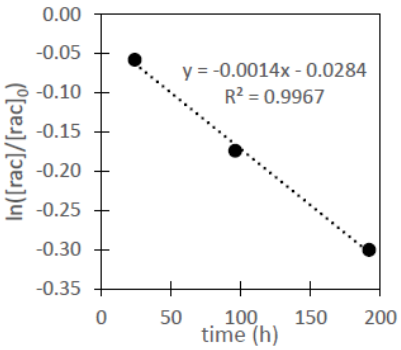

- at 110 °C, in p-xylene. K = 0.38, k = 0.0034.

t (h)	*rac*	*meso*
0	1	0
5.5	0.89	0.11
18	0.83	0.17
60	0.74	0.26
128	0.72	0.28

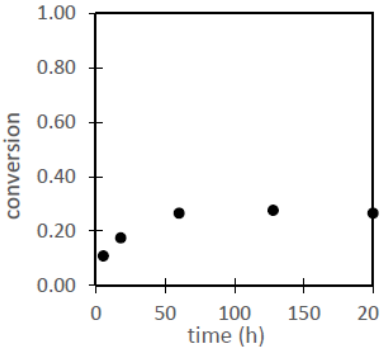

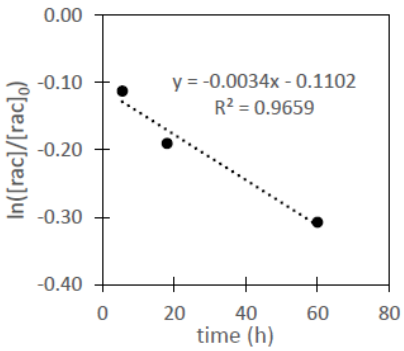

- at 122 °C, in p-xylene. K = 0.42, k = 0.0237.

t (h)	*rac*	*meso*
0	1	0
1	0.97	0.03
2	0.93	0.07
3	0.90	0.10
6	0.85	0.15
9	0.78	0.22
12	0.75	0.25
24	0.70	0.30
61	0.70	0.30

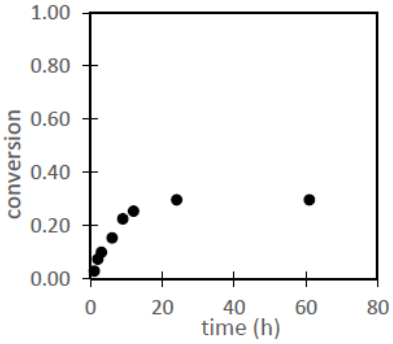

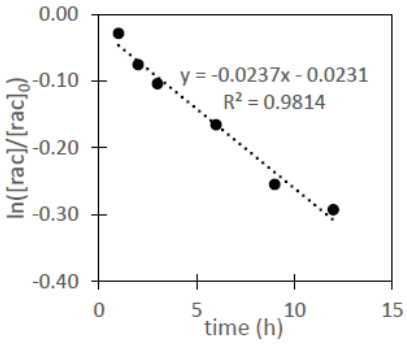

- at 150 °C, in mesitylene. K = 0.50, k = 0.3619.

t (h)	*rac*	*meso*
0	1	0
0.25	0.83	0.17
0.5	0.72	0.28
0.75	0.69	0.31
1	0.68	0.32
4	0.68	0.32
18	0.67	0.33
42	0.67	0.33

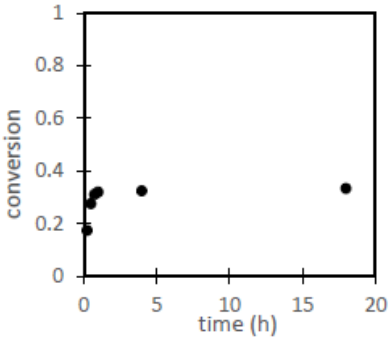

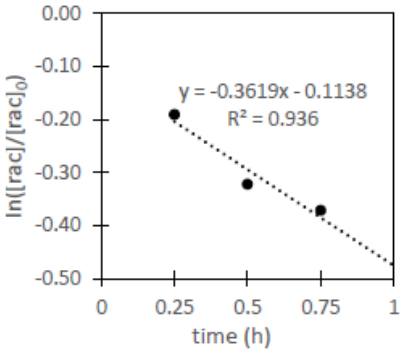

Summary of equilibrium constants and isomerization rate.

T	K	k (h^{-1})
373	0.35	0.0014
383	0.38	0.0034
395	0.42	0.0237
423	0.5	0.3619

Van't Hoff plot and Eyring plot.

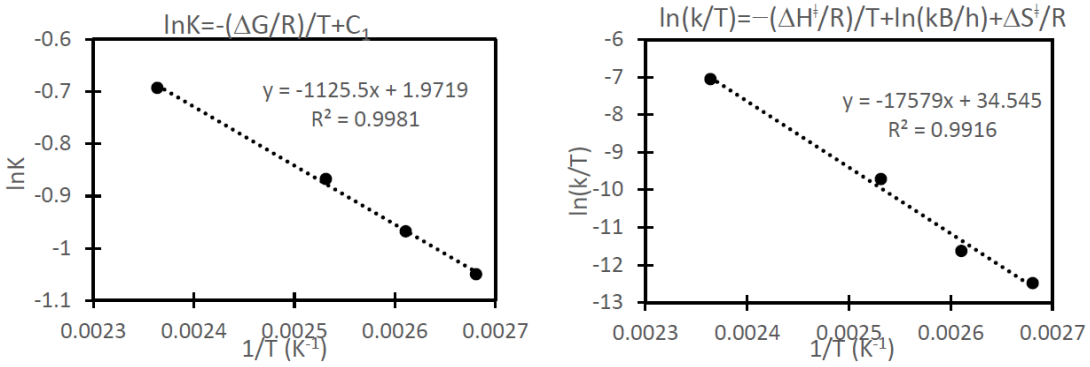

$\Delta H = 1125.5\ K \times 8.31\ J\ K^{-1}\ mol^{-1} = 9353\ J\ mol^{-1} = \underline{2.24\ kcal\ mol^{-1}}$

$\Delta S = 1.9719 \times 8.31\ J\ K^{-1}\ mol^{-1} = 16.4\ J\ K^{-1}\ mol^{-1} = \underline{3.8\ cal\ K^{-1}\ mol^{-1}}$

$\Delta G\ (400\ K) = 9353\ J\ mol^{-1} - 16.4\ J\ K^{-1}\ mol^{-1} \times 400\ K = 2793\ J\ mol^{-1} = \underline{667\ cal\ mol^{-1}}$

$\Delta H^{\ddagger} = 17579\ K \times 8.31\ J\ K^{-1}\ mol^{-1} = 146\ kJ\ mol^{-1} = \underline{34.9\ kcal\ mol^{-1}}$

$\Delta S^{\ddagger} = (-\ln(k_B/h) + 34.545) \times 8.31\ J\ K^{-1}\ mol^{-1} = +10.8\ J\ mol^{-1} = \underline{+2.6\ cal\ K^{-1}\ mol^{-1}}$

$\Delta G^{\ddagger}\ (400\ K) = 146\ kJ\ mol^{-1} - 10.8\ J\ K^{-1}\ mol^{-1} \times 400\ K = 142\ kJ\ mol^{-1} = \underline{33.9\ kcal\ mol^{-1}}$

To clarify the isomerization mechanism, we tested if the thermal isomerization could occur with enantiopure **2**.

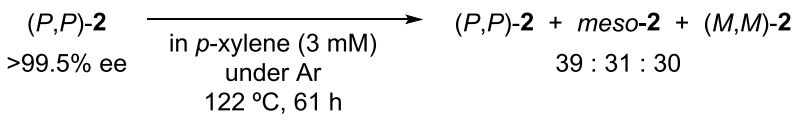

6-4. Investigation of phosphorescence from complex **3**.

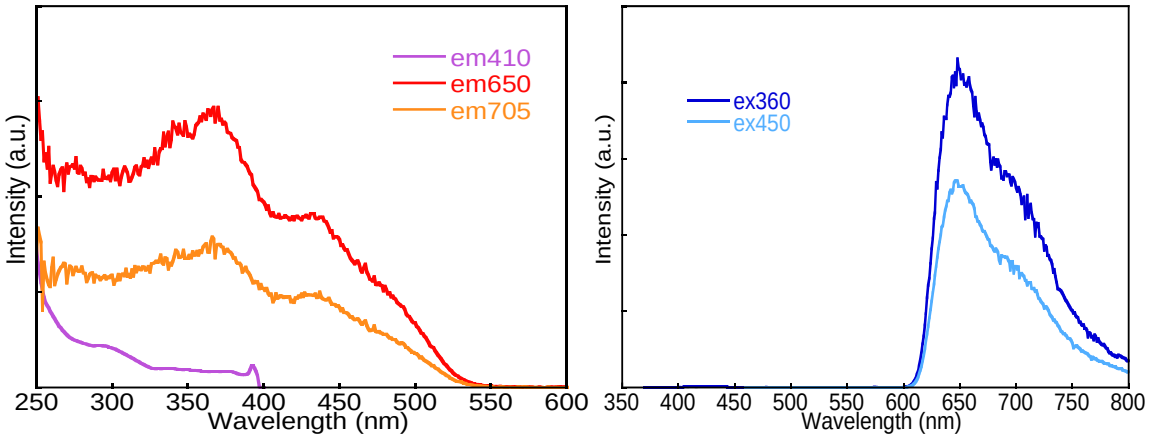

Excitation and emission spectra of **3** in concentrated solution (4.0×10^{-4} M in *n*BuCN, 77 K)

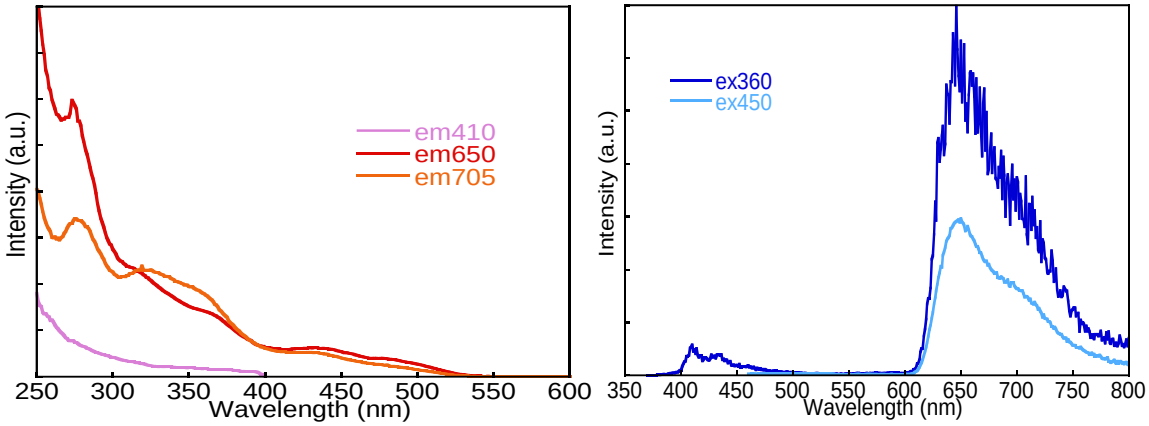

Excitation and emission spectra of **3** in diluted solution (4.0×10^{-5} M in *n*BuCN, 77 K)

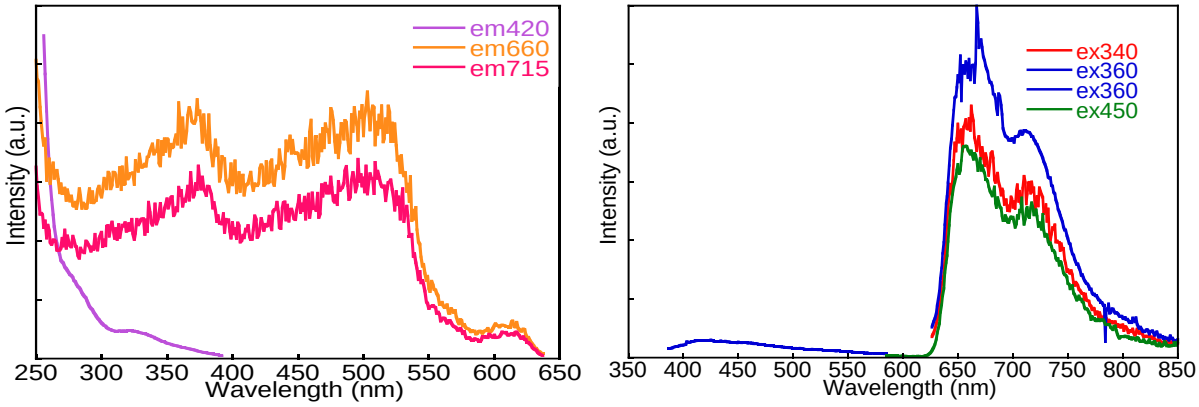

Excitation and emission spectra of **3** in solid state (77 K)

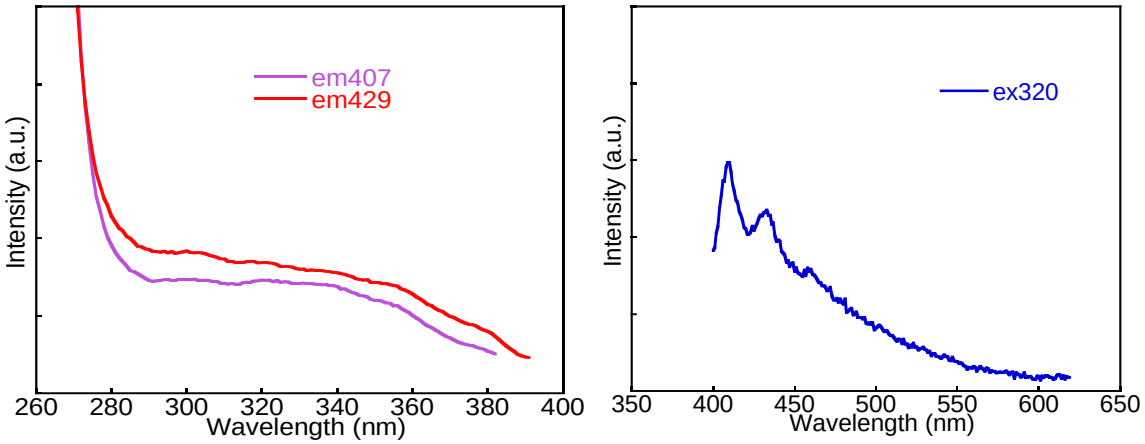

Excitation and emission spectra of **1** (2.6×10^{-4} M in *n*BuCN, 77 K)

(a)

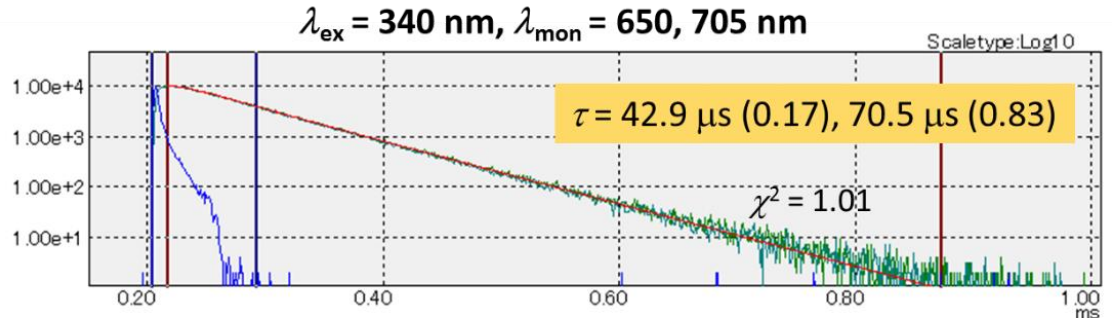

(b)

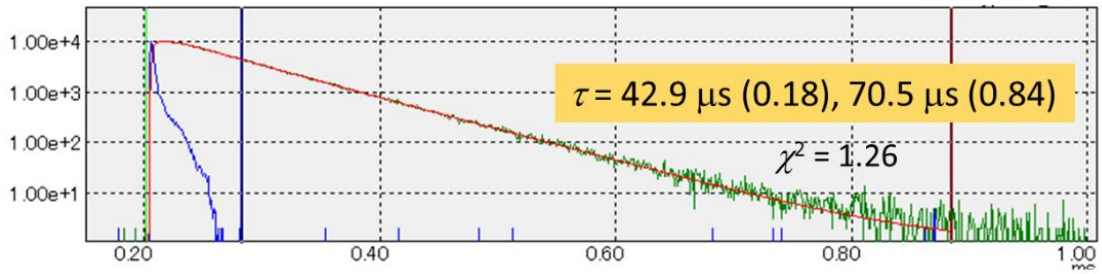

(c)

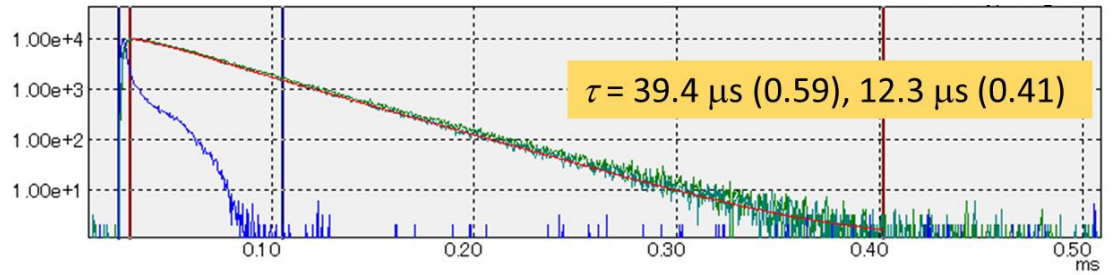

Lifetime measurement of emission from **3**

(a) 4.0×10^{-4} M in *n*BuCN, 77 K. (b) 4.0×10^{-5} M in *n*BuCN, 77 K. (c) solid, 77 K.

6-5. X-ray single crystal analysis

rac-**1**

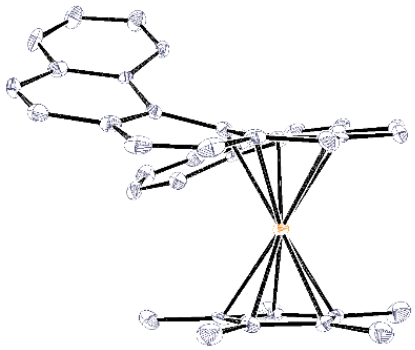

50% thermal ellipsoid. Hydrogen atoms are omitted for clarity.

Formula	$C_{39}H_{32}Ru$	
Formula weight	601.72	
Temperature	93(2) K	
Wavelength	0.71075 Å	
Crystal system	monoclinic	
Space group	$P2_1/c$	
Unit cell dimensions	a = 13.106(3) Å	α = 90 °
	b = 9.570(2) Å	β = 99.867(3) °
	c = 22.256(6) Å	γ = 90 °
Volume	2750.2(11) Å^3	
Z	4	
Density (calculated)	1.453 Mg/cm^3	
Absorption coefficient	0.598 mm^{-1}	
F(000)	1240	
Crystal size	0.10 × 0.08 × 0.01 mm^3	
Theta range for data collection	1.86 to 25.00 °	
Index ranges	–15<=h<=15, –9<=k<=9, –26<=l<=26	
Reflections collected	35916	
Independent reflections	4595	
R_{int}	0.0695	
Max. and min. transmission	0.9940, 0.9427	
Data / restraints / parameters	4595 / 0 / 399	
Goodness-of-fit on F^2	1.307	
Final R indices [I>2sigma(I)]	R_1 = 0.0598, wR_2 = 0.1006	
R indices (all data)	R_1 = 0.0636, wR_2 = 0.1043	
Absolute structure parameter	---	
Largest diff. peak and hole	0.493 and –1.132 e/Å^3	

(*M*)-**1**

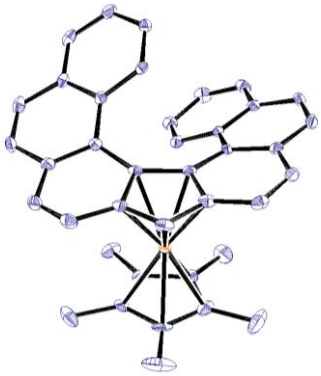

50% thermal ellipsoid. Hydrogen atoms are omitted for clarity.

Formula	$C_{39}H_{32}Ru$	
Formula weight	601.72	
Temperature	93(2) K	
Wavelength	0.71075 Å	
Crystal system	orthorhombic	
Space group	$P2_12_12_1$	
Unit cell dimensions	a = 8.9794(14) Å	α = 90 °
	b = 13.414(2) Å	β = 90 °
	c = 23.349(4) Å	γ = 90 °
Volume	2812.4(8) Å^3	
Z	4	
Density (calculated)	1.421 Mg/cm^3	
Absorption coefficient	0.584 mm^{-1}	
F(000)	1240	
Crystal size	0.40 × 0.10 × 0.02 mm^3	
Theta range for data collection	2.31 to 25.00 °	
Index ranges	–10<=h<=10, –15<=k<=15, –27<=l<=27	
Reflections collected	11109	
Independent reflections	4837	
R_{int}	0.0261	
Max. and min. transmission	0.9884, 0.7999	
Data / restraints / parameters	4837 / 0 / 366	
Goodness-of-fit on F^2	1.156	
Final R indices [I>2sigma(I)]	R_1 = 0.0598, wR_2 = 0.1006	
R indices (all data)	R_1 = 0.0636, wR_2 = 0.1043	
Absolute structure parameter	–0.022(27)	
Largest diff. peak and hole	0.440 and –0.506 e/Å^3	

***rac*-2**

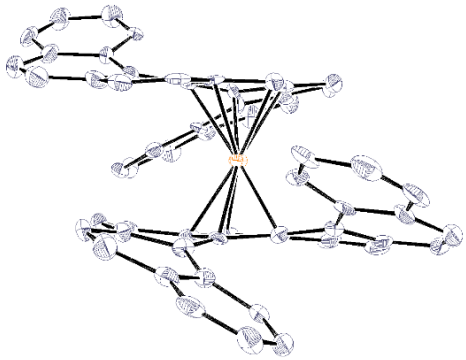

50% thermal ellipsoid. Hydrogen atoms are omitted for clarity.

Formula	$C_{58}H_{34}Ru$	
Formula weight	831.98	
Temperature	93(2) K	
Wavelength	0.71075 Å	
Crystal system	monoclinic	
Space group	*C2*	
Unit cell dimensions	a = 38.88(2) Å	α = 90 °
	b = 8.126(4) Å	β = 115.831(8) °
	c = 27.965(15) Å	γ = 90 °
Volume	7952(7) Å^3	
Z	8	
Density (calculated)	1.390 Mg/cm^3	
Absorption coefficient	0.436 mm^{-1}	
F(000)	3408	
Crystal size	0.28 × 0.13 × 0.01 mm^3	
Theta range for data collection	2.187 to 27.500 °	
Index ranges	–50<=h<=50, –10<=k<=10, –36<=l<=36	
Reflections collected	61644	
Independent reflections	18140	
R_{int}	0.1109	
Completeness to theta = 25.242	99.9%	
Data / restraints / parameters	18140 / 37 / 1079	
Goodness-of-fit on F^2	1.097	
Final R indices [I>2sigma(I)]	R_1 = 0.0879, wR_2 = 0.1404	
R indices (all data)	R_1 = 0.1030, wR_2 = 0.1485	
Absolute structure parameter	0.87(3)	
Largest diff. peak and hole	0.858 and –1.1650 e/Å^3	

meso-**2** containing two THF atoms

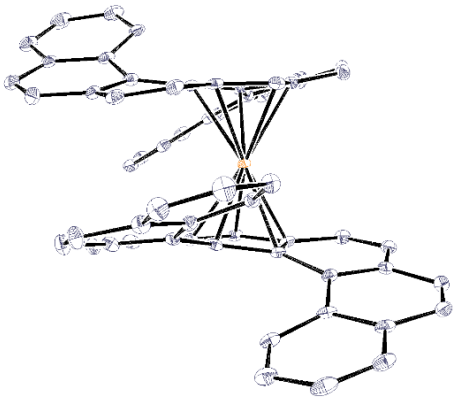

50% thermal ellipsoid. Hydrogen atoms and two THFs are omitted for clarity.

Formula	$C_{66}H_{50}Ru$	
Formula weight	976.13	
Temperature	93(2) K	
Wavelength	0.71075 Å	
Crystal system	monoclinic	
Space group	*P2*	
Unit cell dimensions	a = 9.9254(15) Å	α = 90 °
	b = 15.982(2) Å	β = 107.910(2) °
	c = 14.882(5) Å	γ = 90 °
Volume	2246.3(5) Å^3	
Z	2	
Density (calculated)	1.443 Mg/cm^3	
Absorption coefficient	0.400 mm^{-1}	
F(000)	1012	
Crystal size	0.11 × 0.05 × 0.04 mm^3	
Theta range for data collection	2.877 to 27.498 °	
Index ranges	–12<=h<=12, –20<=k<=20, –19<=l<=19	
Reflections collected	27277	
Independent reflections	10077	
Completeness to theta = 25.242	99.5%	
Max. and min. transmission	1.000, 0.906	
Data / restraints / parameters	10077 / 43 / 668	
Goodness-of-fit on F^2	1.033	
Final R indices [I>2sigma(I)]	R_1 = 0.0307, wR_2 = 0.0672	
R indices (all data)	R_1 = 0.0326, wR_2 = 0.0683	
Absolute structure parameter	0.487(9)	
Largest diff. peak and hole	0.315 and –0.684 e/Å^3	

(*M*)-**1**$_{Fe}$

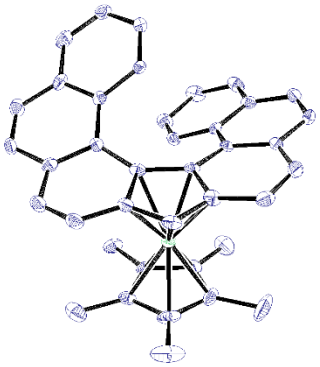

50% thermal ellipsoid. Hydrogen atoms are omitted for clarity.

Formula	$C_{39}H_{32}Fe$	
Formula weight	556.49	
Temperature	93(2) K	
Wavelength	0.71075 Å	
Crystal system	orthorhombic	
Space group	$P2_12_12_1$	
Unit cell dimensions	a = 8.727(3) Å	α= 90 °
	b = 13.550(4) Å	β= 90 °
	c = 23.393(7) Å	γ = 90 °
Volume	2766.2(15) Å^3	
Z	4	
Density (calculated)	1.336 Mg/m^3	
Absorption coefficient	0.572 mm^{-1}	
F(000)	1168	
Crystal size	0.13 × 0.11 × 0.01 mm^3	
Theta range for data collection	2.491 to 25.000 °	
Index ranges	-10<=h<=10, -16<=k<=16, -27<=l<=27	
Reflections collected	36318	
Independent reflections	4866	
Completeness to theta = 25.242	97.2 %	
Data / restraints / parameters	4866 / 0 / 366	
Goodness-of-fit on F^2	1.095	
Final R indices [I>2sigma(I)]	R_1 = 0.0487, wR_2 = 0.0934	
R indices (all data)	R_1 = 0.0542, wR_2 = 0.0960	
Absolute structure parameter	0.050(10)	
Largest diff. peak and hole	0.301 and -0.345 e/Å^3	

rac-**3**

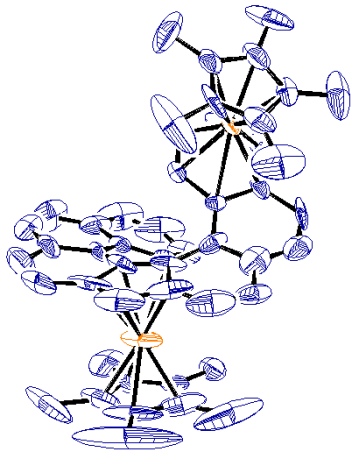

30% thermal ellipsoid. Hydrogen atoms and triflate are omitted for clarity.

Formula	$C_{57}H_{47}F_3O_3Ru_2S$	
Formula weight	987.07	
Temperature	93(2) K	
Wavelength	0.71075 Å	
Crystal system	'monoclinic'	
Space group	'$P2_1/c$'	
Unit cell dimensions	a = 12.569(5) Å	α = 90 °
	b = 22.7095(10) Å	β = 95.332(9) °
	c = 16.208(7) Å	γ = 90 °
Volume	4606(3) Å^3	
Z	4	
Density (calculated)	1.423 Mg/cm^3	
Absorption coefficient	0.753 mm^{-1}	
F(000)	2008	
Crystal size	0.10 × 0.08 × 0.01 mm^3	
Theta range for data collection	2.193 to 24.999 °	
Index ranges	-14<=h<=14, -26<=k<=26, -19<=l<=19	
Reflections collected	47657	
Independent reflections	8094	
R_{int}	0.1160	
Data / restraints / parameters	8094 / 6 / 546	
Goodness-of-fit on F^2	1.133	
Final R indices [I>2sigma(I)]	R_1 = 0.1274, wR_2 = 0.2691	
R indices (all data)	R_1 = 0.1634, wR_2 = 0.2950	
Largest diff. peak and hole	3.087 and –2.826 e/Å^3	

A disordered pentane molecule was squeezed by using PLATON.

6-6. NMR spectra

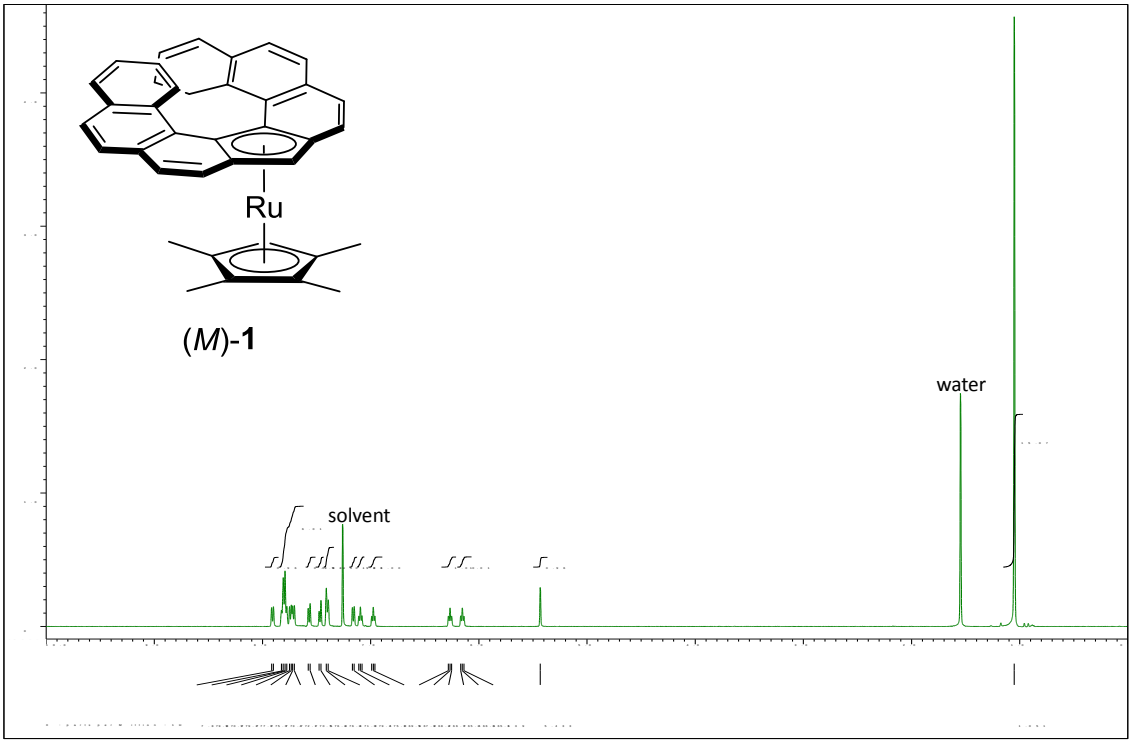

^{1}H NMR spectrum of (*M*)-**1** (400 MHz, $CDCl_3$).

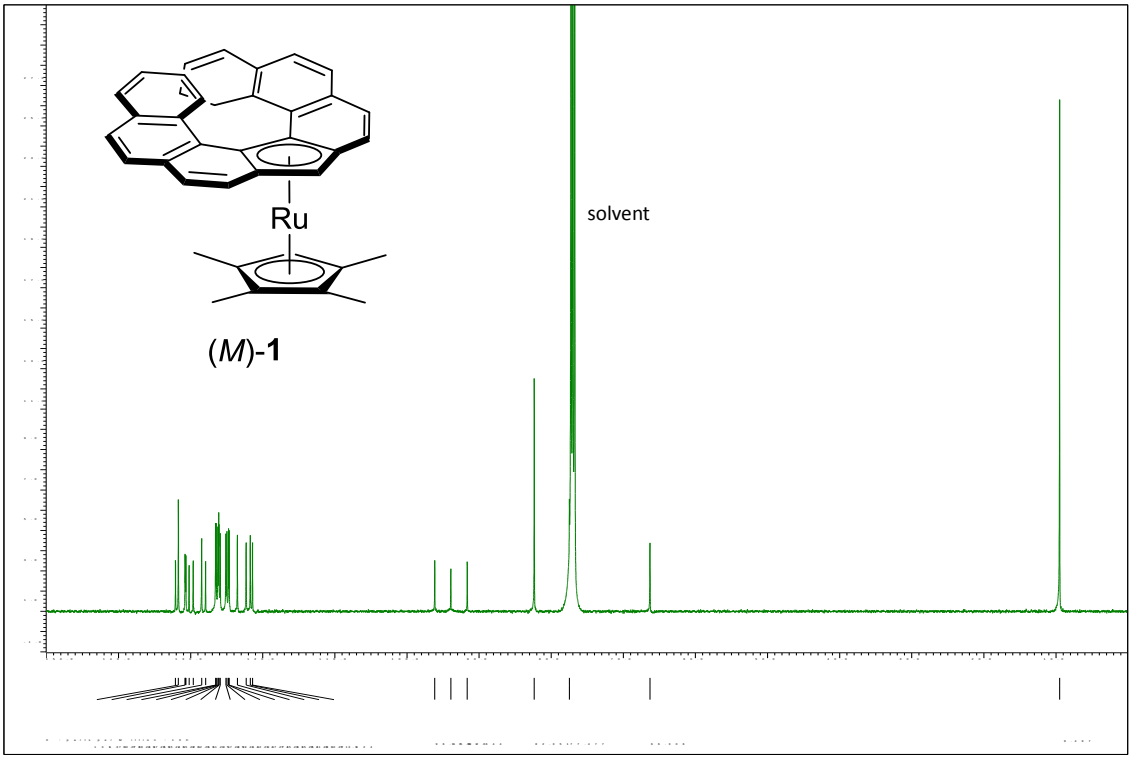

^{13}C{^{1}H } NMR spectrum of (*M*)-**1** (100 MHz, $CDCl_3$).

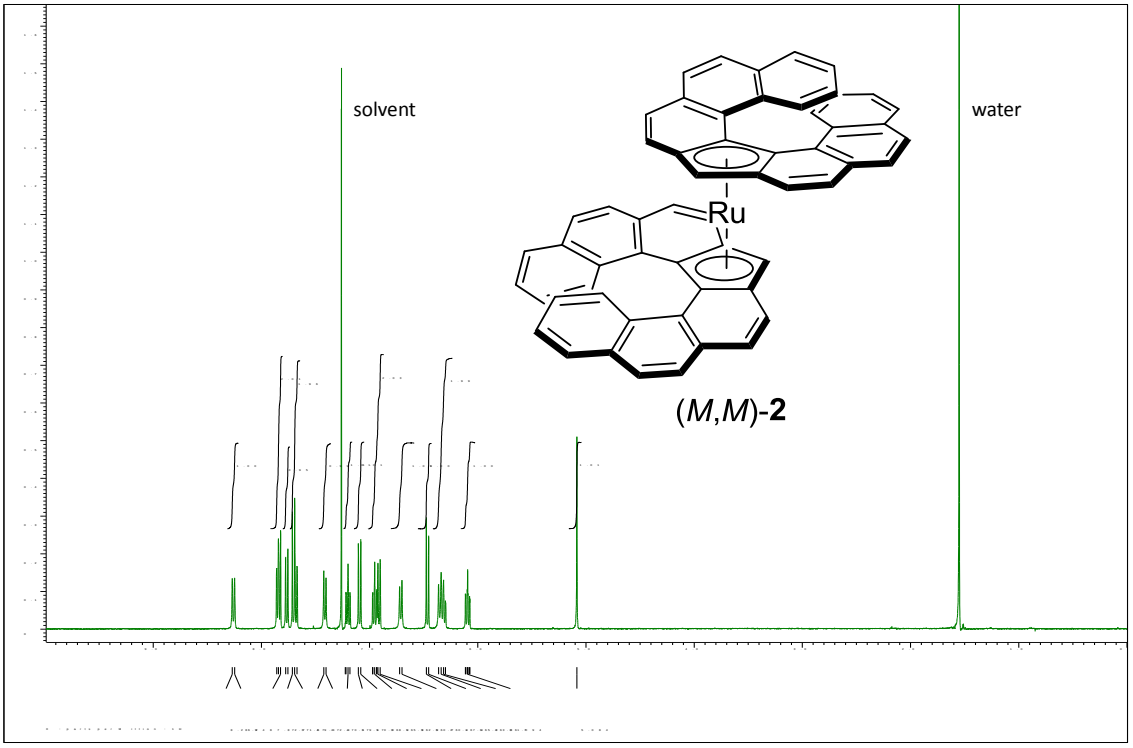

^{1}H NMR spectrum of (*M*,*M*)-**2** (400 MHz, $CDCl_3$).

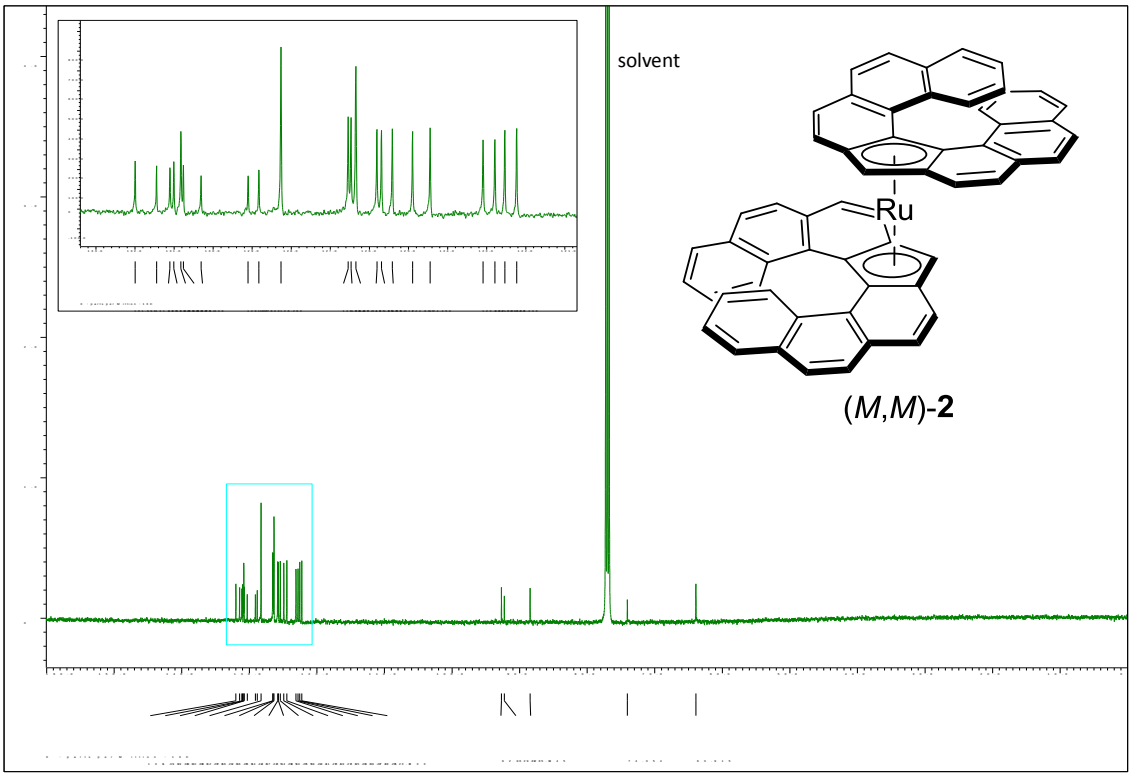

^{13}C{^{1}H } NMR spectrum of (*M*,*M*)-**2** (100 MHz, $CDCl_3$).

Because of very low solubility of *meso*-**2**, we could not obtained its clear NMR charts.

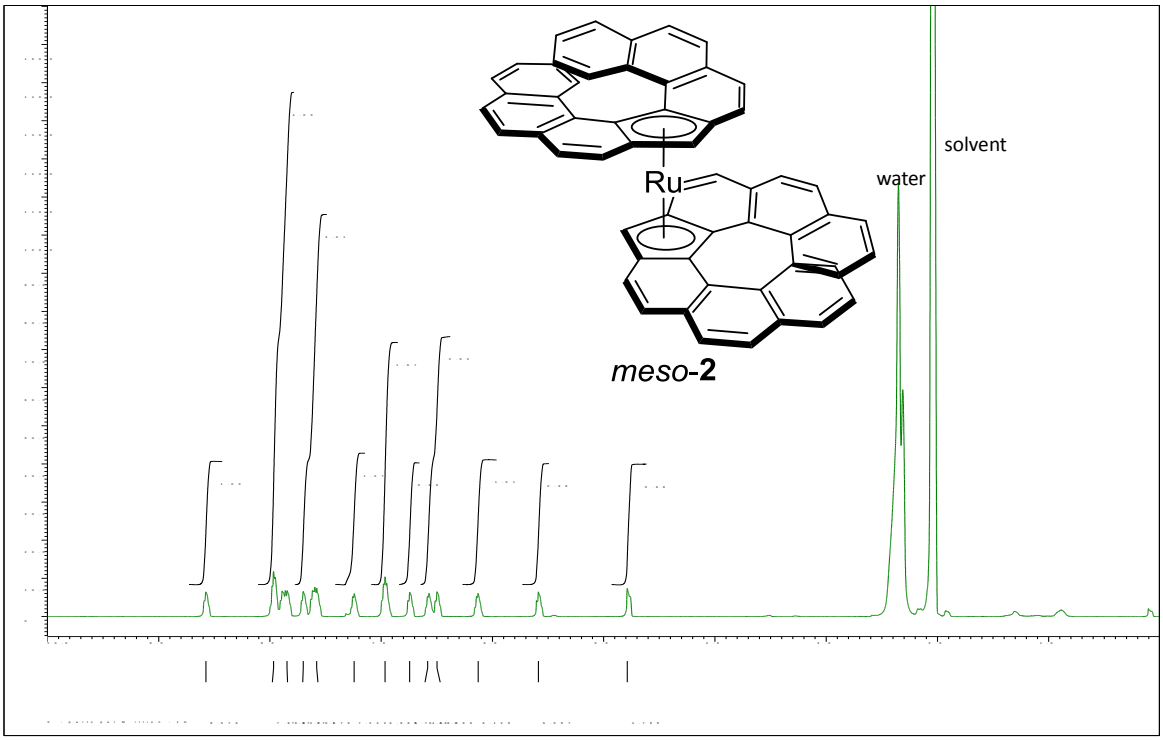

^{1}H NMR spectrum of *meso*-**2** (500 MHz, acetone-d_6/CS_2 (1:2)).

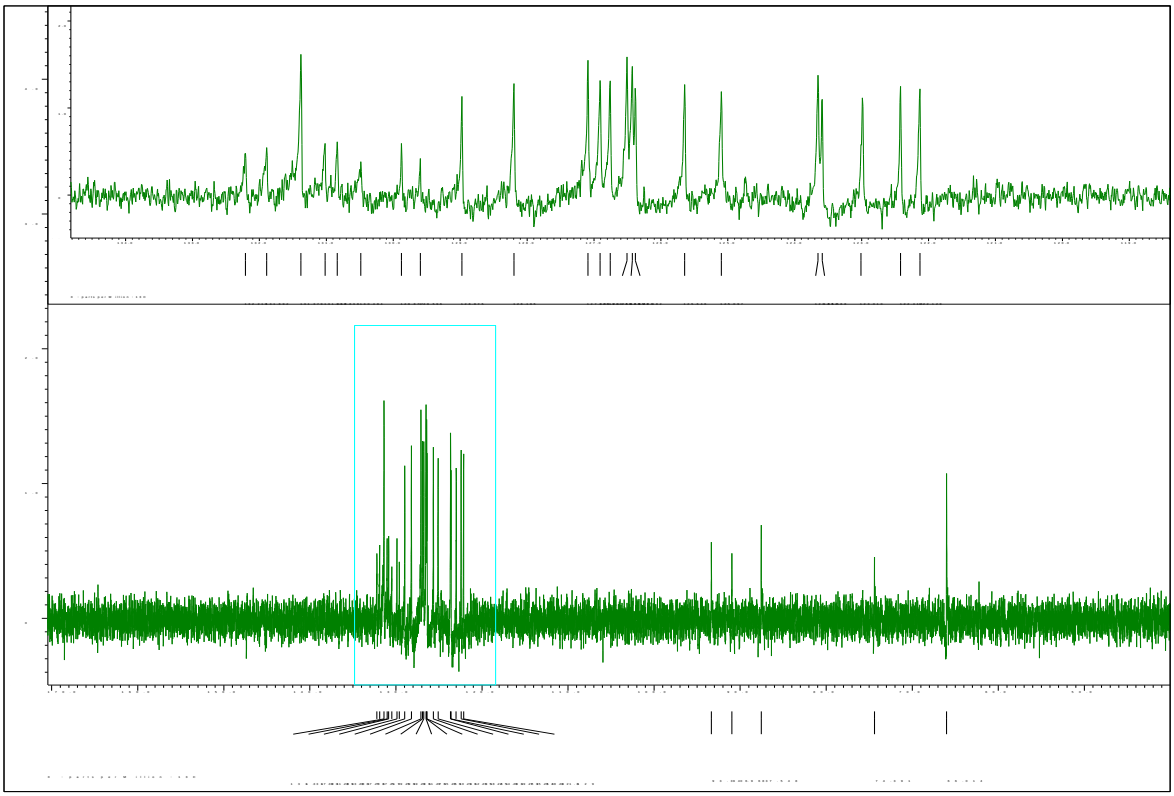

^{13}C{^{1}H } NMR spectrum of *meso*-**2** (126 MHz, acetone-d_6/CS_2 (1:2)).

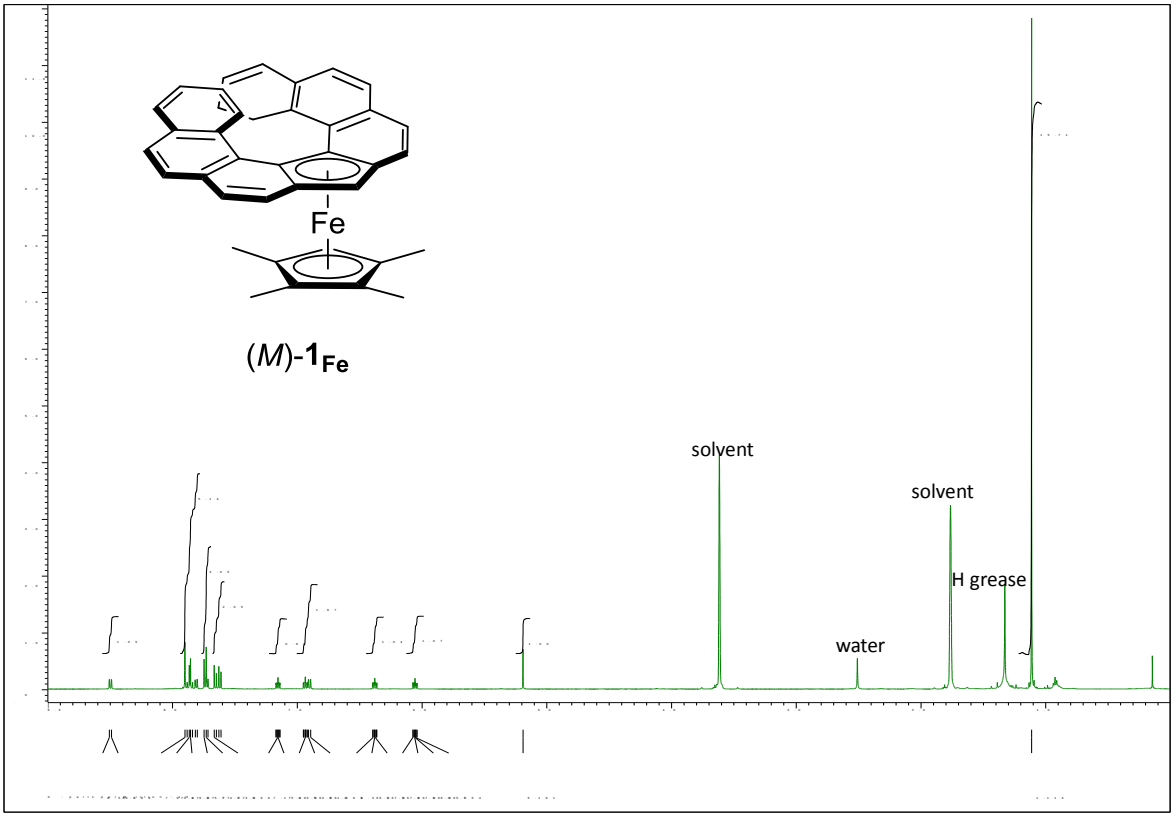

^{1}H NMR spectrum of (*M*)-**1**$_{\mathbf{Fe}}$ (400 MHz, THD-d8).

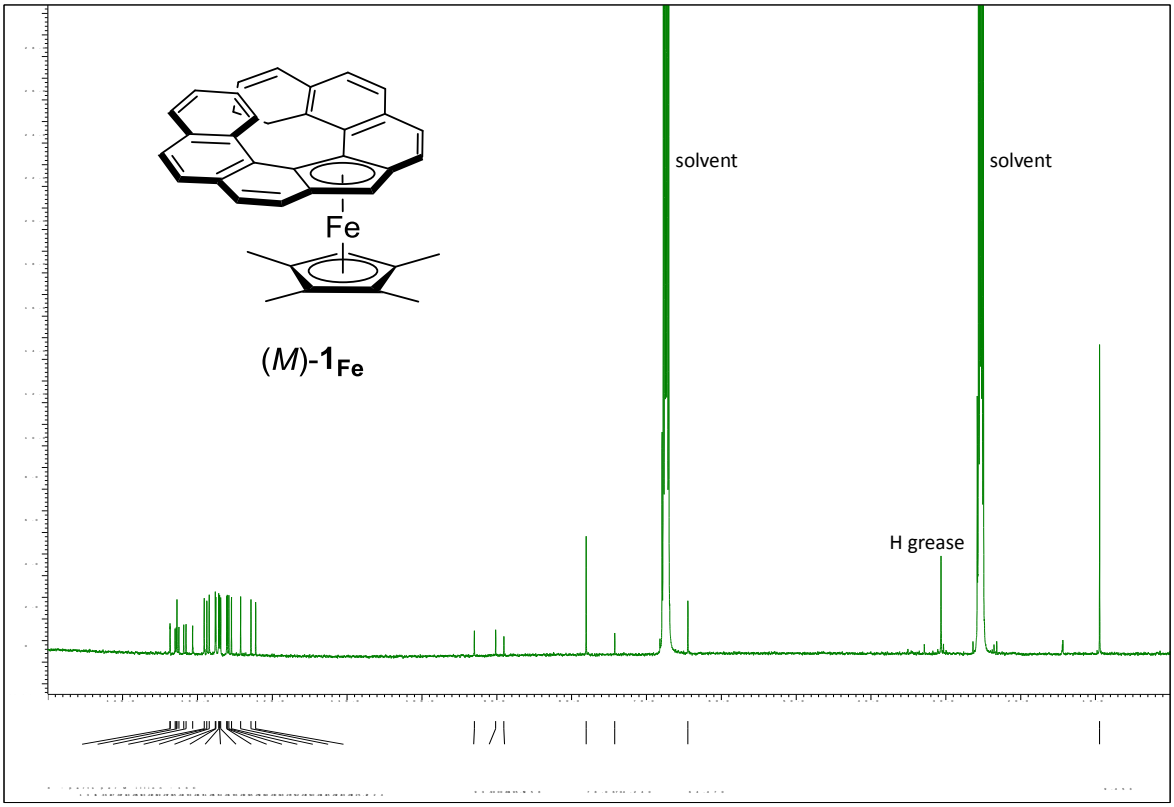

^{13}C{^{1}H } NMR spectrum of (*M*)-**1**$_{\mathbf{Fe}}$ (125 MHz, THF-d8).

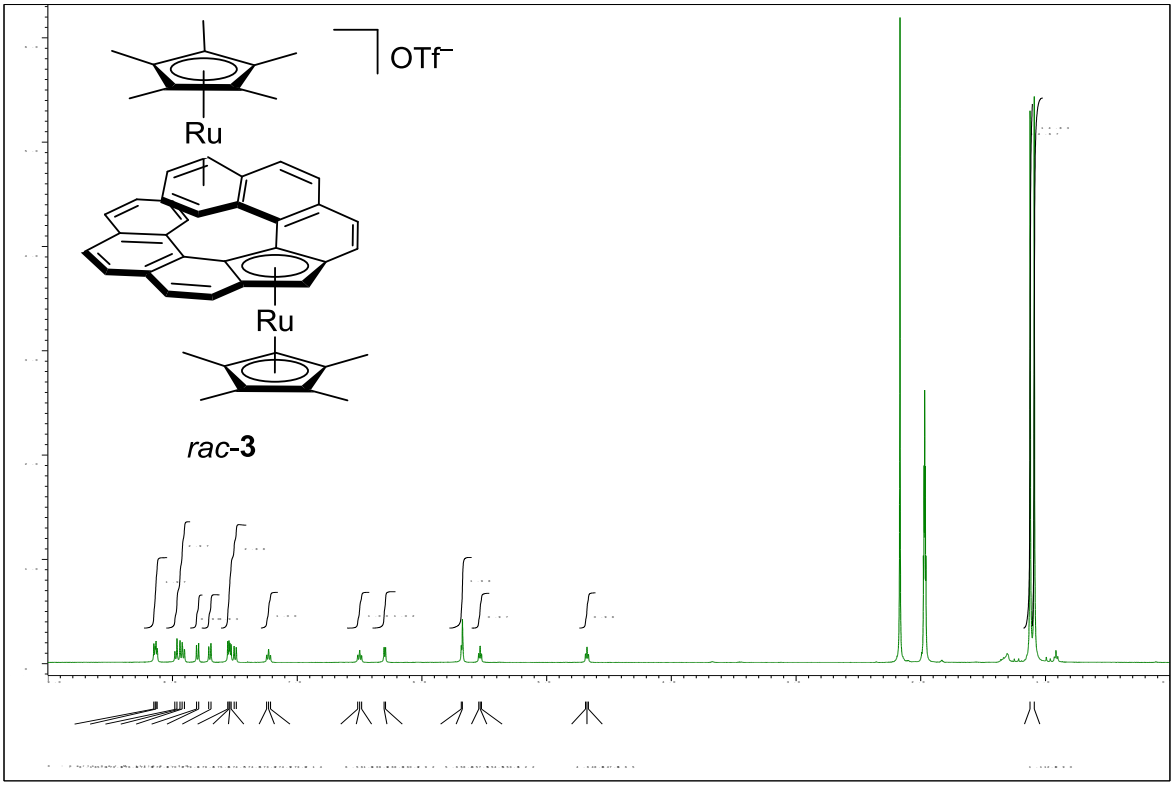

^{1}H NMR spectrum of *rac*-**3** (500 MHz, CD_3CN).

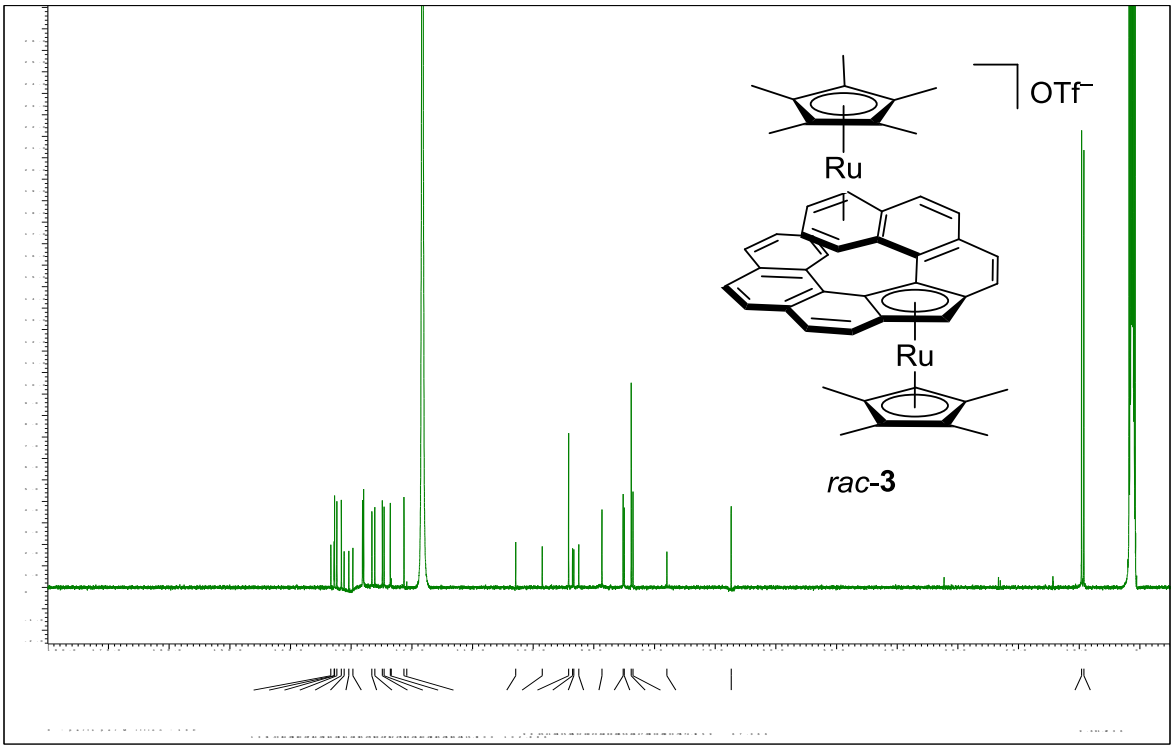

$^{13}C\{^{1}H\}$ NMR spectrum of *rac*-**3** (125 MHz, CD_3CN)

Certain amount of pentane was remained.

6-7. HPLC traces

a Daicel Chiralpak IF-3 column with hexanes/DCM = 3/1, flow = 0.75 mL min^{-1}.

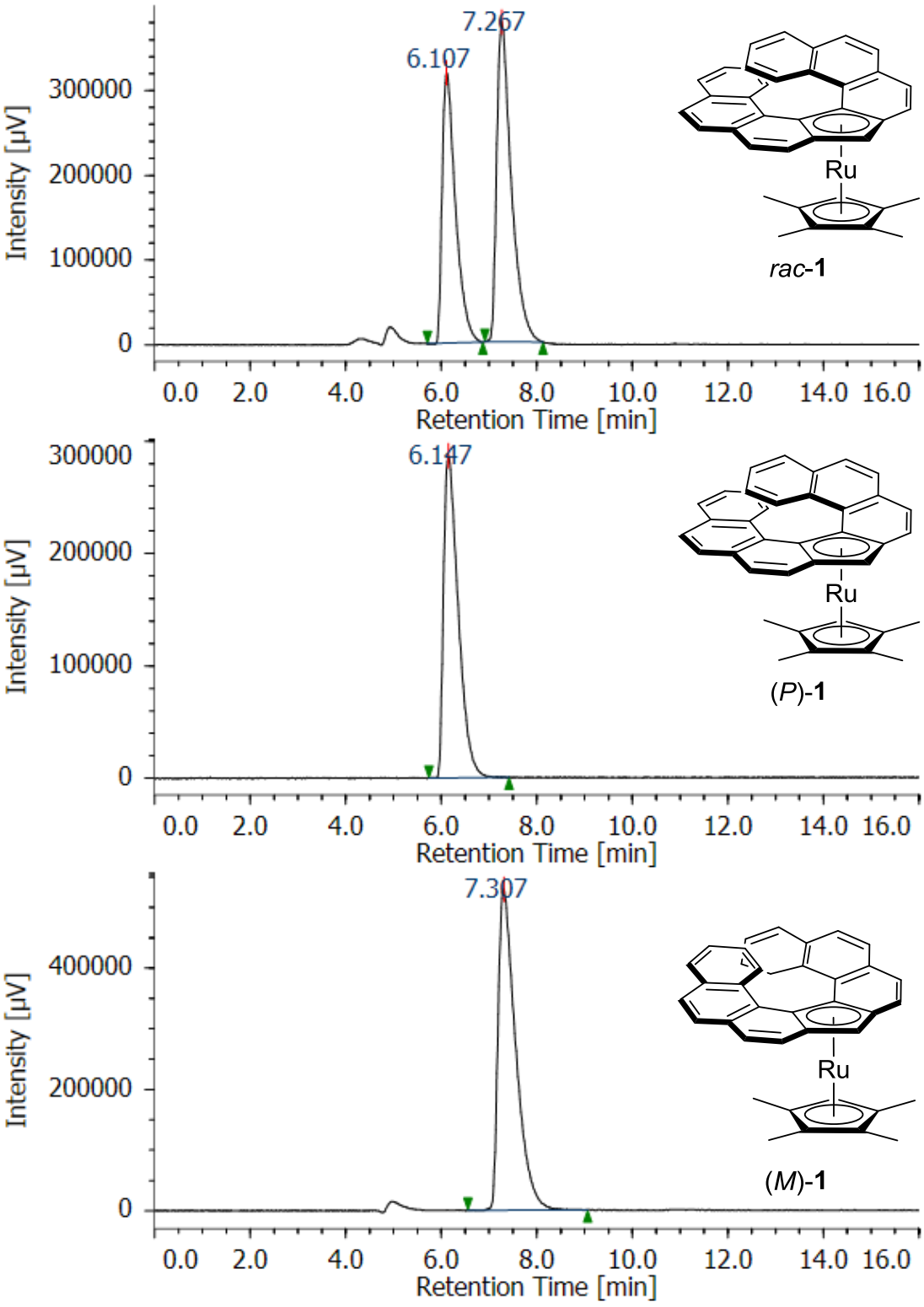

a Daicel Chiralpak IF-3 column with hexanes/DCM = 3/1, flow = 0.75 mL min^{-1}.

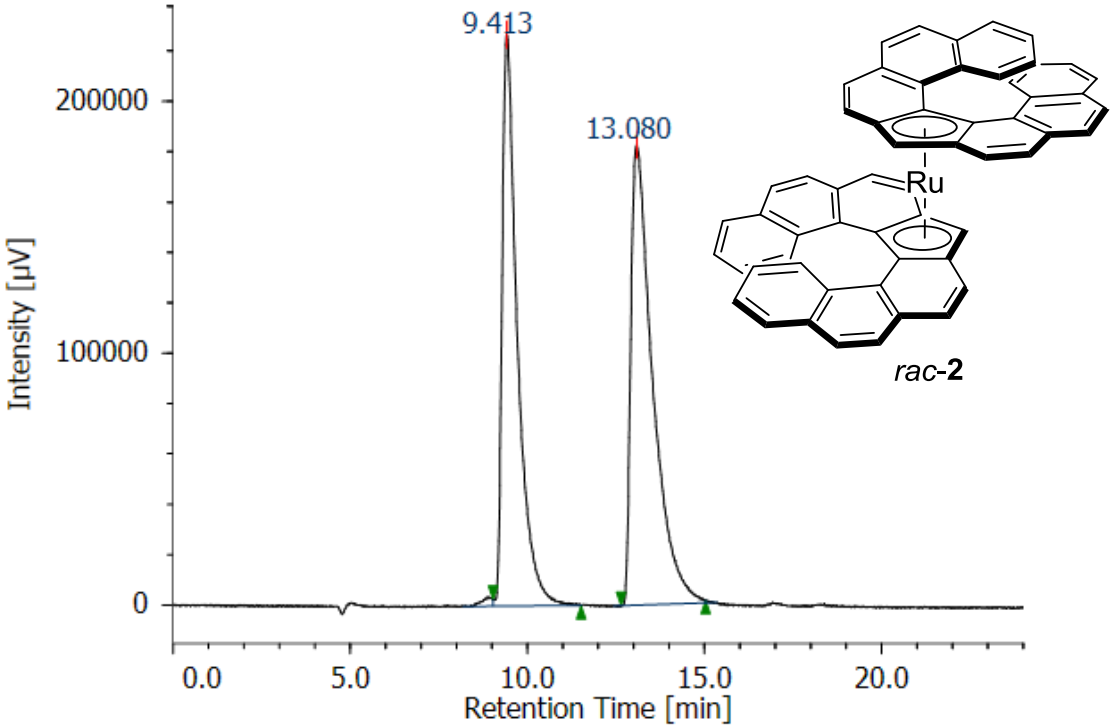

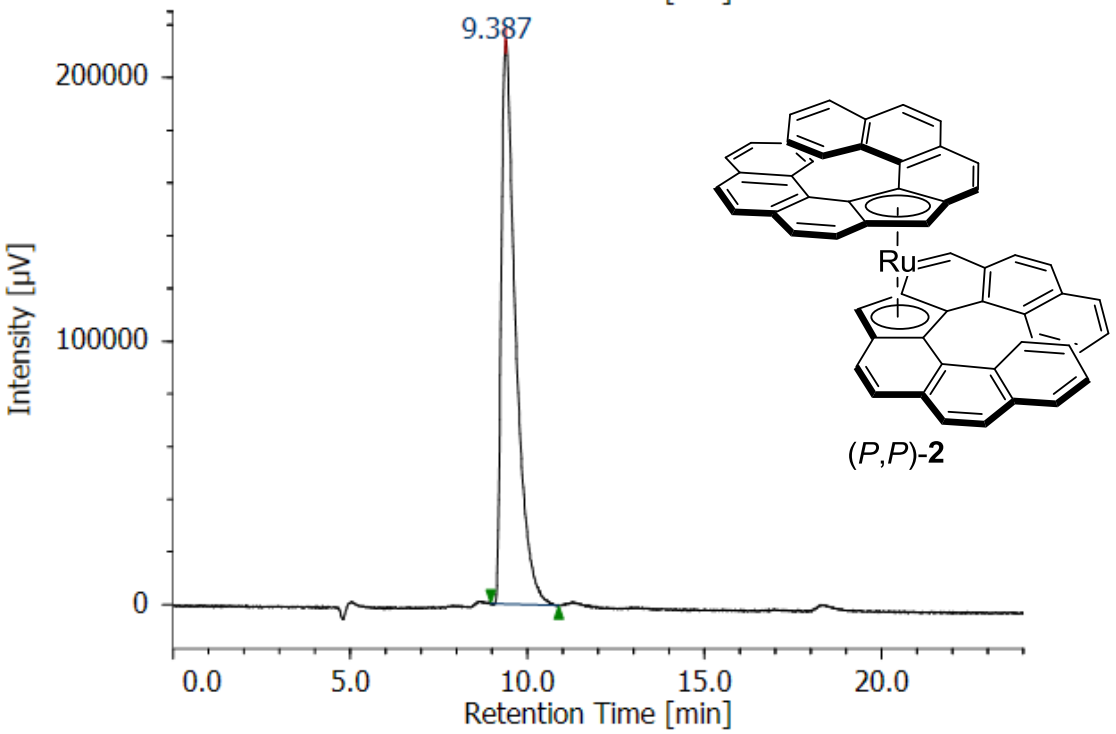

6-8. Reference

(1) Sheldrick, G. M. University of Göttingen: Göttingen, Germany, **2014**.

(2) Frisch, M. J.; Trucks, G. W.; Schlegel, H. B.; Scuseria, G. E.; Robb, M. A.; Cheeseman, J. R.; Scalmani, G.; Barone, V; Mennucci, B.; Petersson, G. A.; Nakatsuji, H.; Caricato, M.; Li, X.; Hratchian, H. P.; Izmaylov, A. F.; Bloino, J.; Zheng, G.; Sonnenberg, J. L.; Hada, M.; Ehara, M.; Toyota, K.; Fukuda, R.; Hasegawa, J.; Ishida, M.; Nakajima, T.; Honda, Y.; Kitao, O.; Nakai, H.; Vreven, T.; Montgomery, J. A.; Peralta, Jr. J. E.; Ogliaro, F.; Bearpark, M.; Heyd, J. J.; Brothers, E.; Kudin, K. N.; Staroverov, V. N.; Keith, T.; Kobayashi, R.; Normand, J.; Raghavachari, K.; Rendell, A.; Burant, J. C.; Iyengar, S. S.; Tomasi, J.; Cossi, M.; Rega, N.; Millam, J. M.; Klene, M.; Knox, J. E.; Cross, J. B.; Bakken, V.; Adamo, C.; Jaramillo, J.; Gomperts, R.; Stratmann, R. E.; Yazyev, O.; Austin, A. J.; Cammi, R.; Pomelli, C.; Ochterski, J. W.; Martin, R. L.; Morokuma, K.; Zakrzewski, V. G.; Voth, G. A.; Salvador, P.; Dannenberg, J. J.; Dapprich, S.; Daniels, A. D.; Farkas, O.; Foresman, J. B.; Ortiz, J. V.; Cioslowski, J.; Fox, D. J. *Gaussian 09, Revision C.01*, Gaussian, Inc., Wallingford CT, **2010**.

(3) a) Becke, A. D. *J. Chem. Phys.* **1993**, *98*, 5648–5652; b) Lee, C.; Yang, W.; Parr, R. G. *Phys. Rev. B* **1998**, *37*, 785–789.

(4) Yanai, T.; Tew, D. P.; Handy, N. C. *Chem. Phys. Lett.* **2004**, *393*, 51.

(5) Zhao, Y.; Truhlar, D. G. *Theor. Chem. Acc.* **2008**, *120*, 215.

(6) Hay, P. J.; Wadt, W. R. *J. Chem. Phys.* **1985**, *82*, 270.

(7) a) Hehre, W. J.; Ditchfield, R.; Pople J. A. *J. Chem. Phys.* **1972**, *56*, 2257 b) Ditchfield, R.; Hehre, W. J.; Pople, J. A. *J. Chem. Phys.* **1971**, *54*, 724.

(8) Fagan, P. J.; Ward, M. D.; Calabrese, J. C. *J. Am. Chem. Soc.* **1989**, *111*, 1698.

(9) Dulière, E.; Devillers, M.; Marchand-Brynaert, J., *Organometallics* **2003**, *22*, 804.

(10) Oyama, H.; Akiyama, M.; Nakano, K.; Naito, M.; Nobusawa, K.; Nozaki, K. *Org. Lett.* **2016**, *18*, 3654.

(11) Gassman, P. G.; Winter, C. H. *J. Am. Chem. Soc.* **1988**, *110*, 6130–6135.

(12) a) Koelle, U.; Salzer, A. *J. Organomet. Chem.* **1983**, *243*, C27–C30; b) Koelle, U.; Grub, J. *J. Organomet. Chem.* **1985**, *289*, 133–139.

(13) Swarts, J. C.; Nafady, A.; Roudebush, J. H.; Trupia, S.; Geiger, W. E. *Inorg. Chem.* **2009**, *48*, 2156–2165.

(14) A. L. Spek, *J. Appl. Cryst.* **2003**, *36*, 7.

Chapter 7.

Summary

7-1. Summary of this thesis

In this thesis, the author accomplished the synthesis of optically pure group 8 complexes with the new [7]helicene ligand, **1**, $\mathbf{1}_{\mathbf{Fe}}$, **2**, and **3**. According to their X-ray structures, the helical part was aromatized and worked as an η^5 ligand like Cp. Successful isolation of each enantiomer of [7]helicene ruthenocenes enabled the investigation of their helical structures, isomerization behaviors, and chiroptical properties. Theoretical calculations suggested that the d-orbitals of the coordinated metals hybridized to the [7]helicene's π-orbitals, which led to unique optical and chiroptical properties. Furthermore, the bimetallic complex **3** was found to exhibit phosphorescence in much higher yield than other reported ruthenocene derivatives, showing a new direction of the Cp complexes serving as a photoluminescence material.

Publication List

Publications included in this thesis

[1] **Akiyama, M.**; Nozaki, K.

"Synthesis of Optically Pure Helicene Metallocenes"

Angewandte Chemie International Edition **2017**, *56*, 2040–2044.

[2] **Akiyama, M.**; Tsuchiya, Y.; Ayumi, I.; Hasegawa, M.; Kurashige, Y.; Nozaki, K.

"Synthesis and Properties of Phosphorescent Bimetallic [7]Helicene Ruthenocene"

to be submitted.

Other publications

[1] Kusumoto, S.; **Akiyama, M.**; Nozaki, K.

"Acceptorless Dehydrogenation of C–C Single Bonds Adjacent to Functional Groups by Metal–Ligand Cooperation"

Journal of the American Chemical Society **2013**, *135*, 18726–18729.

[2] **Akiyama, M.**; Akagawa, K.; Seino, H.; Kudo, K.

"Peptide-Catalyzed Kinetic Resolution of Planar-Chiral Metallocenes"

Chemical Communications **2014**, *50*, 7893–7896.

[3] Akagawa, K.; **Akiyama, M.**; Kudo, K.

"Peptide-Catalyzed Desymmetrization of an Achiral Ferrocenyl Compound To Induce Planar Chirality"

European Journal of Organic Chemistry **2015**, *18*, 3894–3898.

[4] Oyama, H.; **Akiyama, M.**; Nakano, K.; Naito, M.; Nobusawa, K.; Nozaki, K.

"Synthesis and Properties of [7]Helicene-like Compounds Fused with a Fluorene Unit"

Organic Letters **2016**, *18*, 3654–3657.

Review

[1] **Akiyama, M.**; Nakano, K; Nozaki, K.

"Higher-Order π-Electron Systems Based on Helicene Molecules"

in *Chemical Science of π-Electron Systems*

Akasaka, T., Osuka, A., Fukuzumi, S., Kandori, H., Aso, Y. (Eds.), Springer, **2015**, 37–46.

Acknowledgement

This PhD study has been done under supervision of Prof. Kyoko Nozaki at the University of Tokyo from 2014 to 2017. My deepest appreciation goes to her invaluable guidance and warm encouragement. I have learned a wide view for chemistry, a positive way to think, and an enthusiasm to pursue the true nature of things from her.

I would like to express my gratitude to my committee members, Prof. Takuzo Aida, Prof. Kazuaki Kudo, Prof. Hirohiko Houjou, and Prof. Kazuyuki Ishii, for precious advice for this thesis.

I appreciate Prof. Miki Hasegawa, Dr. Ayumi Ishii, and Mr. Yuto Tsuchiya in Aoyama-gakuin University for measurement of photoluminescence spectra, quantum yield, and emission lifetime, and helpful discussions. I am grateful to Prof. Yuki Kurashige in Kyoto University for kind instruction for theoretical calculations and fruitful discussions. I appreciate Prof. Koichi Nozaki in University of Toyama for measurement of CPL and kind advice. I thank Dr. Masanobu Naito in National Institute for Material Science for measurement of CPL. I am grateful to Prof. Takuzo Aida for measurement of photoluminescence and CD spectra. I am grateful to Prof. Yoshiaki Nishibayashi for measurement of CV. I thank Dr. Yousoo Kim and Dr. Junepyo Oh in Riken for STM measurement.

I would like to express my thanks to the staff members in Nozaki group. I am grateful to Prof. Ryo Shintani, who showed me an energetic and steady way to progress research. I am grateful to Dr. Shingo Ito, who taught me the importance to stick to one's principles. I am grateful to Dr. Shuhei Kusumoto, who taught me how to show a passion for chemistry. I would like to thank the past and the present members of the Nozaki group, Prof. Koji Nakano, Prof. Brad P. Carrow, Dr. Takashi Okazoe, Dr. Daisuke Nobuto, Dr. Ryo Tanaka, Dr. Takeharu Kageyama, Dr. Akifumi Nakamura, Dr. Hiromi Oyama, Dr. Yoshitaka Aramaki, Dr. Kohei Takahashi, Dr. Yusuke Ota, Dr. Ryo Nakano, Dr. Collins Obuah, Dr. Keary M. Engle, Dr. Laurence Piche, Dr. Wen-Jie Tao, Dr. Shrinwantu Pal, Dr. Andreas Phanopoulos, Dr. Taishi Maeda, Mr. Motonobu Takahashi, Mr. Shunsuke Kodama, Mr. Fumihiro Ito, Mr. Kazuki Kobayashi, Mr. Masaki Noguchi, Ms. Maki Hasegawa, Mr. Natdanai Wattanavinin, Mr. Jung Jin, Mr. Keita Noguchi, Mr. Ryo Taniguchi, Mr. Yamato Yuki, Mr. Ryuhei Fujie, Mr. Toru Nishiuchi, Mr. Toshiki Tazawa, Mr. Keisuke Takahashi, Mr. Hiroki Goto, Mr. Masahiro Hatazawa, Mr. Yusuke Mitsushige, Mr. Takahiro Ohkawara, Mr. Hideki Omiya, Ms. Midori Yamamoto, Ms. Mapudumo Lephoto, Mr. Ryotaro Takayama, Mr. Wataru Aoki, Ms. Misato Katayama, Mr. Takafumi Kawakami, Mr. Wenhan Wang, Mr. Chihiro

Takagi, Mr. Yosuke Sato, Mr. Ryo Iino, Mr. Yuki Tokimaru, Mr. Koki Matsumoto, Mr. Hiroki Kurata, Mr. Hideaki Ando, Mr. Ryo Takano, Mr. Toshiumi Tatsuki, Mr. Toshiki Murayama, Mr. Tadashi Toyohara, Mr. Fumihiro Horie, Mr. Takashi Omoto, Mr. Shumpei Akita, Mr. Takaaki Kirihara, Mr. Yusuke Makida, Ms. Honami Zaizen, Ms. Nana Misawa, Mr. Taro Nagano, Mr. Tomohiro Tsuda, Ms. Anelisa Matiwane, Mr. Weiwei Wu, Mr. Jing-Yuan Deng, Ms. Chihiro Kengoyama, Ms. Satoko Takaoka, Ms. Hina Yasuda, Mr. Junichi Maeda, Mr. Minoru Koyama, Mr. Kimihiro Nakamura, Ms. Yuko Hirooka. I am also grateful to Ms. Ritsuko Inoue for her kind assistance. I would like to express my thank also to the member of the Kudo group, where I spent my master course, Prof. Kazuaki Kudo, Dr. Kengo Akagawa, Dr. Toshio Takayama, Dr. Masahiro Furutani, Dr. June Park, Mr, Takayuki Ichihara, Mr. Shota Takigawa, Ms. Rieko Suzuki, Mr. Nobutaka Sakai, Mr. Iman Sho Nagamine, Mr. Nobuhiro Nishi, Ms. Zhaonan Du, Mr. Junichi Satou, Mr. Tomoaki Hirata, Mr. Tatsuya Kuremoto.

I am also grateful to Prof. Eric Meggers in Philipps-Universität Marburg and his group members for warmly welcoming me as a visiting student.

This research was supported by JSPS fellowship for young Scientists.

Finally, I would like to express my appreciation to my family, Hidero, Kazuko, and Taiki for their constant support and encouragement throughout my life.

March 2017

Midori Akiyama